NAVAL POSTGRADUATE SCHOOL
Monterey, California

THESIS

ANALYSIS OF PERFORMANCE INDICES
FOR
ALL-POLE, CLOSED-LOOP SYSTEMS

by

Darrell R. Davis

March 1990

Thesis Advisor George J. Thaler

SECURITY CLASSIFICATION OF THIS PAGE

REPORT DOCUMENTATION PAGE

1a. REPORT SECURITY CLASSIFICATION UNCLASSIFIED	1b. RESTRICTIVE MARKINGS
2a. SECURITY CLASSIFICATION AUTHORITY	3. DISTRIBUTION/AVAILABILITY OF REPORT Approved for public release; distribution is unlimited.
2b. DECLASSIFICATION/DOWNGRADING SCHEDULE	
4. PERFORMING ORGANIZATION REPORT NUMBER(S)	5. MONITORING ORGANIZATION REPORT NUMBER(S)
6a. NAME OF PERFORMING ORGANIZATION Naval Postgraduate School Monterey, CA 93943 — 6b. OFFICE SYMBOL (If applicable): 32	7a. NAME OF MONITORING ORGANIZATION Naval Postgraduate School
6c. ADDRESS (City, State, and ZIP Code) Monterey, CA 93943-5000	7b. ADDRESS (City, State, and ZIP Code) Monterey, CA 93943-5000
8a. NAME OF FUNDING/SPONSORING ORGANIZATION — 8b. OFFICE SYMBOL (If applicable)	9. PROCUREMENT INSTRUMENT IDENTIFICATION NUMBER
8c. ADDRESS (City, State, and ZIP Code)	10. SOURCE OF FUNDING NUMBERS PROGRAM ELEMENT NO. — PROJECT NO. — TASK NO. — WORK UNIT ACCESSION NO.

11. TITLE (Include Security Classification)

Analysis of Performance Indices for All-Pole, Closed-Loop Systems

12. PERSONAL AUTHOR(S)

Darrell R. Davis

13a. TYPE OF REPORT	13b. TIME COVERED	14. DATE OF REPORT (Year, Month, Day)	15. PAGE COUNT
Master's Thesis	FROM _____ TO _____	March 1990	150

16. SUPPLEMENTARY NOTATION The views expressed in this thesis are those of the author and do not reflect the official policy or position of the Department of Defense or the U.S. Government.

17. COSATI CODES			18. SUBJECT TERMS (Continue on reverse if necessary and identify by block number)
FIELD	GROUP	SUB-GROUP	Performance Indices, Closed-Loop Systems

19. ABSTRACT (Continue on reverse if necessary and identify by block number)

This study was concerned with the transient performance of servomechanisms. Only those systems with a steady-state-displacement error of zero when subjected to an input-step function were considered. Specific linear and nonlinear systems were optimized by minimizing the cost functionals of the integral of time multiplied by the absolute value of the error and the integral of time multiplied by the absolute value of error plus a weighting factor times the control effort squared. Resultant pole locations were evaluated to determine the existance of progressive and useful patterns. Standard forms were derived for first through seventh-order systems. Active networks were designed using these standard forms. Step responses were evaluated in terms of the components of the cost functionals. Nonlinear and linear optimizations were compared to determine if one was superior to the other. Performance indices were compared to determine if advantages existed for the inclusion of a control cost. Conclusions drawn by previously published material were investigated for validity.

20. DISTRIBUTION/AVAILABILITY OF ABSTRACT	21. ABSTRACT SECURITY CLASSIFICATION
☒ UNCLASSIFIED/UNLIMITED ☐ SAME AS RPT. ☐ DTIC USERS	UNCLASSIFIED
22a. NAME OF RESPONSIBLE INDIVIDUAL Dr. George J. Thaler	22b. TELEPHONE (Include Area Code) (408)646-2134 — 22c. OFFICE SYMBOL 62Tr

DD FORM 1473, 84 MAR — 83 APR edition may be used until exhausted. All other editions are obsolete

SECURITY CLASSIFICATION OF THIS PAGE

Approved for public release; distribution is unlimited

Analysis of Performance Indices for All-Pole, Closed-Loop Systems

by

Darrell R. Davis
Captain, United States Army
B.S., U.S. Military Academy, 1980

Submitted in partial fulfillment of the
requirements for the degree of

MASTER OF SCIENCE IN ELECTRICAL ENGINEERING

from the

NAVAL POSTGRADUATE SCHOOL

March 1990

Author:

Darrell R. Davis

Approved by:

George J. Thaler, Thesis Advisor

Harold A. Titus, Second Reader

John P. Powers, Chairman
Department of Electrical and Computer Engineering

ABSTRACT

This study was concerned with the transient performance of servomechanisms. Only those systems with a steady-state-displacement error of zero when subjected to an input-step function were considered. Specific linear and nonlinear systems were optimized by minimizing the cost functionals of the integral of time multiplied by the absolute value of the error and the integral of time multiplied by the absolute value of error plus a weighting factor times the control effort squared. Resultant pole locations were evaluated to determine the existance of progressive and useful patterns. Standard forms were derived for first- through seventh-order systems. Active networks were designed using these standard forms. Step responses were evaluated in terms of the components of the cost functionals. Nonlinear and linear optimizations were compared to determine if one was superior to the other. Performance indices were compared to determine if advantages existed for the inclusion of a control cost. Conclusions drawn by previously published material were investigated for validity.

TABLE OF CONTENTS

LIST OF TABLES

LIST OF FIGURES

ACKNOWLEDGMENTS

Gratitude is extended to the faculty of the Naval Postgraduate School, many of whom left lasting marks on my character and perspective. To my mentor, Dr. George J. Thaler, I extend special thanks. His expertise, patience, and enthusiasm were inspirational. To Dr. H. A. Titus for his interest, encouragement, and practical approach to both education and life. To Jan Evans for her assistance in typing and moral support. Especially, to my wife, Jennifer, who, when needed, was all things.

I. INTRODUCTION

There are many ways to define an optimum system. What is optimum in any particular case is dependent on the specific application for which the system is to be used. One useful and generally accepted definition of the optimum response is that a system is optimum if it has the least amount of error, with error being defined as the difference between the desired output and the actual output of the system. The primary task of the control systems engineer is to find the most appropriate values for the design parameters that ensures the best performance for the system's application. He must define the parameters so as to produce a response with the closest features, characteristics, and shape to that which he has defined as optimal. In so doing, he has fulfilled his objectives.

A point that is worth stressing is the distinction between an optimum system and one that is not optimum, but acceptable. Good design characteristics might be the outcome of a design that meets certain specifications and general requirements. These systems would be considered good enough, or optimum in the sense that they meet the particular need for which they were created. The truly optimum system is uniquely distinguished from all others by the fact that it defines the best compromise of design parameters to match the ideal output. This study was concerned with the design of servomechanisms, and, as such, the ideal output was the mirror image of the input. More specifically, the study pertained to the class of linear-transfer, single input-single output systems called duplicators.

The most fundamental relationship which gives the dependence of the output on the input is usually the set of differential equations describing the physical system. The Laplace transform ratio between the system output and its input is the transfer

function of the system. Transient response is defined as the system's behavior from the time of its initial disturbance until it reaches its steady state. It is an unavoidable consequence of the nature of dynamic systems. The control engineer must design for the transient response which is compatible with the desired specifications. The problem which arises is the lack of a practical mathematical definition of optimal transient attributes and, as a result, leads to judgment based on intuition.

In an attempt to provide a more quantitative approach to the evaluation of transient responses, the application of various performance criteria or indices have become widely used. The problem encountered in this endeavor is the choosing of a criterion which takes into account most of the system response characteristics; additionally, the criterion must be reliable for a range of various systems, be easy to apply, and be selective in the sense that the optimum system is readily discernible. The performance index is generally an expression of the key variables of the system or control problem that is to be optimized. The choice of the best performance index is one of considerable debate.

Once a performance index has been chosen by the designer, the next step is to bridge the original uncompensated system to the one defined by the performance index. This process is known as system compensation. The selection of an appropriate and suitable compensation scheme remains at the discretion of the engineer. In classical control theory, there are, generally, two basic methods of compensation, adjustment of gain and the addition of poles and zeros. Since gain reduction hampers the system's accuracy, this method is not desirable under ordinary circumstances. The addition of poles and zeros is most frequently used and is accomplished through the use of filters. The addition or adjustment of these poles and/or zeros is done either in the forward path, cascade compensation, or in the minor feedback path, feedback compensation.

In this study, an investigation was made into the results of using performance indices. The effect of different cost functions was examined, with emphasis placed on the weighting within these cost functions. After optimization, the roots of the characteristic equations were studied to identify progressive and useful patterns. Finally, nonlinearities were introduced and their effect on optimal design investigated.

II. BACKGROUND THEORY, EQUATIONS, AND STANDARD PROCEDURES

A. SYSTEMS UNDER INVESTIGATION

The design of a feedback control system starts with a plant, i.e., a process or machine which is to be controlled. A plant function ordinarily expresses the plant characteristics.

It is considered that the plants for the systems of interest may be expressed in the form

$$G_p(S) = \frac{K}{S(S+P_1)(S+P_2)\cdots(S+P_N)} \quad , \tag{2.1}$$

where $P_1, P_2, \cdots P_N$ are plant pole locations and K is the plant gain. As can be seen from Equation 2.1, these are all-pole plants with one pole located at the origin. Due to this one pole at the origin, the plant is often called a type-one system. Given a specific reference input into the plant, an output is received which may or may not be the desired output. To correct any discrepancies, feedback is introduced around the plant to measure and correct its performance. Compensation is generally added either in cascade with the plant, or in a minor feedback path. The feedback not only reduces the system's error between the reference input and system output, but also enhances the system's stability to external disturbances and its sensitivity to plant parameter variations.

Compensation for the plants considered in this study centered around the use of full state feedback. Figure 2.1 shows the block diagram of the proposed system where k_2, k_1 and k_0 are the feedback gains of the second, first, and zero derivatives of the output, $C(S)$.

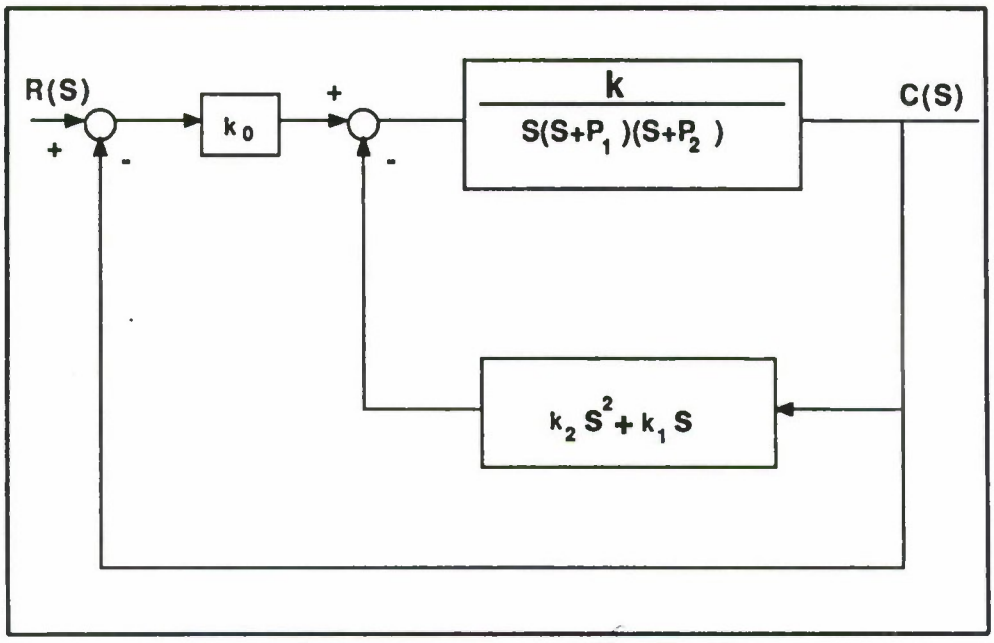

Figure 2.1: Block Diagram of Plant with Feedback Compensation

Since the modelling of different physical systems results in different pole locations, the choice of specific values for the poles was irrelevant to the theory of the study; correspondingly, the initial pole locations were arbitrarily chosen at 0.0, -2.0 and -6.0. As the study of higher-order plants became necessary, additional poles were chosen and added to the existing third-order configuration.

The plant gain, K, directly determined the stability of the uncompensated system and was of greater concern. A poor choice for the value of K provided an unrealistic physical system and, depending on the amount of positive or negative phase margin produced, resulted in abnormally high or low feedback gains. To ensure unbiased results, the gain was chosen to place the uncompensated system at

the limit of stability, or near a zero phase margin. This point was chosen using the Routh criterion. To provide an understanding of the procedure followed for all the N^{th}-order systems, the procedure for the simple third-order system is provided. As previously stated, the third-order plant investigated was

$$G_p(S) = \frac{K}{S(S+2)(S+6)} \quad . \tag{2.2}$$

Using unity feedback as the only form of compensation, the block diagram of the system is presented in Figure 2.2.

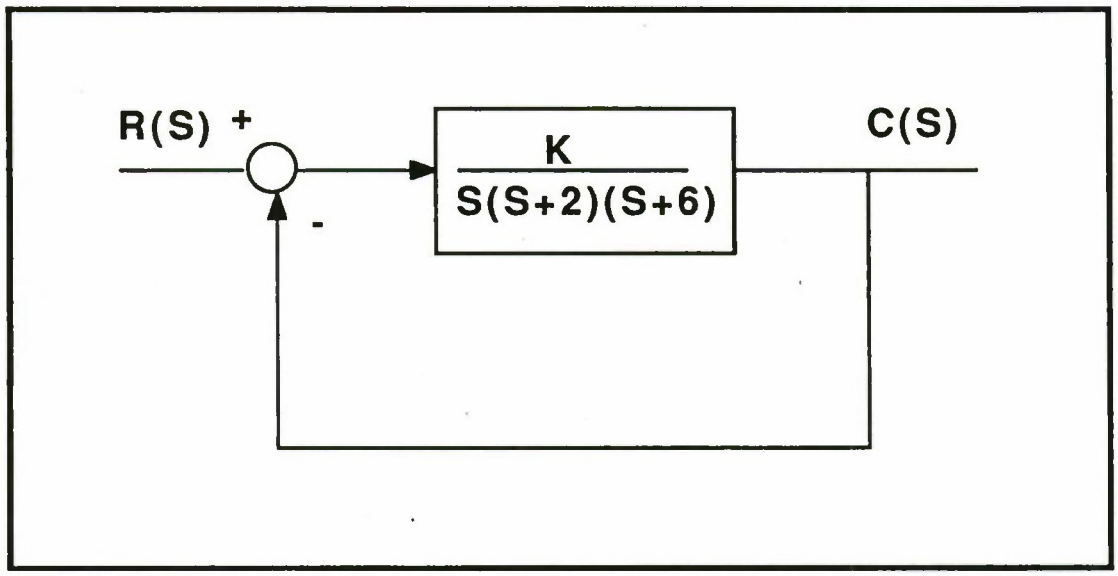

Figure 2.2: Third-Order System with Unity Feedback

Deriving the characteristic equation for the system resulted in Equation 2.3. The corresponding Routh array is given in Figure 2.3. From the array, K had to be

$$C.E. = S^3 + 8S^2 + 12S + K \tag{2.3}$$

positive for the system to be stable. If the S^1 entry was to be positive, it was necessary that K be less than 96.0. Therefore, the bounds of K for a stable system

were $0 < K < 96.0$. The value of K chosen for this study was 48.0. This value provided a small positive phase margin and exemplified a typical physical system. The values of K for higher-order systems were chosen in a like manner.

$$\begin{bmatrix} S^3 & 1 & 12 \\ S^2 & 8 & K \\ S^1 & \frac{96-K}{8} & 0 \\ S^0 & K & 0 \end{bmatrix}$$

Figure 2.3: Routh Array for Equation 2.3

B. COST CRITERION

All compensation schemes are employed to design for accuracy at steady state. Each parameter of the compensation can be adjusted to provide the optimal system performance. In addition to accuracy at steady state, the system must have acceptable dynamics. These dynamics are usually evaluated in terms of the system's percent overshoot of the commanded input, the time required for it to reach a steady-state value, the time for the error to reach its first zero, the time to reach the maximum overshoot, and the frequency of oscillation of the transient. These criteria, or combinations of them, are used to evaluate the optimum performance. Using a step-input signal as the reference, it is desired to develop a single figure of merit or criterion to judge the "goodness" of the time response of the system. Such a criterion must have three basic properties: reliability, ease of application, and selectivity. It must be reliable for a given class of systems so that it can be applied with confidence, it must be easy to apply, and it must be selective so that the "best" system is readily discernible.

Note that the systems studied here had a zero steady-state error with a step input. This meant that the open-loop transfer function had to have at least one pole at the origin. A perfect response required a step-function response identical to the input with no error. Such a system was, of course, impossible, but the amount of total error remained of prime concern and, logically, had to be considered in the performance index. The percent overshoot and the time to the first zero were conflicting characteristics, i.e., their minimum values occurred at different damping ratios; therefore, these two characteristics required an arbitrary compromise and were not used in the cost function. The solution or settling time appeared to combine both properties and was used in the criterion of performance.

Important papers were written by Dunstan Graham and R. C. Lathrop [Refs. 1,2] discussing the general ideas of system response and the various criteria which could be used to evaluate response. Some of the error functions considered were the integral of squared error (ISE), integral of absolute error (IAE), integral of time multiplied by squared error (ITSE), integral of squared time multiplied by squared error (ISTSE), integral of squared time multiplied by the absolute value of error (ISTAE), and integral of time multiplied by the absolute value of error (ITAE). On the basis of the demonstrated superiority of the ITAE criterion when compared to all others from the standpoints of ease of applicability and clear selectivity of optima for various classes of systems, Graham and Lathrop [Refs. 1,2] succeeded in presenting strong arguments for the use of the ITAE criterion as the most suitable measure of system performance. It was this criterion which was initially used during the course of this study.

The ITAE criterion was expressed by the integral

$$J = \int_0^\infty [t\ |e(t)|]\, dt \ , \tag{2.4}$$

where $e(t)$ represented error. It was noted that the t representing time under the integral sign had the effect of penalizing long duration errors. In general, the $e(t)$ was the desired value of the output minus the actual output. Since the input of the follower-type system was, generally, the desired output,

$$e(t) = r(t) - c(t) \tag{2.5}$$

where $r(t)$ and $c(t)$ were input and output, respectively. The system for which the value of Equation 2.4 was a minimum for a step input was then considered to be the optimum solution.

Though useful in the theoretical sense, the ITAE criterion often produced an unrealistic optimal solution. This problem arose from the fact that the ITAE criterion assumed that infinite control input, $r(t)$, was available. In reality, this parameter was limited by the physical limitations of the circuitry or mechanical apparatus. To provide for this reality, a second cost function was designed which penalized the use of the control input. To maintain the customary nomenclature, the control input was annotated as $u(t)$. The performance index used was expressed by the integral

$$J = \int_0^\infty \left[t\,|e(t)| + qu(t)^2 \right] dt \ , \tag{2.6}$$

where $e(t)$ and t represented the error and time, $u(t)$ represented the control input, and q was a weighting factor. The control input, $u(t)$, was squared to account for the fact that the sign of the control input was not important, only the amount of input provided was of concern. The weighting factor q was a number which weighted the control input relative to time multiplied by the absolute value of the error. As q was increased, the cost of the control input was increased; thereby, increasing the penalty for its use. In a physical sense, the control input may have represented fuel consumption and q represented the cost of that fuel. The system which produced

the minimum value of Equation 2.6 for a step input was considered to be the optimal solution.

C. SIMULATION PROCEDURE

Each of the systems examined was modelled using the Dynamic Simulation Language [Ref. 3:p. 556]. An example of the computer code used for the minimization of the fourth-order system using the ITAE cost criterion is included as Appendix A. The code for the minimization of the fourth-order system using the cost function of Equation 2.6 is located in Appendix B.

The general procedure followed for the minimizations was to perform an unconstrained optimization of the feedback gains of Figure 2.1 based on the multiparameter cost functions of Equations 2.4 and 2.6. The minimization algorithm evaluated the cost function at a base point, provided by an initial estimate, and perturbed each parameter by an amount set by the user. It evaluated the cost function at each near point and compared it to the original value of the cost function. If none of these points produced a better value of the cost function, the step sizes were decreased by a factor, set by the user, and the process repeated. If any of these points produced a better value of the cost function, a temporary base point was calculated using the previous base point and the perturbation which produced the best value of the cost function. A search was conducted around this new base point with the same step sizes as the previous search. If this search failed to produce a better value for the cost function, the step sizes were reduced and a new search was conducted. The search continued until either the number of function evaluations exceeded the maximum iterations set by the user, or the difference between the current best value of the cost function and the previous best value of the cost function was less than a limit set by the user. [Ref. 3:p. 557] The stopping limit for these

studies was set at 0.0001, with an infinite limit on the number of iterations allowed. The initial step sizes were chosen as ten percent of the initial estimate.

The derivation of the initial estimate was a design problem. Traditional frequency domain methods were used to choose initial feedback gains which provided some small degree of phase margin. Bode diagrams were the principal tool for this procedure.

The final variable which entered into the minimization procedure was the time period over which the system was to be minimized. If the period was chosen well in excess of the system's settling time, the minimization procedure gave erroneous results. This was due to the program's attempt to eliminate insignificant fluctuations occurring after the settling time. The choice of a minimization period less than the settling time placed undue emphasis on the time to reach the first zero, and caused unusually high values for the lower-order feedback gains. The settling times encountered in this study were between two and ten seconds; thus, the appropriate value within this interval was chosen as the minimization period.

D. RELATED STUDIES

In an article published in 1953 by Dunstan Graham and R. C. Lathrop [Ref. 1], the derivation of the performance index of the integral of time multiplied by the absolute value of the error was investigated. As stated earlier, they provided a pervasive argument in favor of this criterion due to its reliability, selectivity, and ease of use. They concluded that this criterion was reliable in that it selected a damping ratio of about 0.7, a value which was commonly considered to be optimum. It was fairly easy to apply, given the time responses of a system. Finally, they suggested that it was selective in that the difference between the optimum value and other values was easy to distinguish.

Their paper, as was this study, was concerned with the transient performance of servomechanisms or similar transfer systems. Only those systems with a steady-state displacement error of zero when subjected to an input step function were considered.

The underlying importance of their work was not their conclusion of the best performance index to use, but their derivation and subsequent study of characteristic-equation standard forms. Using the step responses and standard forms of the Butterworth filters as a mark against which to measure, Graham and Lathrop performed an iterative experimental determination of the optimum unit-numerator transfer functions by the application of the minimum criterion of Equation 2.4. They found that when this minimum criterion was applied to the determination of the optimum unit-numerator transfer functions of various orders, the standard forms of Table 2.1 were obtained. The corresponding pole locations and step-function responses were also studied to determine if the application of this arbitrary cost criterion resulted in a family of systems with similar and progressive characteristics. Unfortunately, no such trend was discovered.

In comparing the standard forms of Table 2.1 with the standard Butterworth forms presented in Table 2.2, the standard forms of Table 2.1 had coefficients which were slightly higher for the lower orders, and slightly lower for the higher orders.

In their paper, Graham and Lathrop [Ref. 1] took a large step in a more logical approach to systems design. When one kept in mind the limitations of the analytical tools available at that time period, namely the analog computer, their work demanded even more respect. It was the first large-scale attempt to formulate the specific transfer functions that satisfied a given error criterion.

TABLE 2.1: The Minimum ITAE Standard Forms for Zero-Displacement-Error Systems

$$s + \omega_o$$

$$s^2 + 1.40\omega_o s + \omega_o^2$$

$$s^3 + 1.75\omega_o s^2 + 2.15\omega_o^2 s + \omega_o^3$$

$$s^4 + 2.10\omega_o s^3 + 3.40\omega_o^2 s^2 + 2.70\omega_o^3 s + \omega_o^4$$

$$s^5 + 2.80\omega_o s^4 + 5.00\omega_o^2 s^3 + 5.50\omega_o^3 s^2 + 3.40\omega_o^4 s + \omega_o^5$$

$$s^6 + 3.25\omega_o s^5 + 6.60\omega_o^2 s^4 + 8.60\omega_o^3 s^3 + 7.45\omega_o^4 s^2 + 3.95\omega_o^5 s + \omega_o^6$$

$$s^7 + 4.475\omega_o s^6 + 10.42\omega_o^2 s^5 + 15.08\omega_o^3 s^4 + 15.54\omega_o^4 s^3 + 10.64\omega_o^5 s^2 + 4.58\omega_o^6 s + \omega_o^7$$

$$s^8 + 5.20\omega_o s^7 + 12.80\omega_o^2 s^6 + 21.60\omega_o^3 s^5 + 25.75\omega_o^4 s^4 + 22.20\omega_o^5 s^3 + 13.30\omega_o^6 s^2 + 5.15\omega_o^7 s + \omega_o^8$$

E. OBJECTIVES OF THE STUDY

The objective of this study was not to prove the superiority of one error criterion over another. No one criterion served all needs. The proper criterion was implied by the application and may have required that emphasis be placed on speed rather than damping, or on accuracy rather than the time to the first zero error. The study centered around the integral of time multiplied by the absolute value of the error. This criterion appeared to be a criterion that was preferred, and one which adequately defined or evaluated the transient performance of a zero-error transfer function to a step input. The adequacy of this criterion was based upon the fact that it gave recognition to the concept that the sign of the error was not important;

TABLE 2.2: The Butterworth Standard Forms

$$s + \omega_o$$

$$s^2 + 1.40\omega_o s + \omega_o^2$$

$$s^3 + 2.00\omega_o s^2 + 2.00\omega_o^2 s + \omega_o^3$$

$$s^4 + 2.60\omega_o s^3 + 3.40\omega_o^2 s^2 + 2.60\omega_o^3 s + \omega_o^4$$

$$s^5 + 3.24\omega_o s^4 + 5.24\omega_o^2 s^3 + 5.24\omega_o^3 s^2 + 3.24\omega_o^4 s + \omega_o^5$$

$$s^6 + 3.86\omega_o s^5 + 7.46\omega_o^2 s^4 + 9.13\omega_o^3 s^3 + 7.46\omega_o^4 s^2 + 3.86\omega_o^5 s + \omega_o^6$$

$$s^7 + 4.50\omega_o s^6 + 10.10\omega_o^2 s^5 + 14.60\omega_o^3 s^4 + 14.60\omega_o^4 s^3 + 10.10\omega_o^5 s^2 + 4.50\omega_o^6 s + \omega_o^7$$

$$s^8 + 5.12\omega_o s^7 + 13.14\omega_o^2 s^6 + 21.84\omega_o^3 s^5 + 25.69\omega_o^4 s^4 + 21.84\omega_o^5 s^3 + 13.14\omega_o^6 s^2 + 5.12\omega_o^7 s + \omega_o^8$$

furthermore, it recognized that the existence of an initial error had to be accepted, but that the system had to be penalized if any error existed after this initial period.

Initially accepting this criterion, the study delved into the manner and effect of its use with both linear and nonlinear systems. The second objective was to determine if the standard forms presented by Graham and Lathrop in Table 2.1 were accurate enough to be used in modern design. Thirdly, this study examined the root patterns resulting from minimization using this criterion to determine if a standard, predictable, and useful trend emerged. The study concluded with the effects of adding a control cost to the performance index.

III. OPTIMIZATION USING THE INTEGRAL OF TIME MULTIPLIED BY THE ABSOLUTE VALUE OF ERROR

A. PROBLEM OF INCREASING BANDWIDTH

When used in conjunction with full-state-feedback compensation, the cost criterion of the integral of time multiplied by the absolute value of the error did not reach a minimum value unless a specific value was chosen for the system's bandwidth. Consider the system of Figure 3.1 which utilized the plant of Equation 2.2. As stated in Chapter I, the pole locations were arbitrarily chosen and the plant gain of 48.0 was chosen to place the uncompensated plant near the stability limit. In order to maintain the error definition given in Equation 2.5 and correctly measure the cost function, a block diagram manipulation was performed. The resulting system maintained a unity-feedback loop, and is presented in Figure 3.2. As shown in Figure 3.2, when unity feedback was added, the gain of the zero-order derivative became a forward-path gain. Reducing this system to an equivalent open-loop transfer function, Equation 3.1 was obtained.

$$G_{ol}(S) = \frac{(48)(k_0)}{S\left[S^2 + (8 + 48k_2)S + (12 + 48k_1)\right]} \tag{3.1}$$

The minimization of this transfer function adjusted the k_2, k_1 and k_0 terms until the cost function of Equation 2.4 was at its smallest value. By inspection of this cost function, it was seen that a reduction in settling time or a reduction in total error drove the function to lower values. Control theory suggested that these two criteria were in conflict, i.e., a reduction in settling time caused an increase in total error. As the system increased its speed to finish its transient in a smaller

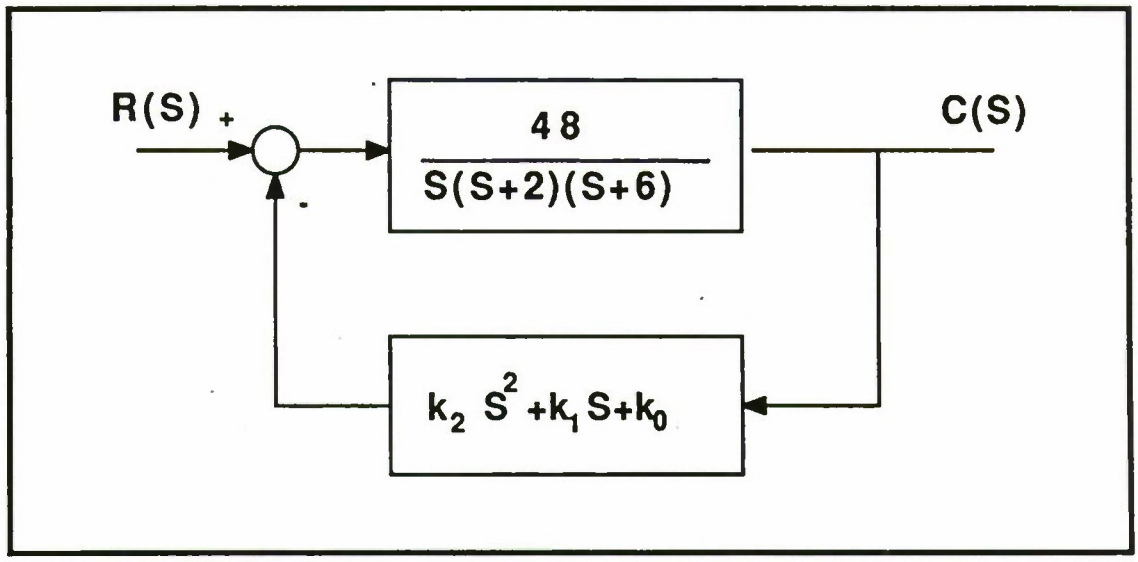

Figure 3.1: Block Diagram of Compensated Third-Order System

time period, its percent overshoot of the steady-state value increased; this caused a corresponding increase in error. Following this theory, one might assume that there was a minimization point where the conflict between settling time and total error was resolved; consequently, the system would converge to an optimum value. In practice, this optimum value was never reached. Using full-state feedback with all gains variable, minimization using the integral of time multiplied by the absolute value of the error could not be accomplished. The explanation of this phenomena was that although settling time and error were in conflict, a substantial increase in gain caused a decrease in settling time; consequently, the value of the cost index could always be reduced by increasing the gain of the system. The increase in the magnitude of the error caused by the increase in gain was not enough to offset the reduction in the settling time. At any operating point, the value of the cost function could be reduced by simply increasing the gain of the zero-order derivative.

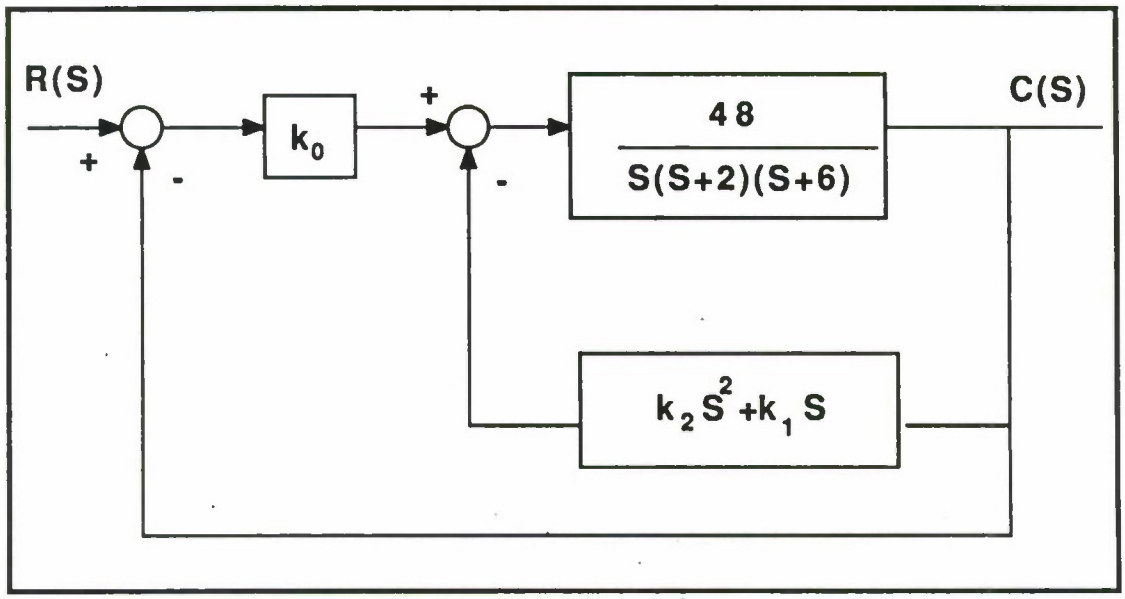

Figure 3.2: Block Diagram of Compensated System with Unity Feedback

Effectively, the resonant frequency of the system was being increased. In polynomial form, the plant transfer function is given by Equation 3.2.

$$G_p(S) = \frac{48}{S(S^2 + 8S + 12)} \tag{3.2}$$

This implied a resonant frequency of $\sqrt{48}$ or 6.93. After full-state-feedback compensation, the closed-loop transfer function is given by Equation 3.3.

$$\frac{C(S)}{R(S)} = \frac{48k_0}{S^3 + (8 + 48k_2)S^2 + (12 + 48k_1)S + 48k_0} \tag{3.3}$$

In this form, it was seen that the resonant frequency was now a function of the zero-order derivative, k_0. In this case, the resonant frequency was $\sqrt[3]{48k_0}$. Clearly, as k_0 increased, the resonant frequency increased. The result was a substantial and unrealistic increase in the bandwidth of the system.

These relationships were discovered by examining the results of a partial optimization of various third-order systems. The results are presented in Tables 3.1 and

3.2. Using Equation 2.2 with a gain of 48.0, the pole at S = -6.0 was varied between -0.01 and -1000.0 in order to ascertain the pole's effect on the value of the cost index. From Table 3.1, it could be seen that a partial minimization always resulted in an unusually high value for the k_0 term and no definite pole pattern; furthermore, the cost function remained short of minimization. Realizing that k_0 was, in effect, a forward gain, the plant of Equation 2.2 was studied using various values for the plant gain. The results of this constant-pole, variable-gain minimization are presented in Table 3.2. Rather than attempt a complete minimization, which had henceforth proved unfruitful, a partial minimization was conducted to bring the cost index to an arbitrary value of approximately 0.002. From Table 3.2, it can be seen that as the plant gain was raised to higher values, the k_0 term compensated by lowering its value; correspondingly, as the plant gain was lowered, the k_0 term compensated by raising its value. No definite pole pattern was discovered. The trend in the k_0 term indicated that the minimization was responding to changes in the plant gain which was, in effect, a changing of the bandwidth. To maintain the cost function at a predetermined figure, the k_0 maintained an inverse relationship to the value of the plant gain.

TABLE 3.1: Partial Minimization of Third-Order System with Constant Gain and Varying Pole Locations

PLANT	COST	FEEDBACK GAINS		ROOTS	
$\frac{48}{S(S+2)(S+.01)}$	0.00250	$k_2 =$	8.69	-125.2	$+ j196.8$
		$k_1 =$	2,010.00	-125.2	$- j196.8$
		$k_0 =$	191,000.00	-168.0	
$\frac{48}{S(S+2)(S+1)}$	0.00257	$k_2 =$	2.37	-25.4	$+ j61.1$
		$k_1 =$	161.00	-25.4	$- j61.1$
		$k_0 =$	6,020.00	-66.0	
$\frac{48}{S(S+2)(S+5)}$	0.00255	$k_2 =$	2.52	-29.0	$+ j61.6$
		$k_1 =$	181.00	-29.0	$- j61.6$
		$k_0 =$	6,760.00	-69.9	
$\frac{48}{S(S+2)(S+6)}$	0.00259	$k_2 =$	2.04	-22.4	$+ j61.3$
		$k_1 =$	145.00	-22.4	$- j61.3$
		$k_0 =$	5,410.00	-60.9	
$\frac{48}{S(S+2)(S+10)}$	0.00254	$k_2 =$	2.31	-27.1	$+ j61.2$
		$k_1 =$	171.00	-27.1	$- j61.2$
		$k_0 =$	6,420.00	-68.71	
$\frac{48}{S(S+2)(S+100)}$	0.00254	$k_2 =$	1.79	-47.3	$+ j64.9$
		$k_1 =$	314.00	-47.3	$- j64.9$
		$k_0 =$	12,500.00	-93.2	
$\frac{48}{S(S+2)(S+1000)}$	0.00254	$k_2 =$	8.93	-54.7	$+ j49.1$
		$k_1 =$	308.00	-54.7	$- j49.1$
		$k_0 =$	149,000.00	-1,321.0	

TABLE 3.2: Partial Minimization of $\frac{k}{s(s+2)(s+6)}$ With Varying Gains

PLANT GAIN	COST	FEEDBACK GAINS		ROOTS	
1.2	0.00277	$k_2 =$	91.70	-29.1	$+ j64.2$
		$k_1 =$	7,040.00	-29.2	$- j64.2$
		$k_0 =$	247,000.00	-59.0	
12.0	0.00259	$k_2 =$	10.00	-30.2	$+ j62.4$
		$k_1 =$	743.00	-30.2	$- j62.4$
		$k_0 =$	27,400.00	-68.0	
48.0	0.00259	$k_2 =$	2.04	-22.38	$+ j61.3$
		$k_1 =$	145.00	-22.38	$- j61.3$
		$k_0 =$	5,410.00	-60.9	
96.0	0.00256	$k_2 =$	1.73	-52.9	$+ j85.6$
		$k_1 =$	181.00	-52.9	$- j85.6$
		$k_0 =$	7,230.00	-68.6	
600.0	0.00251	$k_2 =$	1.85	-90.8	$+ j55.9$
		$k_1 =$	155.00	-90.8	$- j55.9$
		$k_0 =$	6,930.00	-306.0	
1,200.0	0.00250	$k_2 =$	0.70	-76.7	$+ j52.6$
		$k_1 =$	95.70	-76.7	$- j52.6$
		$k_0 =$	4,990.00	-691.9	
12,000.0	0.00251	$k_2 =$	0.58	-69.9	$+ j50.7$
		$k_1 =$	79.70	-69.9	$- j50.7$
		$k_0 =$	4,220.00	-6790.5	
120,000.0	0.00251	$k_2 =$	0.53	-69.1	$+ j50.2$
		$k_1 =$	73.70	-69.1	$- j50.2$
		$k_0 =$	3,840.00	-63,900.0	

To prove the failure of the cost index to minimize the system in the absence of a set bandwidth, several complete minimizations were attempted. None of these were successful. As an example, the transfer function of Equation 3.4

$$G_p(S) = \frac{48.0}{S(S+2.00)(S+0.01)} \tag{3.4}$$

was attempted. Minimization found feedback gains of $k_2 = 33.19$, $k_1 = 33,560.00$ and $k_0 = 110,260,000.00$ with a cost-index value of 6.25×10^{-6}. The system remained unminimized. Theoretically, the system could only be minimized for k_0 equal to infinity. The resonant frequency of the uncompensated plant was 6.93 radians/second. Using full-state feedback with partial minimization, the characteristic equation became

$$S^3 + (1.6 \times 10^3)s^2 + (1.61 \times 10^6)S + 5.29 \times 10^9 = 0 \ . \tag{3.5}$$

This equation implied a resonant frequency of 1,742.69 radians/second. The increase was, obviously, unrealistic.

B. FIXING THE BANDWIDTH

In the previous section, the problem of an ever-increasing natural frequency was presented. This problem was encountered because of the nature of the compensation used. The zero-order derivative had the effect of a forward gain in the system, thereby limiting the ability to optimize the system using the integral of time multiplied by the absolute value of the error. In this section, the compensation scheme was adjusted to alleviate this problem. In the next section, the effects of a nonlinear system was investigated.

The general form of the characteristic equation for a third-order system is given in Equation 3.6, where ω_0 is a selected frequency commonly used to

$$S^3 + A\omega_0 S^2 + B\omega_0^2 S + \omega_0^3 = 0 \tag{3.6}$$

approximate the natural frequency; A and B are constants. Throughout the remainder of the study, ω_0 was referred to as the natural or resonant frequency. Though this equality actually only held true for second-order systems, ω_0 was proportional to the natural frequency for higher-order systems. The equation of the closed-loop transfer function of a system using full-state feedback compensation is given in Equation 3.7,

$$G_p(S) = \frac{(G)(k_0)}{S^3 + (A + Gk_2)S^2 + (B + Gk_1)S + Gk_0} \tag{3.7}$$

where G is the gain of the uncompensated plant and all other variables are as previously defined. Equating terms of Equations 3.6 and 3.7, the value of ω_0 was

$$\omega_0 = \sqrt[3]{Gk_0} \ . \tag{3.8}$$

Since the gain, G, was presumed to be a fixed parameter, the k_0 term could be adjusted to provide the desired natural or resonant frequency. Notice that this now fixed k_0 to a constant value and left the designer with $N - 1$ gains with which to adjust the optimal response.

For the third-order system under study, the gain was 48.0. The resonant frequency was approximated by ω_0 and set at 10.0 radians/second; therefore, the k_0 term was set at 20.83. The block diagram of the compensated system with the resonant frequency fixed at a value of 10.0 radians/second is given in Figure 3.3.

This system was optimized using the integral of time multiplied by the absolute value of the error. Unlike the results obtained in the absence of a fixed resonant frequency, the cost index of this system possessed an absolute minimum of 3.1386×10^{-2}. It was important to note that the value of the cost function, by itself, had no real meaning. It served as only a benchmark against which other similar systems could be compared. Its numerical value was dependent on the integration method used, the duration of the minimization effort, and other procedural techniques. It

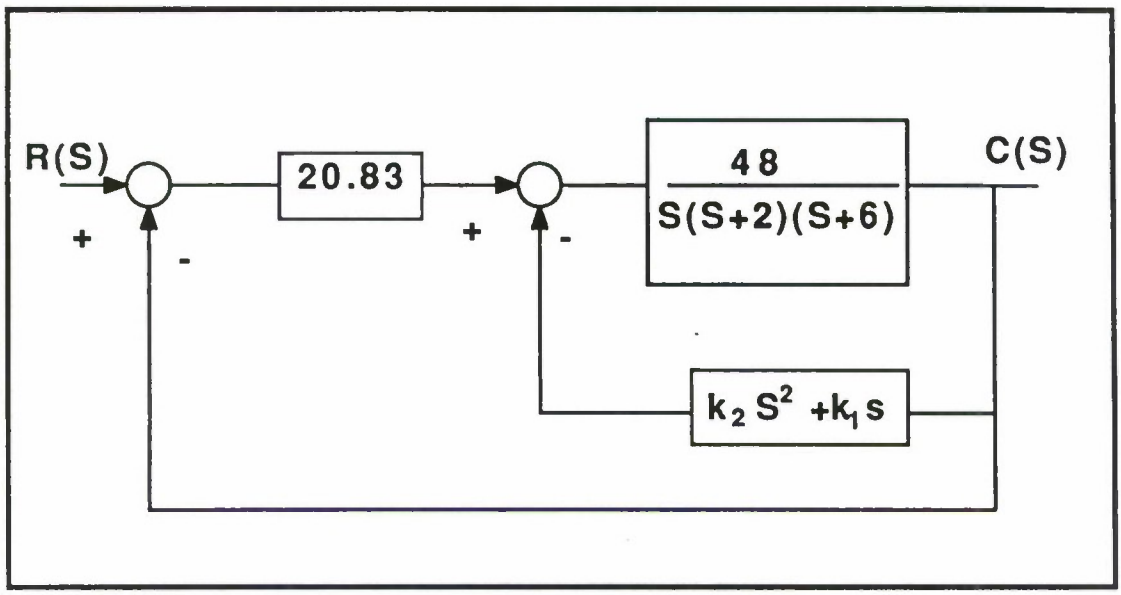

Figure 3.3: Block Diagram of Compensated System with Resonant Frequency Set At $\omega_o = 10.0$

was, therefore, critical to maintain a constant methodology in the minimization effort.

Desiring to compare the results obtained with a set resonant frequency with those obtained when the resonant frequency was variable, the study described in Chapter III, Section A was repeated. The pole located at $S = -6.0$ was varied in order to determine its effect on the optimal solution. In this case, the pole was varied between -1.0 and -1000.0. The results are presented in Table 3.3.

TABLE 3.3: Minimization of Third-Order System with Constant Gain, Constant Resonant Frequency, and Varying Pole Locations

UNCOMPENSATED PLANT	COST	FEEDBACK GAINS	GRAHAM AND LATHROP PREDICTED GAINS	ROOT LOCATIONS
$\frac{48}{S(S+2)(S+1)}$	3.1380×10^{-2}	$k_1 = 4.48$ $k_2 = 0.31$	$k_1 = 4.44$ $k_2 = 0.30$	-5.37 $\pm j$10.60 -7.07
$\frac{48}{S(S+2)(S+6)}$	3.1386×10^{-2}	$k_1 = 4.28$ $k_2 = 0.21$	$k_1 = 4.23$ $k_2 = 0.20$	-5.40 $\pm j$10.50 -7.07
$\frac{48}{S(S+2)(S+10)}$	3.1382×10^{-2}	$k_1 = 4.11$ $k_2 = 0.12$	$k_1 = 4.06$ $k_2 = 0.12$	-5.37 $\pm j$10.50 -7.08
$\frac{48}{S(S+2)(S+100)}$	3.1265×10^{-2}	$k_1 = 0.34$ $k_2 = -1.76$	$k_1 = 0.31$ $k_2 = -1.76$	-5.31 $\pm j$10.65 -7.04
$\frac{48}{S(S+2)(S+1000)}$	2.9625×10^{-1}	$k_1 = -37.26$ $k_2 = -20.51$	$k_1 = -37.19$ $k_2 = -20.51$	-5.12 $\pm j$10.53 -7.28

By examination of the table, it was seen that the value of the cost index remained, essentially, constant; moreover, the roots of the characteristic equation remained fixed. It was noted that the feedback gains steadily decreased in magnitude as the plant pole location was increased from -1.0 to -1000.0. These results were in congruence with control theory. The roots of the denominator polynomial of the closed-loop transfer function determined the transient characteristics of the system. Using the integral of time multiplied by the absolute value of the error, there was only one root pattern which provided the optimal response. Since the use of full-state feedback assumed that the roots of the system could be placed at any location, the feedback gains adjusted themselves to attain the optimum root pattern of $-5.0 \pm j10.0$ and -7.0. As the pole location moved farther into the left-half plane, its effect on the system's response became negligible; accordingly, the need for high feedback gains was reduced. The gains steadily decreased and, at the pole location of $S = -100.0$, actually became positive feedback.

To illustrate the standard optimal response, the step response of the system was conducted for pole locations at the extremes of $S = -1.0$ and $S = -100.0$. These responses, as shown in Figures 3.4 and 3.5, were almost identical. From another point of view, the error, cost, and control versus time are plotted in Figures 3.6 and 3.7. As viewed from this perspective, the transient dynamics again showed identical characteristics. Figure 3.8 is a plot of the root locations for the systems optimized in Table 3.3. This root pattern remained constant for all third-order systems optimized with this cost index. The radial distance of these roots from the origin was a function of the chosen natural frequency. As the natural frequency was increased, the pattern moved further into the left-half plane; likewise, if the frequency was decreased, the roots moved toward the right-half plane. The roots, of course, never crossed into the right-half plane.

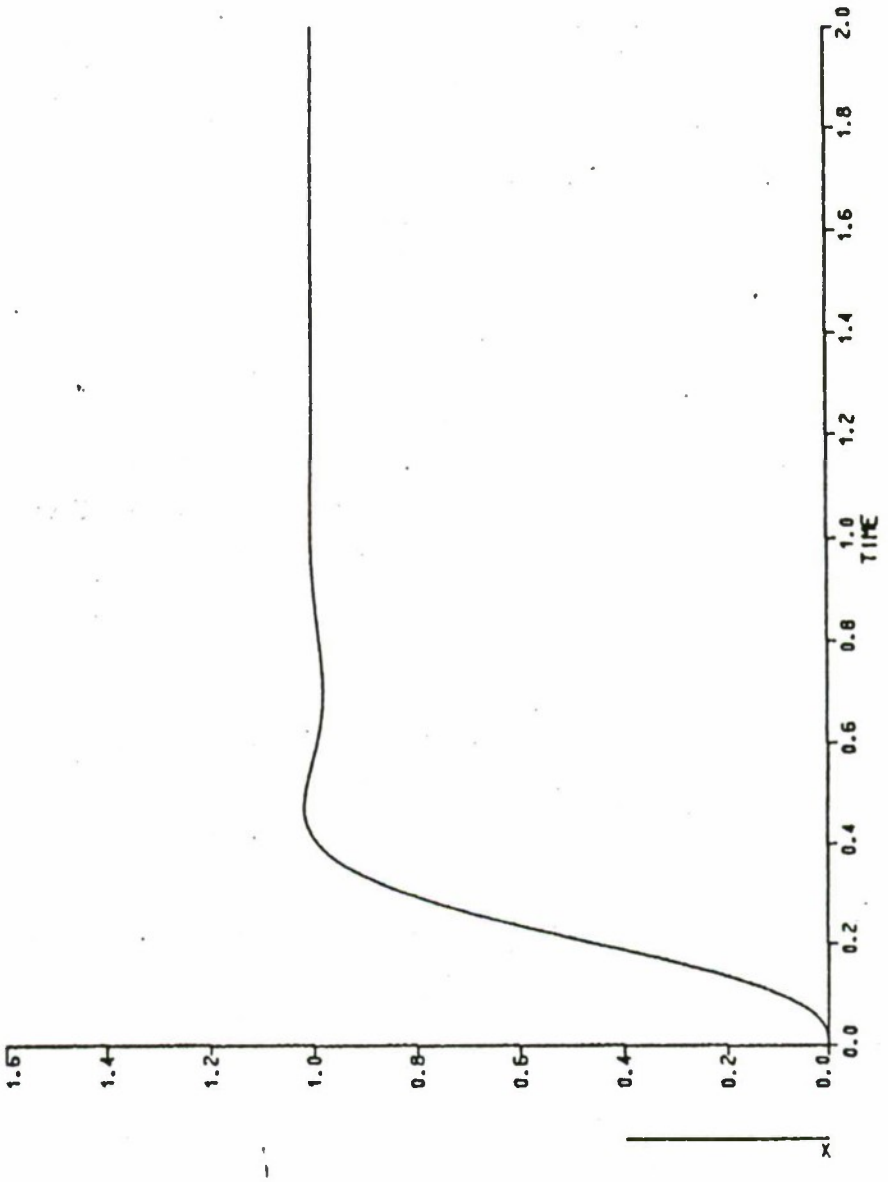

Figure 3.4: Step Response of Minimized Third-Order System with Pole at S=-1.0

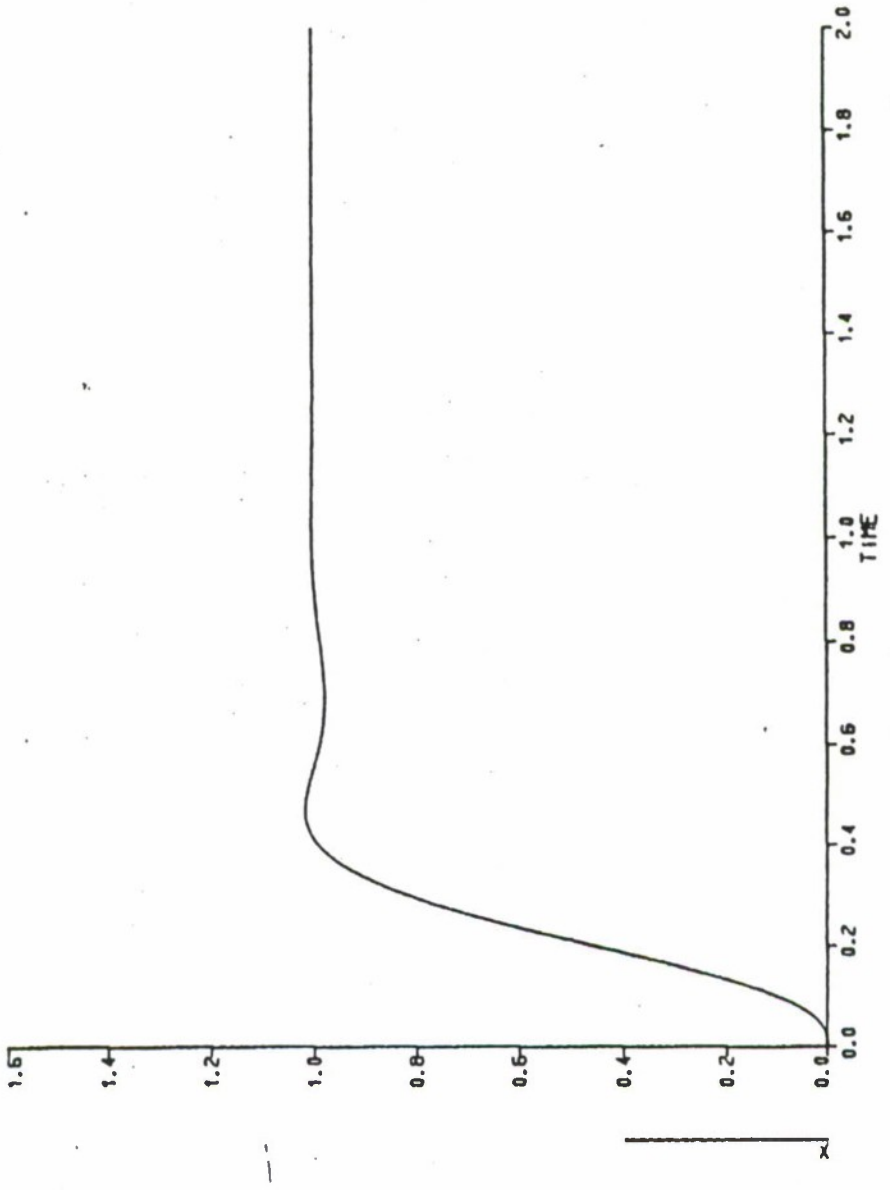

Figure 3.5: Step Response of Minimized Third-Order System with Pole at S=-100.0

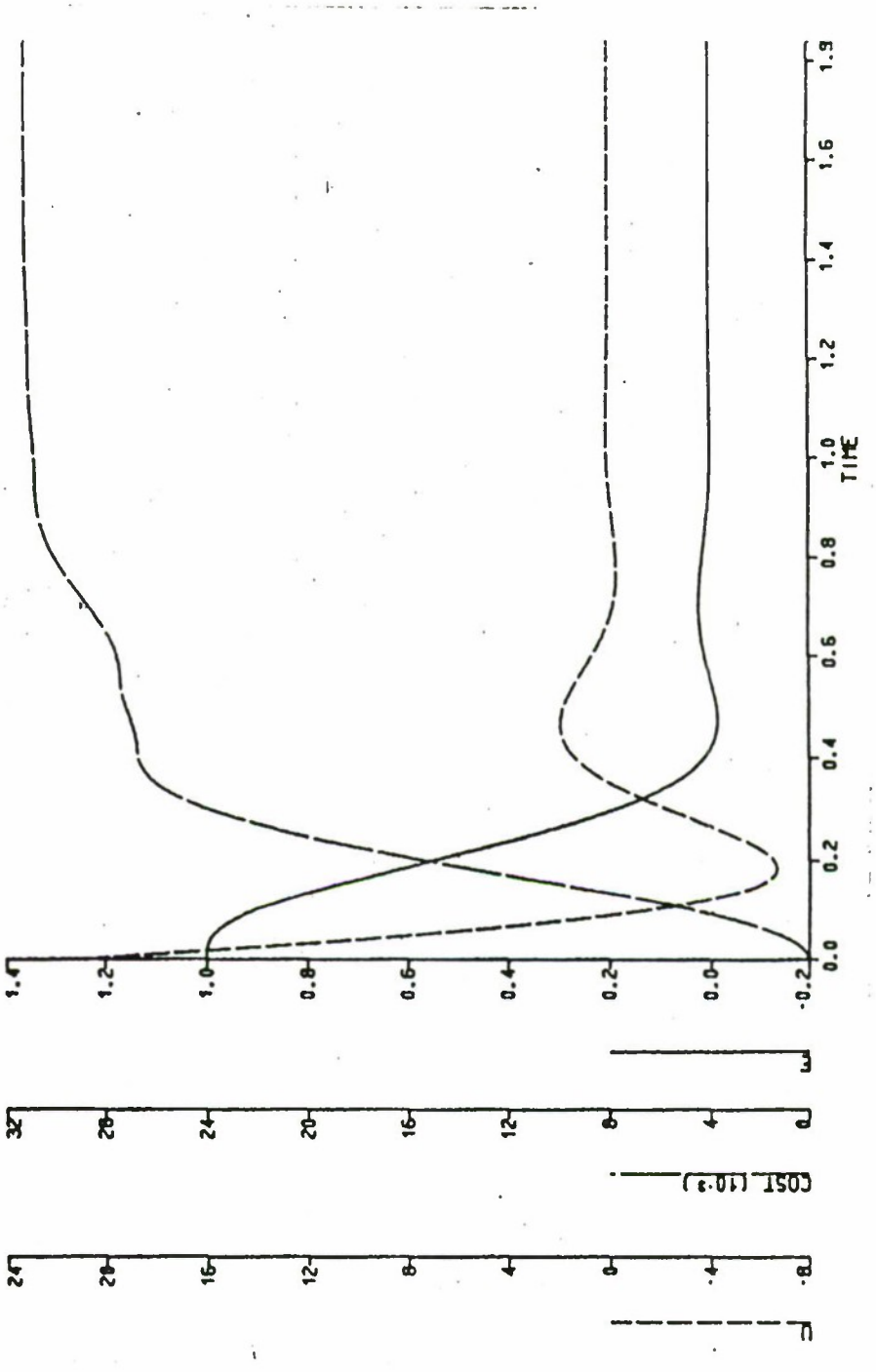

Figure 3.6: Plot of Error, Cost, and Control Versus Time for Third-Order System with Pole at S=-1.0

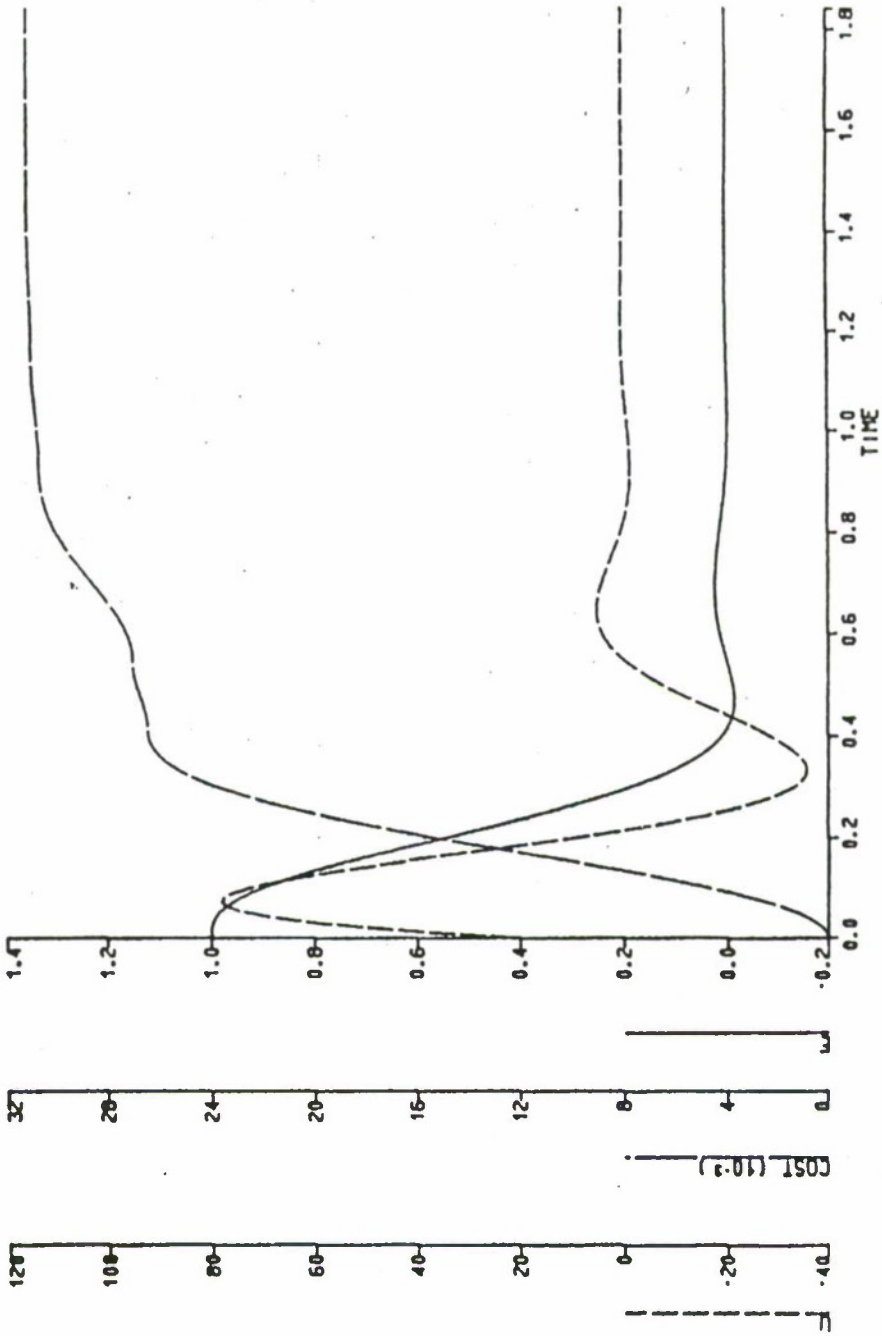

Figure 3.7: Plot of Error, Cost, and Control Versus Time for Third-Order System with Pole at S=-100.0

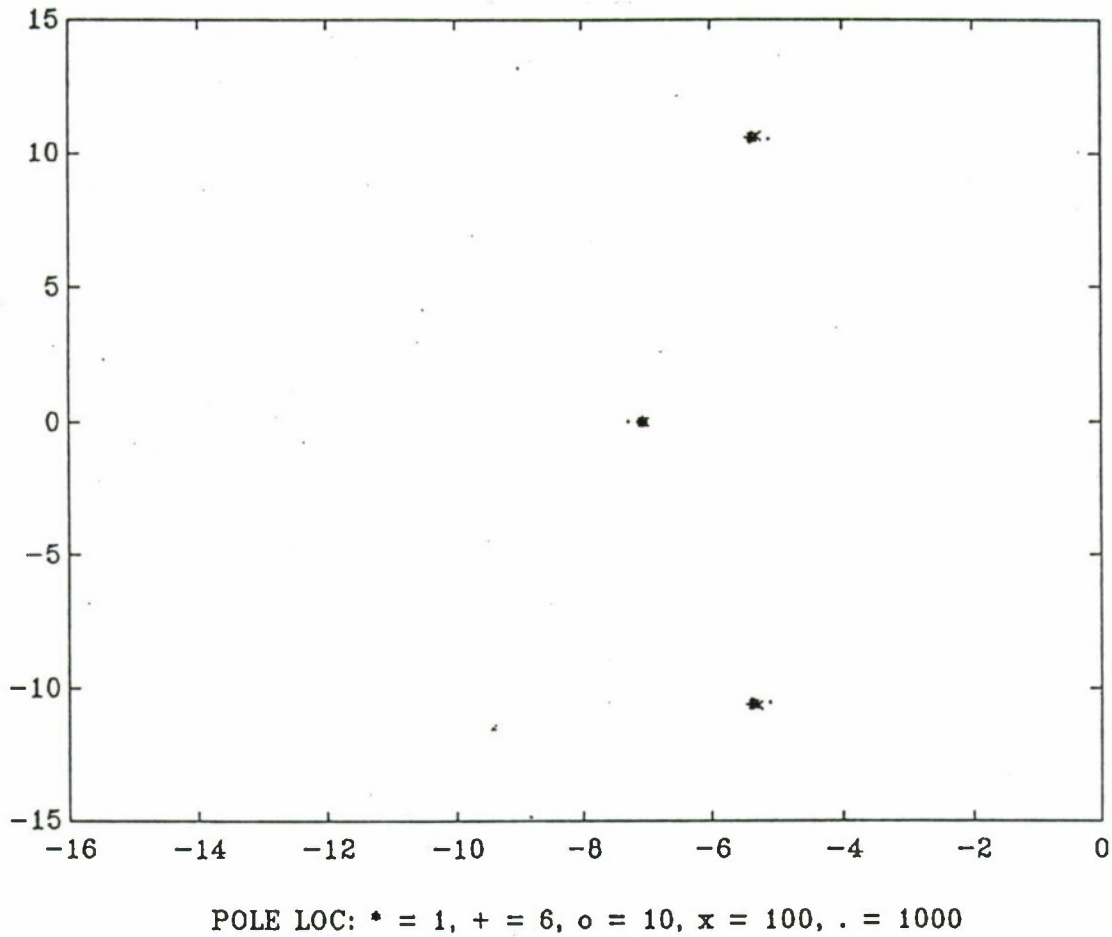

Figure 3.8: Plot of Root Locations for Third-Order System with Varying Pole Locations

It was of interest to compare these results with those produced by the Graham and Lathrop standard forms as presented in Table 2.1. For the third-order system, the standard form was given as

$$S^3 + 1.75\omega_o S^2 + 2.15\omega_o^2 S + \omega_o^3 \ . \tag{3.9}$$

From Equation 3.6, the characteristic equation of the compensated system was

$$S^3 + (A + Gk_2)S^2 + (B + Gk_1)S + Gk_0 \ . \tag{3.10}$$

Given an ω_o equal to 10.0 radians/seconds, it was possible to simply solve for the feedback gains. As an example, the uncompensated plant of Equation 3.2 was considered. The value of A was 8.0, the value of B was 12.0, and the value of G was 48.0. Equating the coefficients of Equations 3.8 and 3.9 resulted in

$$8 + 48(k_2) = 1.75(10) \tag{3.11}$$

and

$$12 + 48(k_1) = (2.15)(10)^2 \ . \tag{3.12}$$

Solving for the feedback gains, Graham and Lathrop predicted $k_2 = 0.198$ and $k_1 = 4.230$. This procedure was repeated for the various pole locations studied, and the results are presented in the data of Table 3.3. Graham and Lathrop's calculations proved, at least for the third-order system, to be correct within one-hundredth of the actual value. This topic is examined in more detail later in the study.

All of the results found with the third-order system were generalized to higher-order systems, i.e., all systems have a definite pole pattern which minimizes the cost index. If the system parameters change, resulting in a change of pole locations within the plant, the state feedback gains adjust themselves to return the roots to their optimal locations. An increase in ω_0 causes a shift of the pole pattern to the left, and a decrease in ω_0 causes the pattern to shift to the right.

C. THE EFFECTS OF NONLINEARITIES

Up to this point, only linear systems or those that could be approximated as linear systems were considered. Because of the relative simplicity and straightforwardness of such systems, much insight was gained as to the dynamics of linear systems designed by the use of the cost index; however, linear systems never truly exist in practice. All physical systems are nonlinear to some extent. Linear feedback control systems are idealized models that are fabricated by the analyst purely for the ease of design. When the magnitude of the signals in a control system is limited to a range in which system components exhibit linear characteristics, the system is essentially linear. These linear characteristics are usually tested through the principle of superposition. If superposition applies, the system is linear. When the magnitude of the signals are extended beyond the range of linear operation, the system can no longer be considered linear. Quite often, nonlinear characteristics are intentionally introduced in a control system to improve its performance or provide more effective control. An on-off (bang-bang) type of controller is often used to achieve minimum-time control. This type of control is found in many missile or spacecraft control systems. In the altitude control of missiles, jets are mounted on the sides of the vehicle to provide reaction torque. These jets are controlled in a full-on or full-off fashion.

Nonlinearities can be continuous or discontinuous. Continuous nonlinearities are, as their name implies, present for the duration of the system's function. The relationship between an applied force and the resulting deformation of a spring is considered to be a continuous nonlinearity. The second type of nonlinearity is the discontinuous nonlinearity. Up to a certain size input, the output is directly proportional; but, for greater or smaller inputs, the output remains constant. It

was with discontinuous nonlinearities that this study was concerned. Henceforth, the term nonlinearity refers to those of a discontinuous nature.

Several forms of nonlinearities are very often encountered. These nonlinearities are frequently referred to as fast nonlinearities, which implies that their range of operation changes at a fast rate compared to the response time of the system. [Ref. 4:p. 601] The most common of these fast nonlinearities are dead zone, backlash or hysteresis, and saturation or limiting. A dead zone is a range of input for which there is no output. Backlash is most commonly associated with the dead play between coupled gear members. This study, however, dealt solely with the nonlinearity of saturation. Many components are linear up to a given input signal. For larger signals, the output may not be proportional to the input or may even be limited to some constant value. Although the transition between this linear and nonlinear region may be gradual, the transfer characteristic is often represented by straight line segments. The system is then said to be piecewise linear. [Ref. 4:pp. 600-603] Figure 3.9 shows the ideal saturation curve that was used in this study.

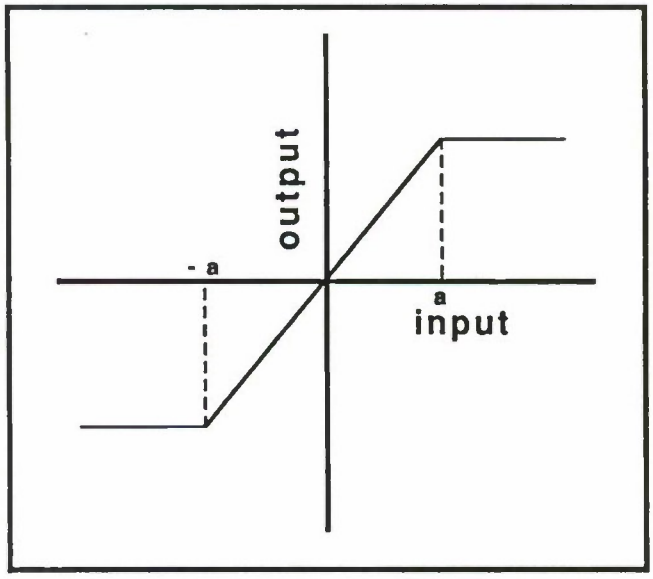

Figure 3.9: Ideal Saturation Curve

For linear systems, there are a large number of analytical and graphical techniques for design and analysis; however, nonlinear systems are very difficult to treat mathematically, and there are no general methods that may be used to solve a wide class of nonlinear systems. The treatment of nonlinearities in this study attempted only to be illustrative and, most certainly, not exhaustive. It dealt only with the effects of saturation on all-pole systems which were optimized using either Equation 2.4 or Equation 2.6.

The effect of the nonlinearity depends on its position within the system. Saturation effects are, normally, present in one of two areas, at the input into the plant or at the input into the system. The most common of these is at the input into the plant where it limits the amount of control input used. Referring to Figure 3.10, saturation points 1 and 2 respectively depict the relative position of system and plant saturation.

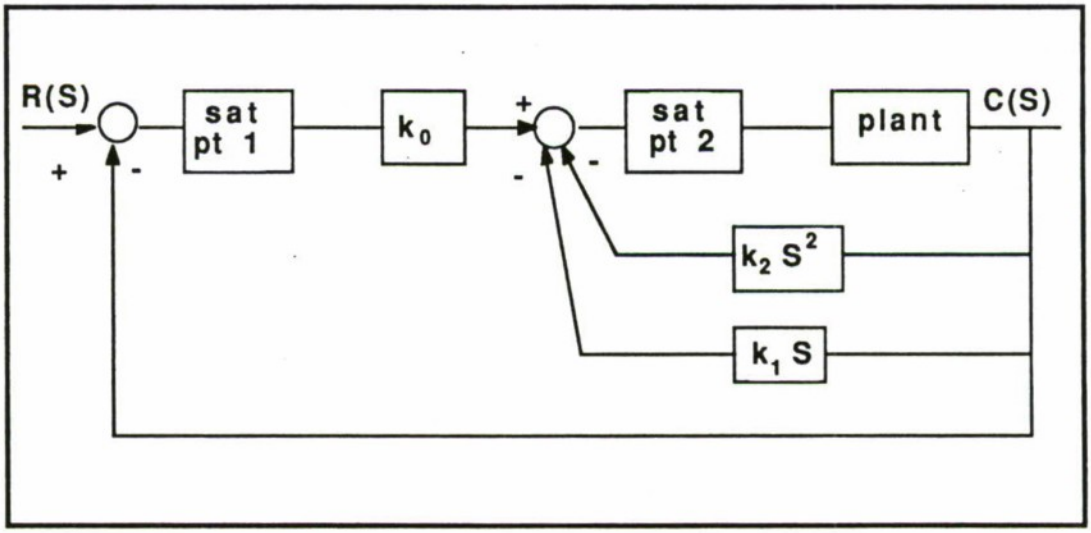

Figure 3.10: Block Diagram Showing Points of Possible Saturation

Saturation point 2 effectively limits the control to the plant. This point could represent an amplifier with specific saturation limits, or a motor whose magnetic field has saturation properties. To study the effects of this type of saturation, the piecewise-linear saturation curve of Figure 3.9 was used with upper and lower saturation limits of 30.0 and -30.0. The plant of Equation 3.2 was used and compensated with full-state feedback. A block diagram of the system is shown in Figure 3.11.

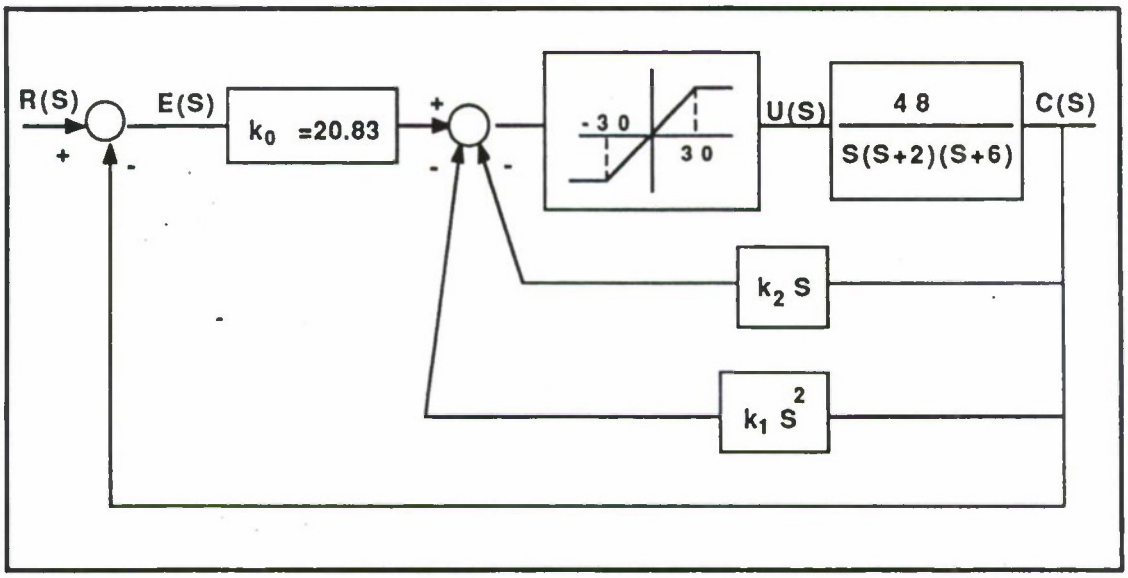

Figure 3.11: System with Nonlinearity Present

As before, the resonant frequency was set to 10.0 radians/second by fixing the value of the zero-derivative feedback gain at 20.83.

The objective of this investigation was to evaluate the performance of the given cost index in the presence of nonlinearities. The approach used was to first set the feedback gains at the value obtained through the optimization of the linear system. The system was then simulated for various amplitudes of step input, and

the value of the cost index recorded. The saturation nonlinearity was then inserted into the system at saturation point 2 in Figure 3.10. Using the same "linear" feedback gains and step inputs, the system was, again, simulated and the value of the cost index recorded. Finally, the minimization process was repeated with the nonlinearity present. New optimal feedback gains were determined and used in a third simulation of the system. The resulting values for this three-part procedure are presented in Table 3.4.

TABLE 3.4: Comparison of Cost Index in the Presence of Nonlinearity at Point 2

STEP SIZE	NONLINEAR OPTIMAL GAINS	COST OF LINEAR SYSTEM WITH LINEAR OPTIMAL GAINS	COST OF NONLINEAR SYSTEM WITH LINEAR OPTIMAL GAINS	COST OF NONLINEAR SYSTEM WITH NONLINEAR OPTIMAL GAINS
1.0	$k_0 = 20.830$ $k_1 = 4.281$ $k_2 = 0.205$	0.031	0.031	0.031
1.5	$k_0 = 20.830$ $k_1 = 4.382$ $k_2 = 0.206$	0.047	0.640	0.680
10.0	$k_0 = 20.830$ $k_1 = 4.382$ $k_2 = 0.206$	0.314	0.690	0.680
20.0	$k_0 = 20.830$ $k_1 = 4.842$ $k_2 = 0.265$	0.628	2.510	2.270
50.0	$k_0 = 20.830$ $k_1 = 5.483$ $k_2 = 0.269$	1.569	14.510	12.600
100.0	$k_0 = 20.830$ $k_1 = 5.812$ $k_2 = 0.271$	3.139	55.580	51.230

At a step input of 1.0, the initial input into the nonlinearity was 1.0 multiplied by the k_0 term. Refer to Figure 3.11. This input was well below that needed to reach the nonlinear region of saturation and had no effect on the dynamic response of the system. The cost index and optimal gains remained unchanged. As the step input was raised to the point where the step input multiplied by k_0 exceeded the saturation value of 30.0, nonlinear effects deteriorated the system's performance. Due to the nonlinearity remaining in saturation for longer periods of time, the effects of larger step inputs were more dramatic than those of smaller step sizes. In general, the presence of the nonlinearity caused a decrease in the system's damping. The decreased damping resulted in a larger overshoot of the final value and a longer transient period; however, the general shape of the response remained constant. The system maintained one overshoot and one undershoot. The change in the damping had dramatic effects on the relative values of the cost index. Even with input steps causing only minor amounts of saturation, the cost index doubled from that of a linear system. For larger step inputs, cost indexes of at least an order of magnitude higher than its linear counterpart were common. This result was to be expected. During the optimization of the linear system, the cost index penalized long duration errors and adjusted the feedback gains to provide as fast a system as possible. The introduction of the nonlinearity initially limited the control input to 30.0, and resulted in a slower system.

Although the presence of the saturating element caused a large rise in the value of the cost index, it can be seen from Table 3.4 that minimization with the nonlinearity inserted showed relatively little change. Even for large amounts of saturation, the cost function was only reduced by a few units. In congruence with this was the fact that the nonlinear optimal gains changed very little from the linear optimal gains. Each feedback gain increased in value proportional to the increase

in the step input with the higher-order feedback gains increasing at a faster rate than those of lower orders. In terms of the transient response, this had the effect of increasing the damping coefficient by moving the dominant complex roots farther into the left half of the complex plane. This resulted in less overshoot and a smoother transient response. To illustrate this phenomena, the step responses for the extreme case of saturation caused by a step input of 50.0 are given in Figures 3.12, 3.13, and 3.14. Figure 3.12 shows the typical step response obtained with the use of this cost index. This illustration is for linear optimal gains with a linear system. Figure 3.13 shows the effects of using linear optimal gains with a nonlinear system. Note the increase in the settling time and maximum percent overshoot. Figure 3.14 shows the nonlinear system with the nonlinear optimal gains. Both overshoot and transient were reduced. Due to the limit on the control input, the minimization only nominally reduced the settling time. The majority of the decrease in the cost index came from the reduction of overshoot, which resulted in less total error.

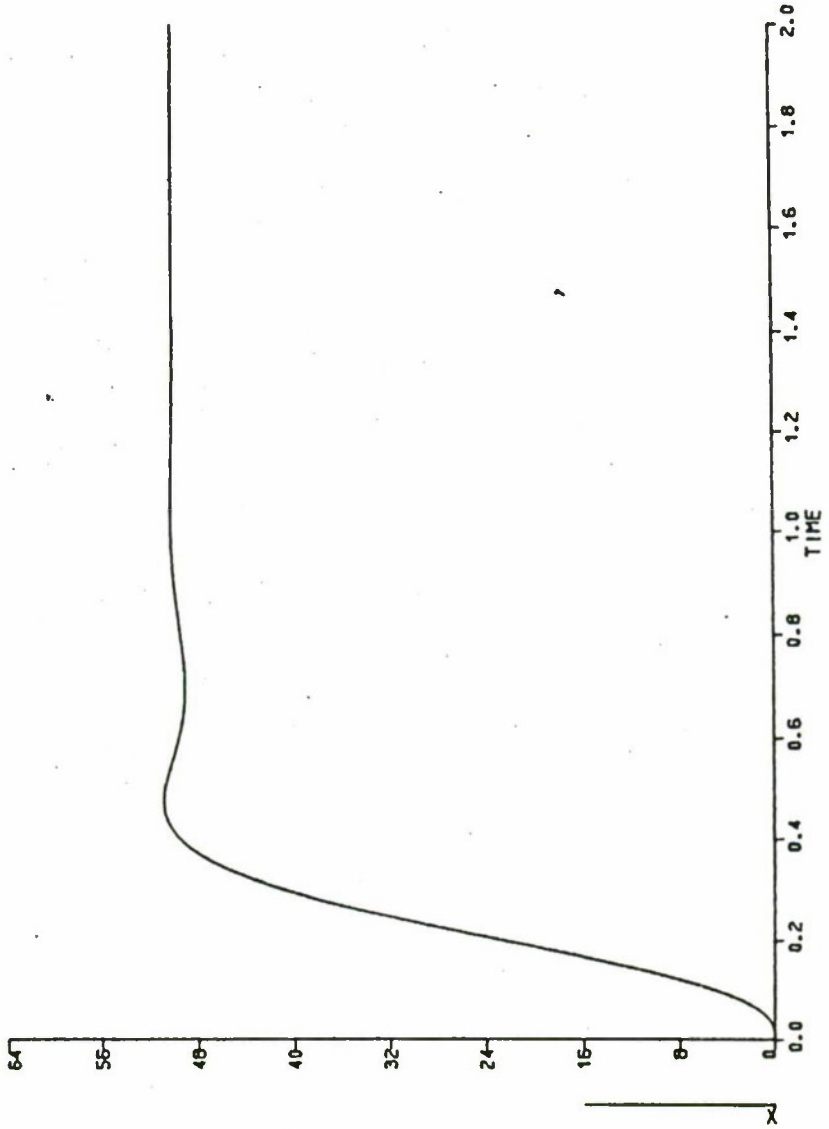

Figure 3.12: Linear Step Response, Step=50.0, X=Output

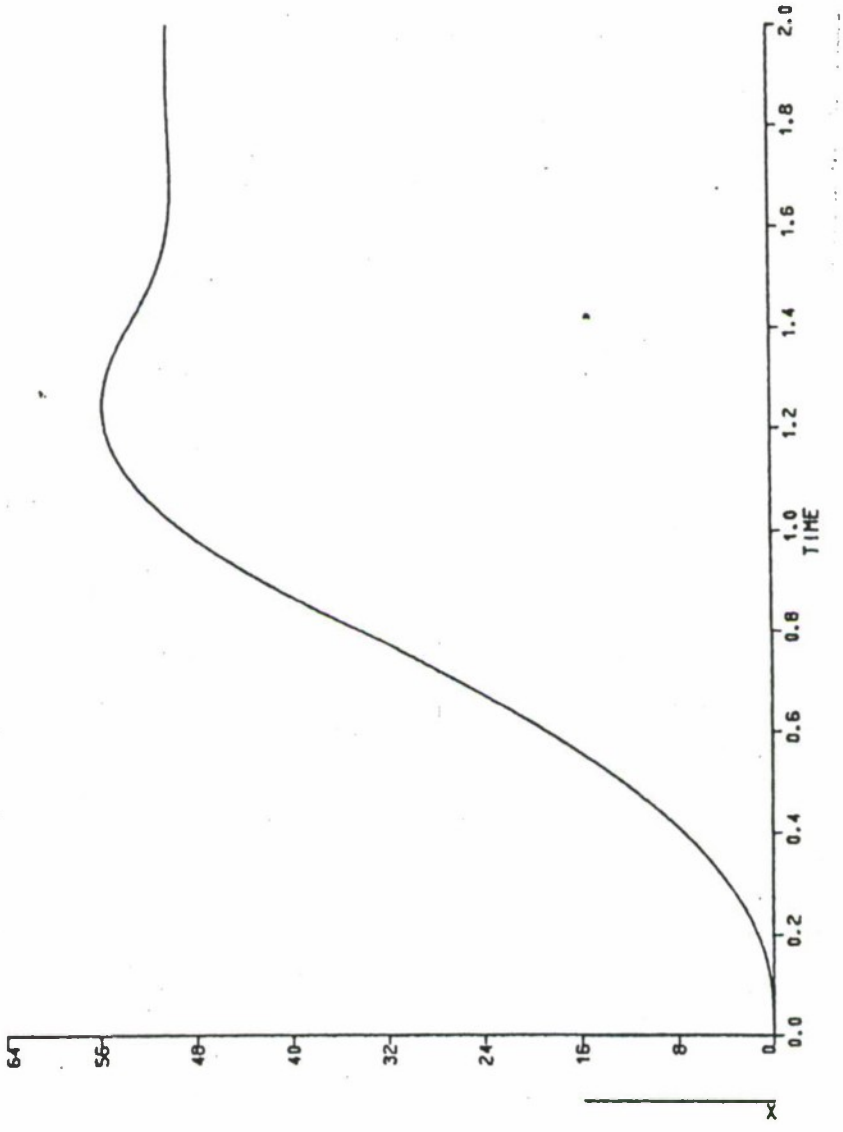

Figure 3.13: Nonlinear Step Response Using Linear Optimal Gains, Step=50.0, X=Output

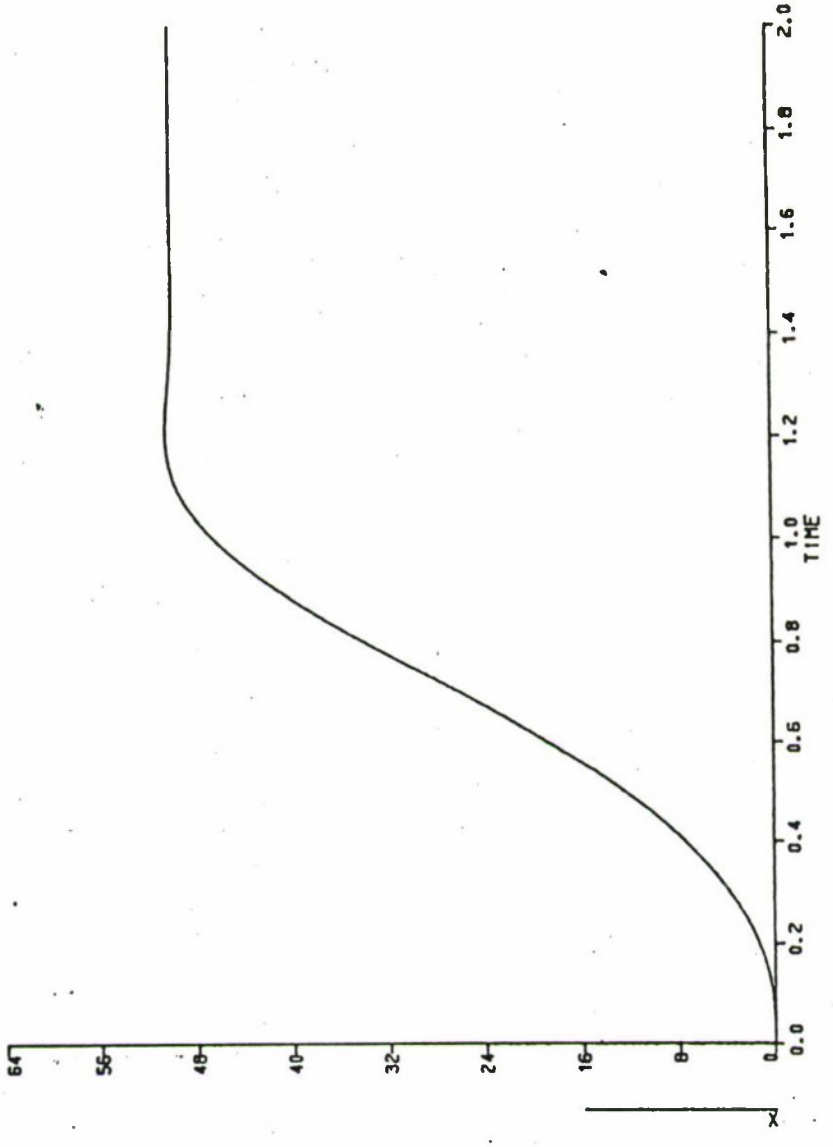

Figure 3.14: Nonlinear Step Response Using Nonlinear Optimal Gains, Step=50.0, X=Output

Perhaps a better understanding of the dynamics of the system could be gained by examining Figures 3.15, 3.16, and 3.17. These figures correspond to the systems described for Figures 3.12, 3.13, and 3.14, respectively. In these figures, the cost, control input, and error were plotted as a function of time. In the linear system of Figure 3.15, no saturation occurred. In Figure 3.16, it was clear that the control input, shown by the curve NLU, remained saturated at ± 30.0 for well over half of the transient period. After nonlinear minimization, Figure 3.17 shows that the new optimal gains reduced the total saturation time. Figure 3.18 shows the effect of the nonlinear optimal gains on the linear system. All overshoots and undershoots were eliminated.

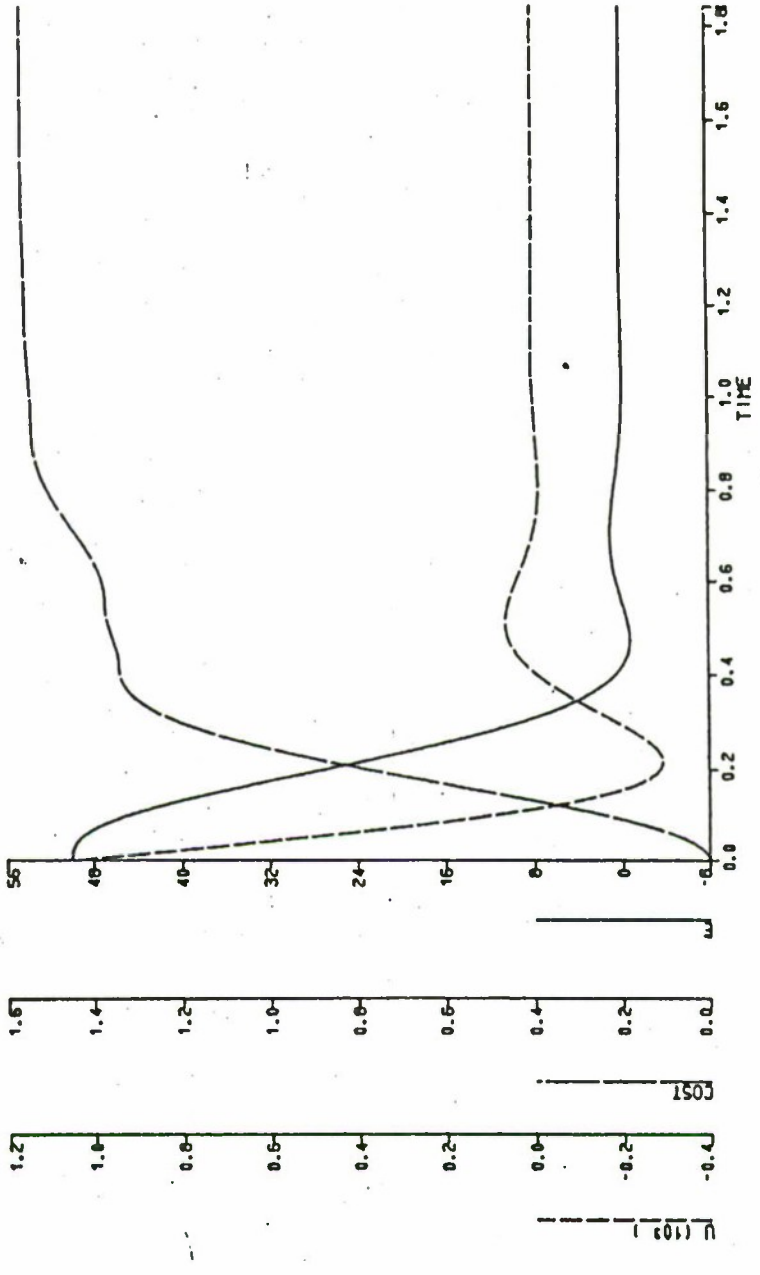

Figure 3.15: Linear System; U = Control Input, Cost = Value of Cost Index, E = Error, Step = 50.0

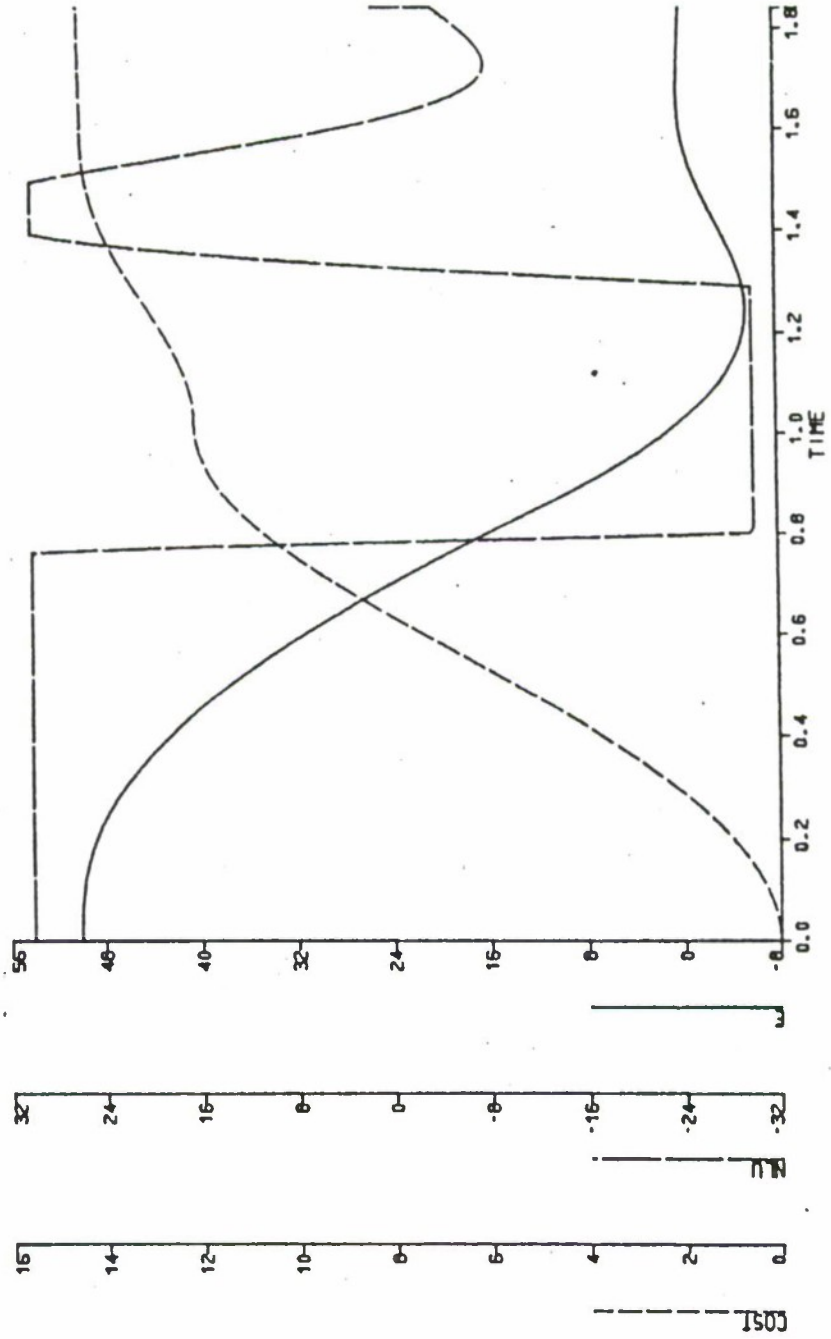

Figure 3.16: Nonlinear System with Linear Gains; NLU = Control Input, Cost = Value of Cost Index, E = Error, Step = 50.0

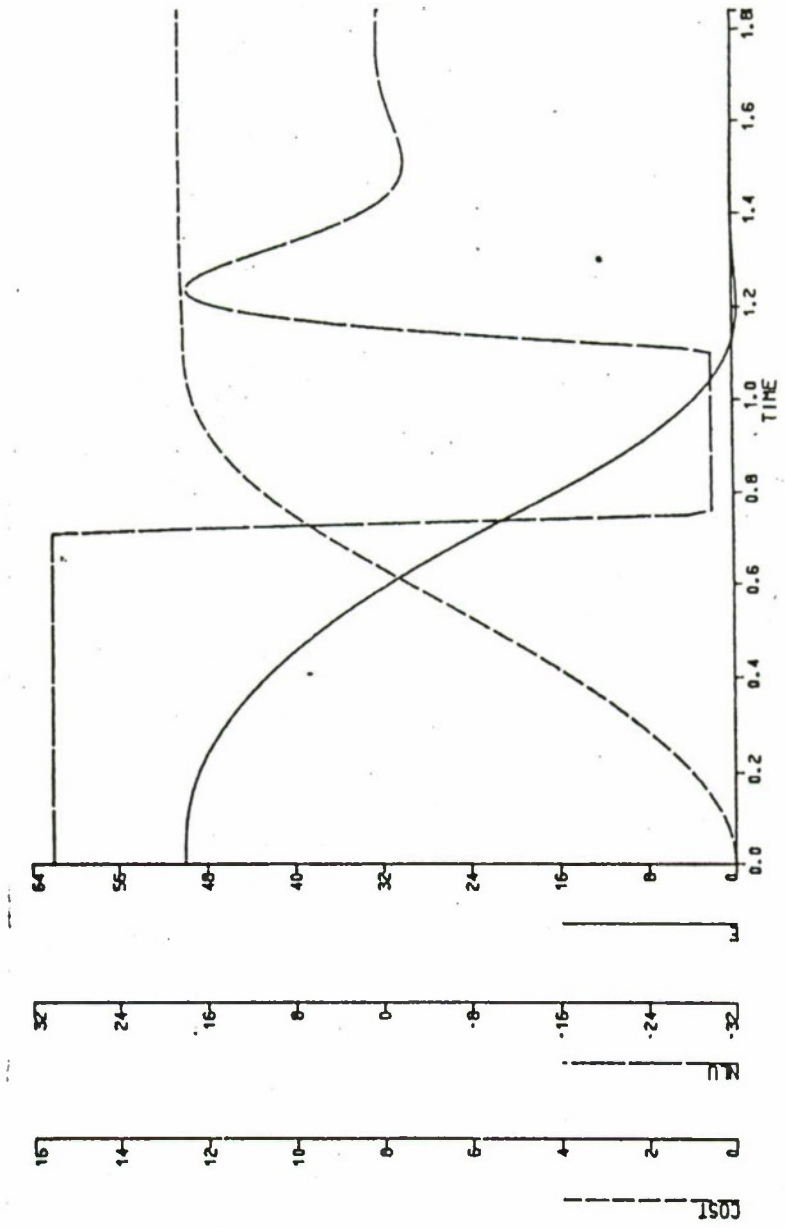

Figure 3.17: Nonlinear System with Nonlinear Gains; NLU = Control Input, Cost = Value of Cost Index, E = Error, Step = 50.0

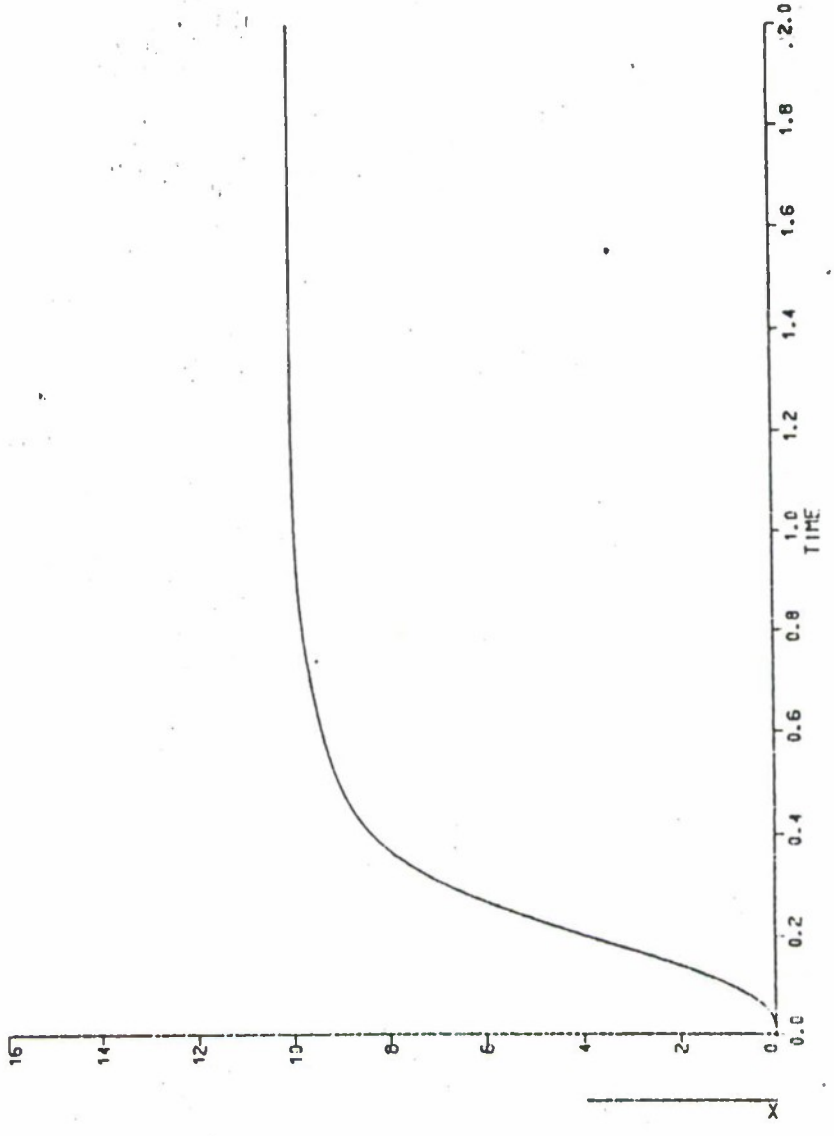

Figure 3.18: Linear System with Nonlinear Optimal Gains; Step = 50.0, X = Output

The results of this study indicated that the integral of time multiplied by the absolute value of the error remained a viable design tool in the presence of saturation. The optimal feedback gains attained through a linear minimization remained near optimal when the nonlinearity was introduced. Realizing the decreased damping brought about by the control input limit, the control systems engineer could lightly increase the feedback gains to quickly attain the desired response.

The question now arises as to the effect of moving the nonlinearity to saturation point 1 in Figure 3.10. In order to perform the simulations of this new system, the nonlinear element of Figure 3.9 was moved to saturation point 1 and the limits of saturation reset to ± 5.0. This new saturation limit was used in order that the nonlinear effects could be observed at lower step inputs. The general procedure of the simulation remained as it did for saturation point 2.

While the nonlinearity at saturation point 2 served to reduce the damping, saturation point 1 had the opposite effect. The nonlinearity at point 1 served to increase the damping of the system. The resulting values for various step inputs are presented in Table 3.5. At the step input of 5.0, the system remained in the linear region of operation and the value of the cost index and optimal gains remained constant for all simulations. As the step input exceeded the linear area of operation, increased damping effects were seen whose magnitude was dependent on the amount of saturation present. This increase in damping resulted in greatly reduced overshoot of the steady-state value and relatively little increase in the transient period. Generally, the resulting system maintained a smooth transition to its final value. As with saturation point 2, point 1 had dramatic effects on the relative values of the cost index. For an input of 5.0 units over the saturation value, the cost index approximately doubled from that of a linear system. Though there was no linear

relationship between the increase in the cost index and the value of the step input, larger step inputs caused higher values for the cost index.

TABLE 3.5: Comparison of Cost Index in the Presence of Nonlinearity at Point 1

STEP SIZE	NONLINEAR OPTIMAL GAINS	COST OF LINEAR SYSTEM WITH LINEAR OPTIMAL GAINS	COST OF NONLINEAR SYSTEM WITH LINEAR OPTIMAL GAINS	COST OF NONLINEAR SYSTEM WITH NONLINEAR OPTIMAL GAINS
5.0	$k_0 =$ 20.831 $k_1 =$ 4.280 $k_2 =$ 0.206	0.157	0.157	0.159
6.0	$k_0 =$ 20.831 $k_1 =$ 4.192 $k_2 =$ 0.195	0.188	0.209	0.208
10.0	$k_0 =$ 20.831 $k_1 =$ 3.713 $k_2 =$ 0.131	0.319	0.617	0.526
20.0	$k_0 =$ 20.831 $k_1 =$ 2.902 $k_2 =$ 0.063	0.628	3.451	2.239

Although the presence of the saturating element caused a large rise in the value of the cost index, Table 3.5 shows that minimization with the nonlinearity inserted gave relatively little change in the optimal gains. For a step input of 20.0, causing an initial saturation of 15.0, the cost index was reduced by less than 2.0 units. In order to reduce the damping and increase the transient time, the minimization reduced the values of the feedback gains. In terms of the transient response, this had the effect of decreasing the damping coefficient by moving the dominant complex roots closer to the right half of the plane. The response of the linear system with a step input of 10.0 is shown in Figure 3.19 and shows the typical transient response of a system designed using the integral of time multiplied by the absolute value of the error. Figure 3.20 is the step response of the same system with the nonlinearity inserted. The saturation, effectively, slowed the system down and resulted in less

overshoot and undershoot; furthermore, a smoother transition to steady state was noted. In Figure 3.21, the cost index was minimized with the nonlinearity present. The oscillatory response returned due to a lower damping coefficient caused by the reduction in feedback gains. The effect of these new feedback gains could best be seen in Figure 3.22 where the nonlinear optimal gains were used with the linear system. The step response became much more oscillatory with two overshoots and two undershoots.

The effects of the saturation located at points 1 and 2 were opposite. Point 1 caused an increase in damping, while point 2 caused a decrease in damping. The nonlinear optimal gains of point 1 reduced in value with an increase in step size; conversely, increases in gain were observed at point two. The result of most importance here was the fact that the presence of this type of saturation had predictable effects which could be used to provide the needed response. As an example, consider that the control systems engineer desired fast response, little error, and no overshoot; further, there was some sort of limiting device at saturation point 1. The engineer linearizes the system, utilizes the integral of time multiplied by the absolute value of the error criterion, and obtains his desired response. Adjustment of the system is enhanced by the knowledge that a decrease in feedback gains allows less damping and an increase in feedback gains causes more damping.

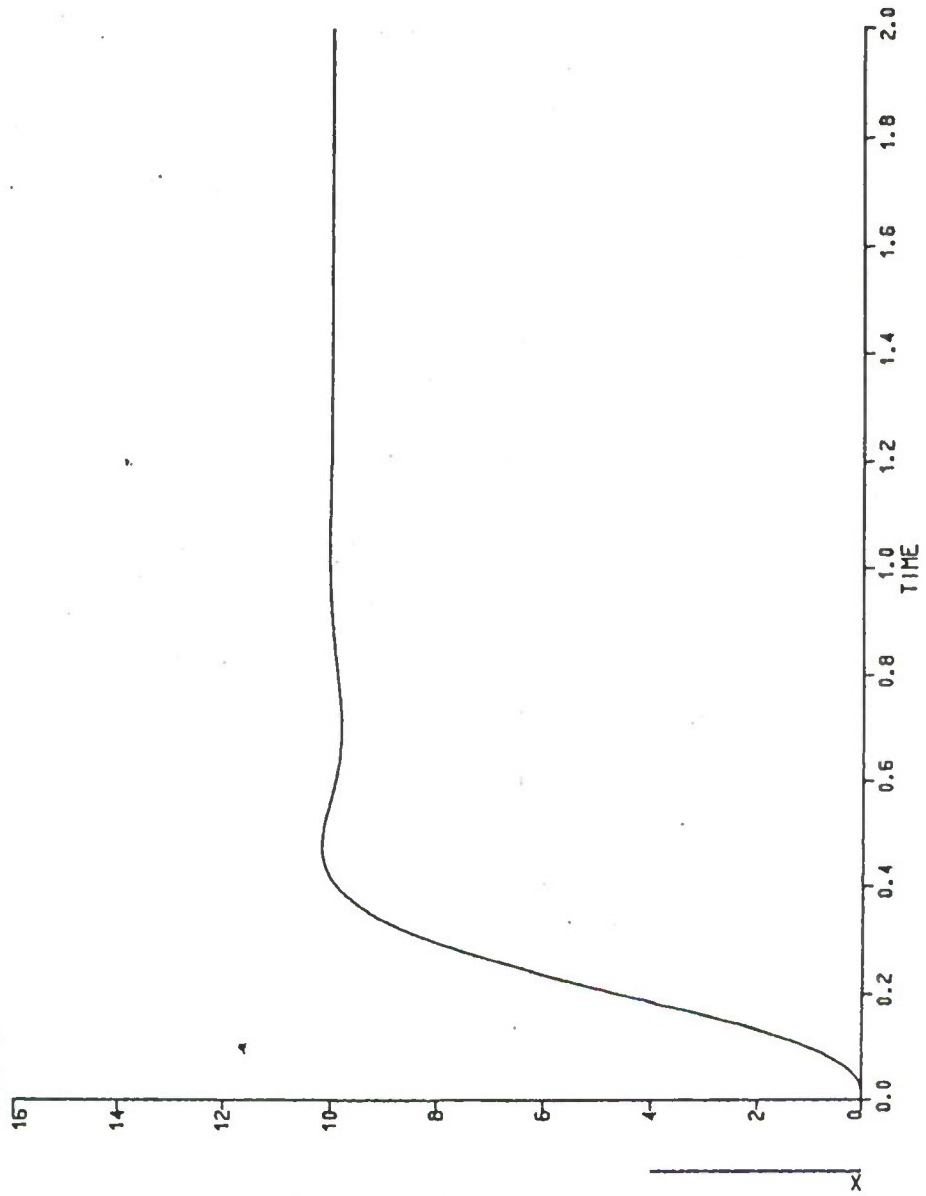

Figure 3.19: Linear Step Response, Step = 10.0, X = Output

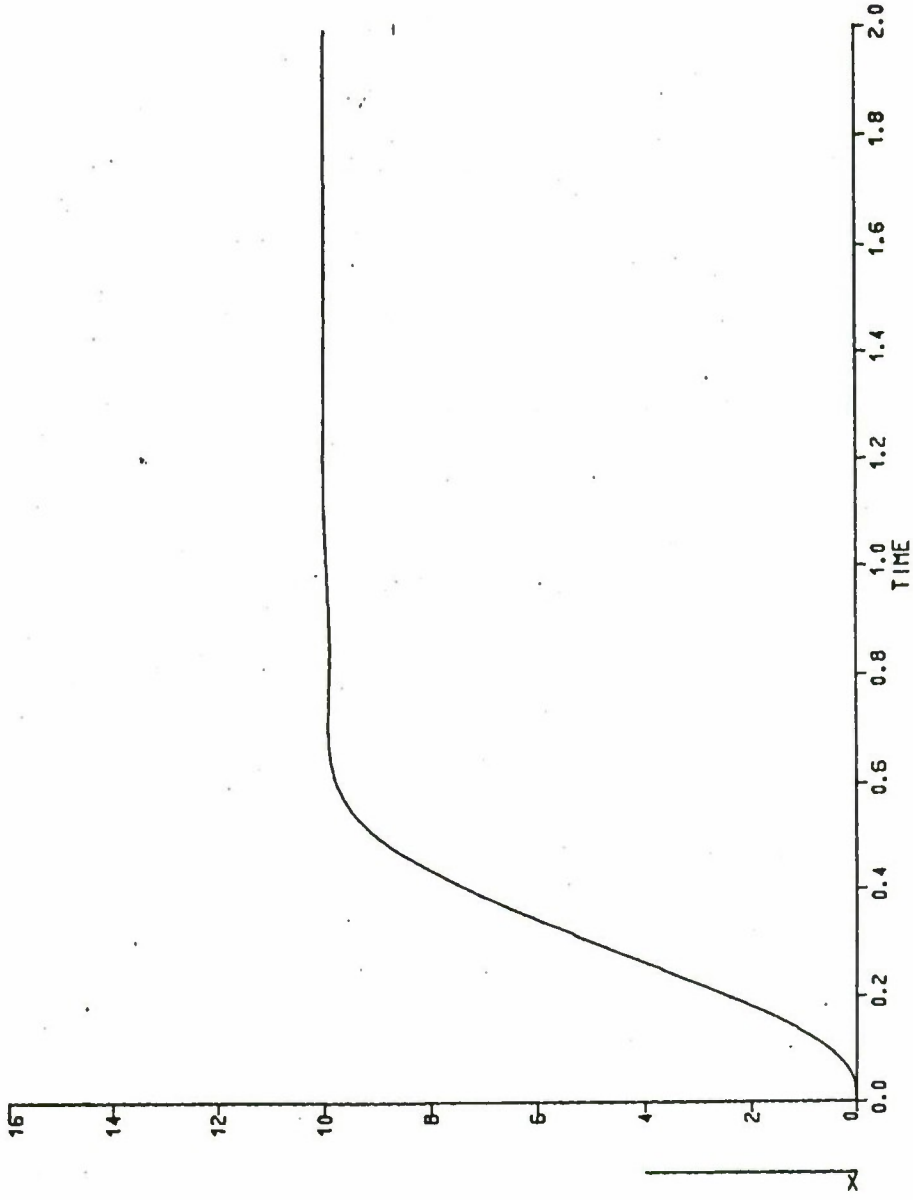

Figure 3.20: Nonlinear Step Response Using Linear Optimal Gains, Step = 10.0, X = Output

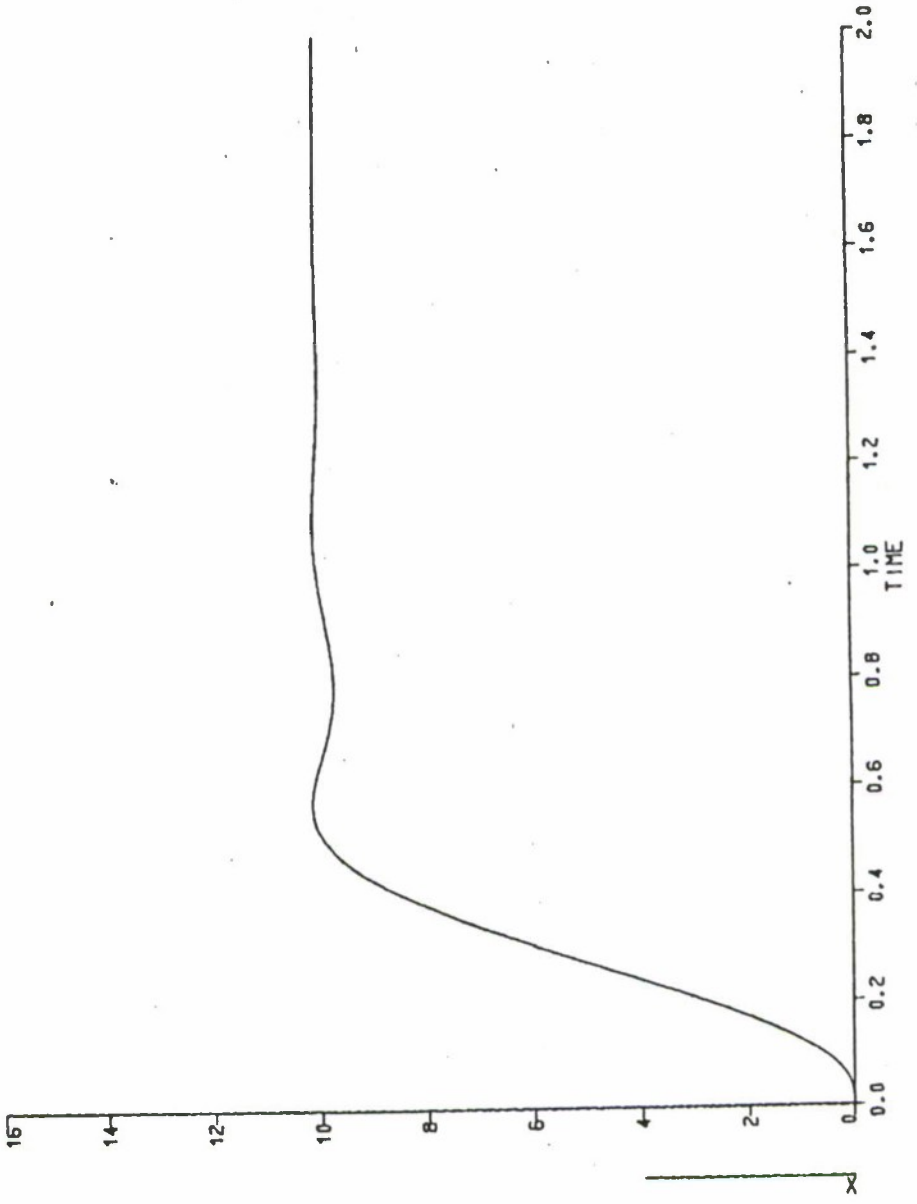

Figure 3.21: Nonlinear Step Response Using Nonlinear Optimal Gains, Step = 10.0, X = Output

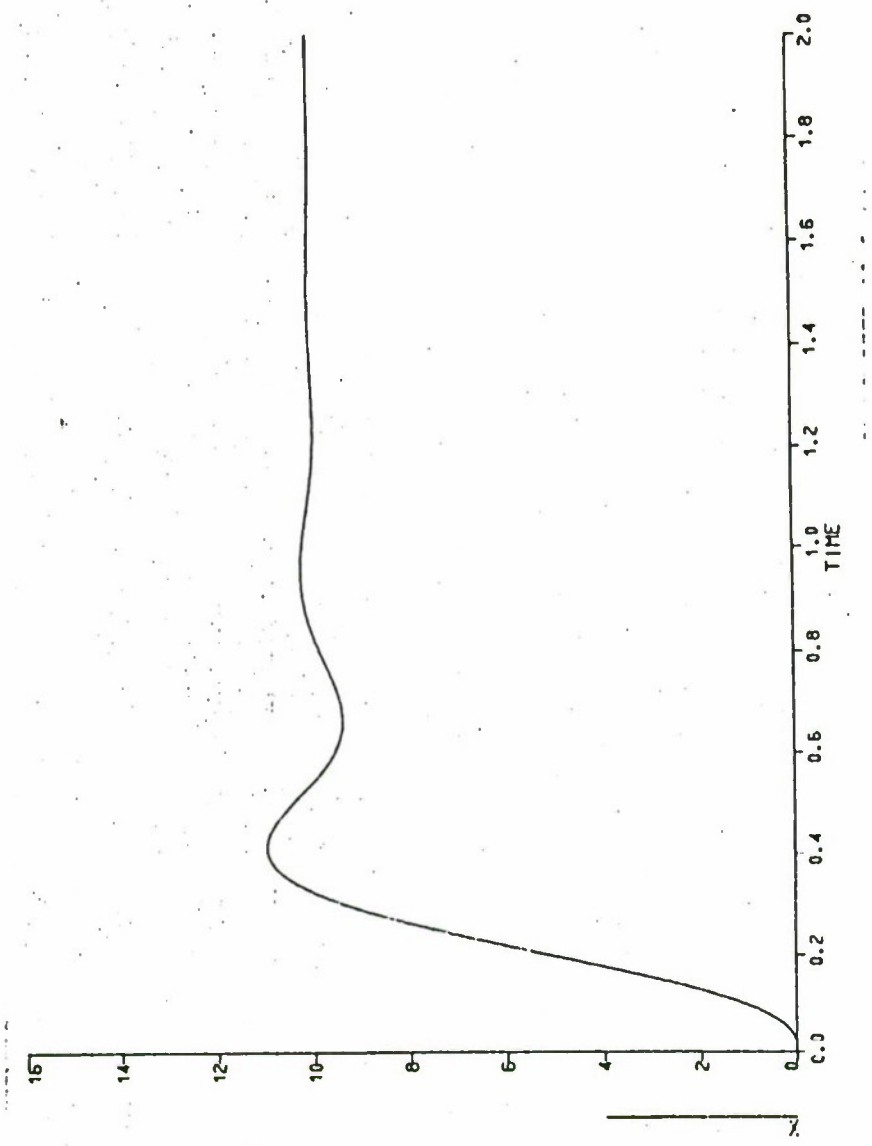

Figure 3.22: Linear Step Response Using Nonlinear Optimal Gains, Step = 10.0, X = Output

IV. STANDARD FORMS

Chapter II presented the standard forms derived by Graham and Lathrop [Ref. 1] and based on the integral of time multiplied by the absolute value of error. These standard forms were based on their simulations of linear systems on an analog computer which, at the time, was the most convenient computing device. Their work started by normalizing the closed-loop transfer function of the linear system to be optimized to the form

$$\frac{C(S)}{R(S)} = \frac{A_m S^m + A_{m-1} S^{m-1} + \cdots A_1 S + 1}{S^N + B_{N-1} S^{N-1} + \cdots B_1 S + 1} \quad . \tag{4.1}$$

In this normalized form, the coefficients of the first and last terms of the denominator were unity.

Each coefficient of the normalized transfer function was then varied separately until the value of the cost index became a minimum. The coefficients obtained at the minimum value of the cost index were considered to be the optimum parameters. These optimum parameters became the basis for their standard forms. Though their work was widely heralded as a success, they were personally disappointed by their failure to find a progressive root pattern. Since their work, the development of advanced techniques in simulation analysis along with a wealth of numerical optimization algorithms have provided more efficient and effective methods to study the problem. In this chapter, these advanced methods were used to derive and study a new set of standard forms.

The investigations dealt with type-1 plants which utilized full-state feedback. The closed-loop transfer function could be written as

$$\frac{C(S)}{R(S)} = \frac{\omega_0^N}{S^N + A_1 \omega_0 S^{N-1} + \cdots A_{N-1} \omega_0^{N-1} + \omega_0^N} \quad , \tag{4.2}$$

where N and ω_o denoted the order and angular frequency of the system; $A_1 \ldots A_{N-1}$ were the transfer-function coefficients. To facilitate problem manipulation and ease computational tasks, all systems were considered to have an angular frequency of 1.0 radian/second. This allowed Equation 4.2 to be re-written as

$$\frac{C(S)}{R(S)} = \frac{1.0}{S^N + A_1 S^{N-1} + \cdots A_{N-1} S + 1.0} \quad . \tag{4.3}$$

Using a unity-feedback loop to provide the error signal, the transfer function of the plant became

$$G_p(S) = \frac{1.0}{S^N + A_1 S^{N-1} + \cdots A_{N-1} S} \quad . \tag{4.4}$$

The unity-feedback system was modeled using the Dynamic Simulation Language and coupled with the minimization algorithm. [Ref. 3] The unit step was used as the test input. In most cases, the coefficients of the Butterworth standard forms served as the initial guesses to start the optimization process. The settling time was calculated for each system and used as the time interval for minimization. The optimum, normalized transfer function coefficients of each model resulted from the iterative computations performed. Standard forms for the first- through seventh-order systems were derived.

What was expected was roughly the same coefficients as Graham and Lathrop found, only with improved accuracy. This was the case for the initial minimization results which are presented in Table 4.1.

TABLE 4.1: Minimization #1; Minimum ITAE Standard Forms

$$s + \omega_o$$

$$s^2 + 1.42\omega_o s + \omega_o^2$$

$$s^3 + 1.74\omega_o s^2 + 2.15\omega_o^2 s + \omega_o^3$$

$$s^4 + 1.87\omega_o s^3 + 3.29\omega_o^2 s^2 + 2.61\omega_o^3 s + \omega_o^4$$

$$s^5 + 2.09\omega_o s^4 + 4.47\omega_o^2 s^3 + 4.68\omega_o^3 s^2 + 3.25\omega_o^4 s + \omega_o^5$$

$$s^6 + 2.81\omega_o s^5 + 6.27\omega_o^2 s^4 + 8.22\omega_o^3 s^3 + 7.42\omega_o^4 s^2 + 3.98\omega_o^5 s + \omega_o^6$$

$$s^7 + 4.41\omega_o s^6 + 9.67\omega_o^2 s^5 + 15.06\omega_o^3 s^4 + 15.50\omega_o^4 s^3 + 11.03\omega_o^5 s^2 + 4.81\omega_o^6 s + \omega_o^7$$

$$s^8 + 5.02\omega_o s^7 + 12.09\omega_o^2 s^6 + 21.31\omega_o^3 s^5 + 25.85\omega_o^4 s^4 + 22.91\omega_o^5 s^3 + 14.01\omega_o^6 s^2 + 5.40\omega_o^7 s + \omega_o^8$$

Comparing Table 4.1 with Graham and Lathrop's standard forms as presented in Table 2.1 in Chapter II, the coefficients were, essentially, the same. The minor differences were attributed to the greater accuracy of the digital computer and minimization algorithm. The results of Table 4.1 were obtained using step sizes on the order of 0.1 in the minimization search. These small steps closely resembled the continuous nature of the analog computer used by Graham and Lathrop.

The minimization was then repeated with larger step sizes. Surprising results were obtained. Although the coefficients of the lower-order systems (first- through fourth-order) remained unchanged, the higher-order systems showed drastic changes which could not be attributed to the increased accuracy of the digital computer. The revised standard forms are presented in Table 4.2.

TABLE 4.2: Minimization #2; Minimum ITAE Standard Forms

$$s + \omega_o$$

$$s^2 + 1.42\omega_o s + \omega_o^2$$

$$s^3 + 1.74\omega_o s^2 + 2.15\omega_o^2 s + \omega_o^3$$

$$s^4 + 1.87\omega_o s^3 + 3.29\omega_o^2 s^2 + 2.61\omega_o^3 s + \omega_o^4$$

$$s^5 + 1.93\omega_o s^4 + 4.38\omega_o^2 s^3 + 4.52\omega_o^3 s^2 + 3.22\omega_o^4 s + \omega_o^5$$

$$s^6 + 1.61\omega_o s^5 + 5.28\omega_o^2 s^4 + 5.87\omega_o^3 s^3 + 6.43\omega_o^4 s^2 + 3.54\omega_o^5 s + \omega_o^6$$

$$s^7 + 1.59\omega_o s^6 + 6.37\omega_o^2 s^5 + 7.57\omega_o^3 s^4 + 10.85\omega_o^4 s^3 + 7.82\omega_o^5 s^2 + 4.19\omega_o^6 s + \omega_o^7$$

When comparing the new standard forms with the original forms of Table 4.1, large changes were seen in the fifth- through seventh-order systems. Clearly, Graham and Lathrop found only a local minimum for these higher-order systems. To quantify the reduction, the value of the cost index was calculated for all systems of Table 4.1 and compared with the revised systems of Table 4.2. The results are presented in Table 4.3.

TABLE 4.3: Value of Relative Cost Indexes

SYSTEM ORDER	COST MINIMIZATION #1	COST MINIMIZATION #2	SETTLING TIME
1	18.000	18.000	6
2	1.936	1.936	8
3	3.085	3.085	11
4	4.512	4.512	12
5	6.227	6.201	14
6	8.761	8.251	15
7	13.082	10.676	20

While the first- through fourth-order costs remained constant, increasingly lower costs were realized as the system's order was increased. The largest decrease in cost was for the seventh-order system, as its cost went from 13.1 units to approximately 10.7 units.

The failure of Graham and Lathrop to find the absolute or global minimum thwarted their effort to find a progressive or predictable root pattern. The revised root locations for the third- through seventh-order systems, as plotted in Figure 4.1, show a definitive pattern.

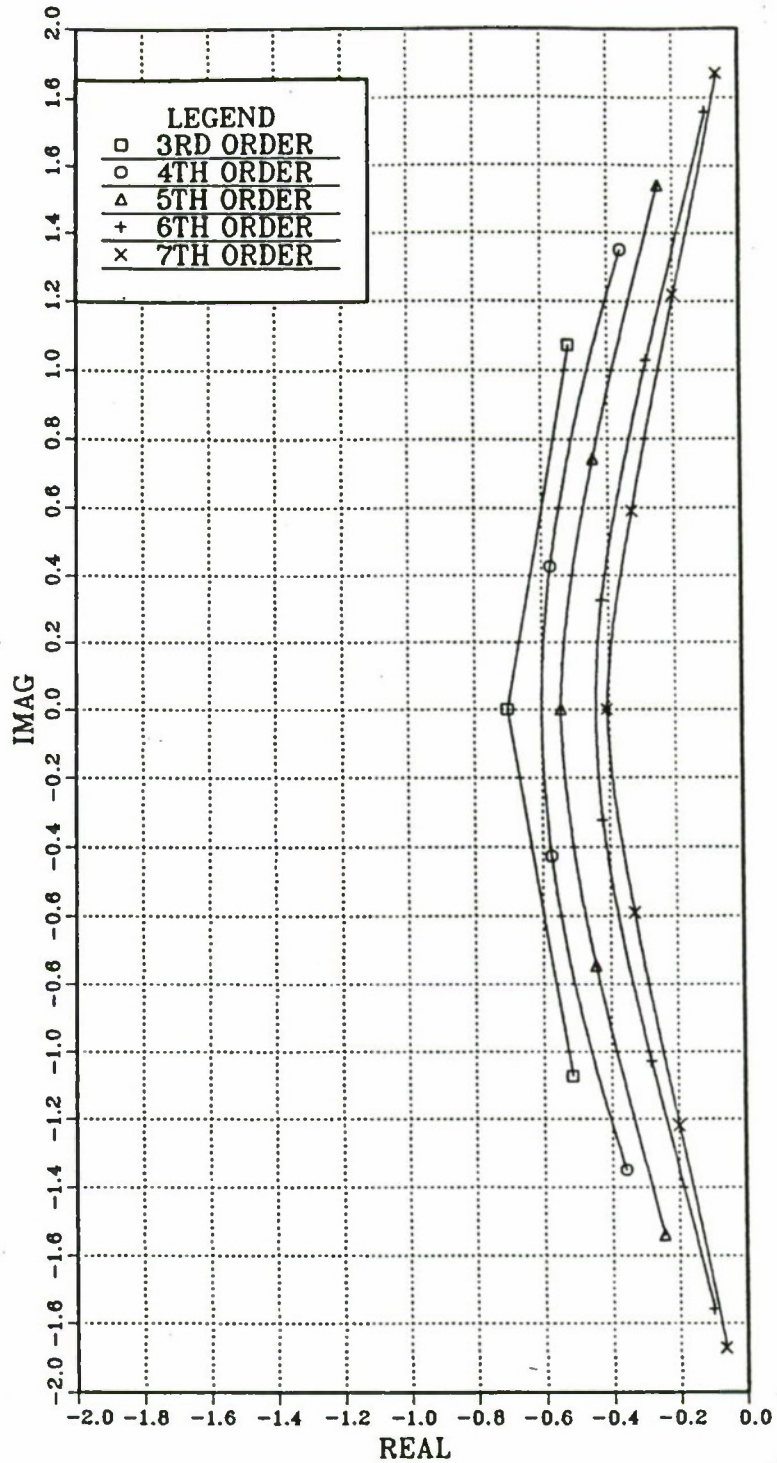

Figure 4.1: Root Locations for Systems of TABLE 4.2 Plotted on the S-Plane

In general, the optimum systems' roots tended to move closer toward the imaginary axis as the order of the system was increased. All even-ordered, optimum-system poles were complex conjugates, as was the case with the second-, fourth- and sixth-order systems. All odd-ordered optimum systems had one real root which was always the furthest distance from the origin, and the rest of the roots were complex conjugates. It was found that the closer the conjugate roots were to the imaginary axis, the larger their imaginary values; moreover, it was found that all of the roots were evenly spaced on an arc running between the two conjugate roots having the greatest absolute imaginary value. Though the results seemed to indicate a definite configuration, no geometric pattern was established.

The optimal systems obtained in Table 4.2 resulted in step responses possessing similar characteristics. Figure 4.2 shows the step responses for the first- through seventh-order systems.

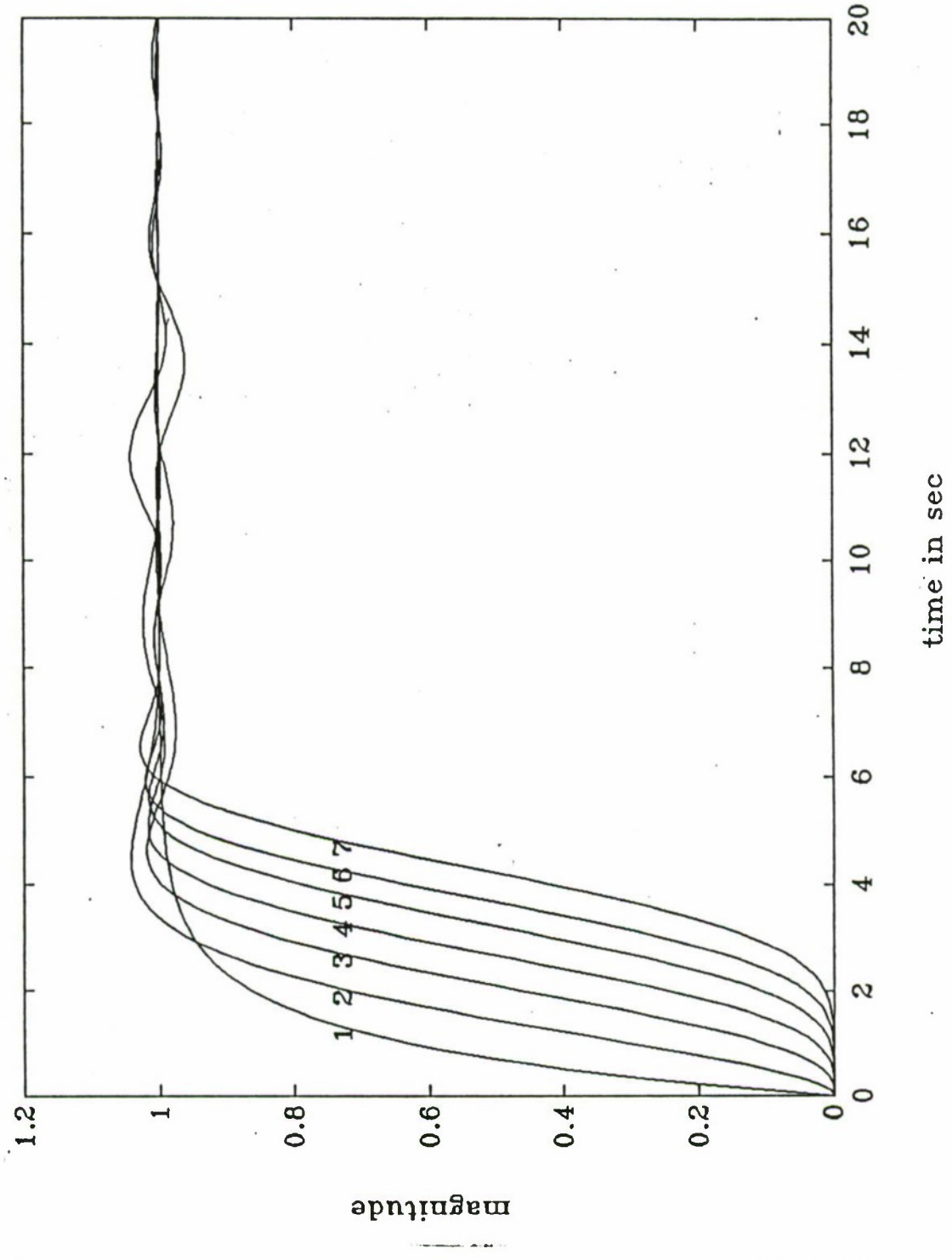

Figure 4.2: Step Response of Optimal Systems of TABLE 4.2

All of these systems had fast responses, negligible over and undershoots, and fast rates of decay.

In reference to Table 4.2, it may be observed that the natural frequency of every system, approximated by ω_0, appeared in the standard forms as a literal quantity. No attempt was made to optimize the system with respect to ω_0. It should be noted that the value of the integral of time multiplied by the absolute value of the error was affected by varying ω_0. In fact, the value of the cost index decreased with increasing ω_0. This indicated that the largest possible value of ω_0 should be used in follower-type systems. In terms of the S-plane, this meant that the radial distance from the origin to the roots of the characteristic equation increased with larger values of ω_0. Figure 4.3 shows the movement of roots away from the origin of the S-plane as ω_0 was increased from 1.0 to 2.0, 4.0, 6.0, 8.0, and 10.0. Realistically, practical considerations set an upper limit on the natural frequency and, thus, upon the frequency of ω_0.

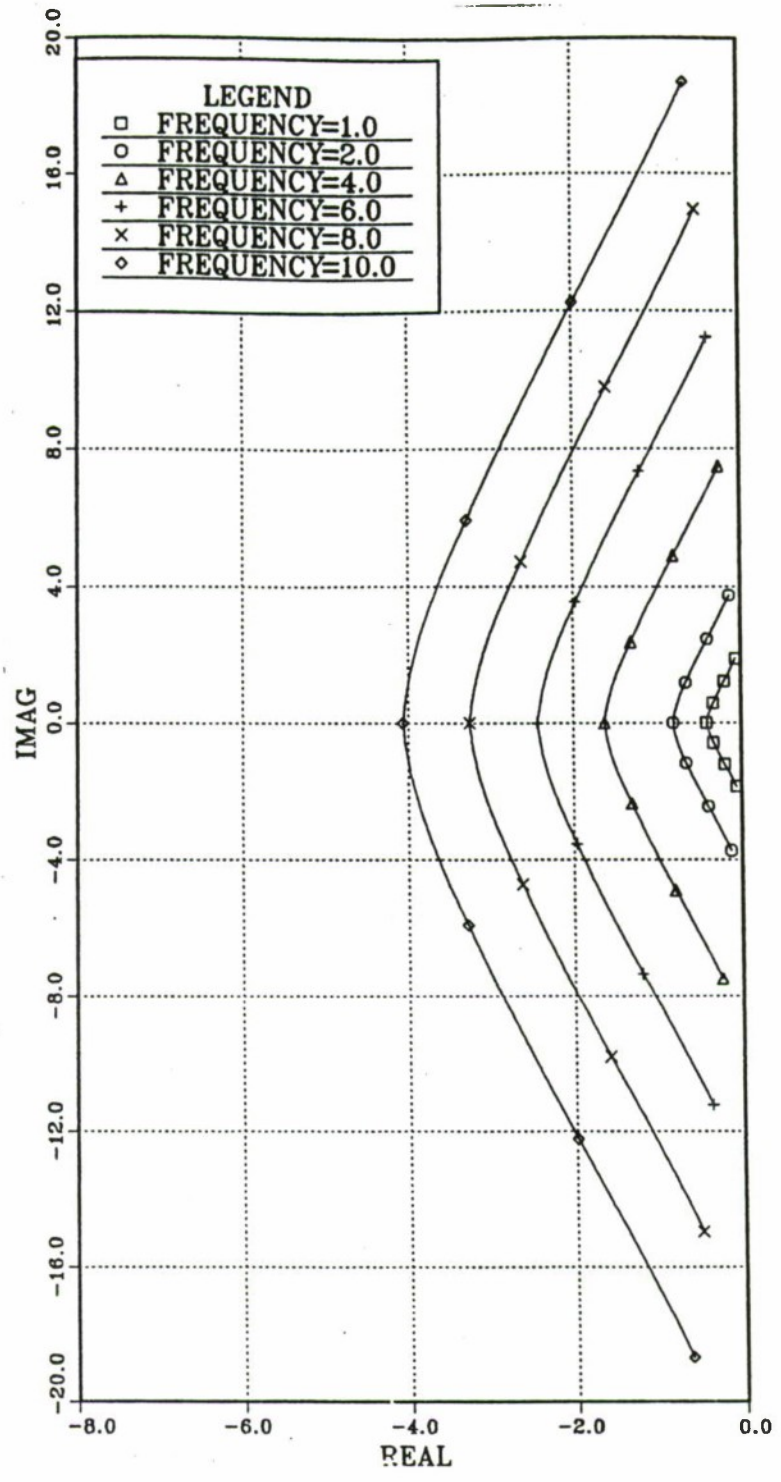

Figure 4.3: Root Movement for a Seventh-Order System as a Function of ω_0

The usefulness of these standard forms was best illustrated by examples. Consider the system of Figure 4.4.

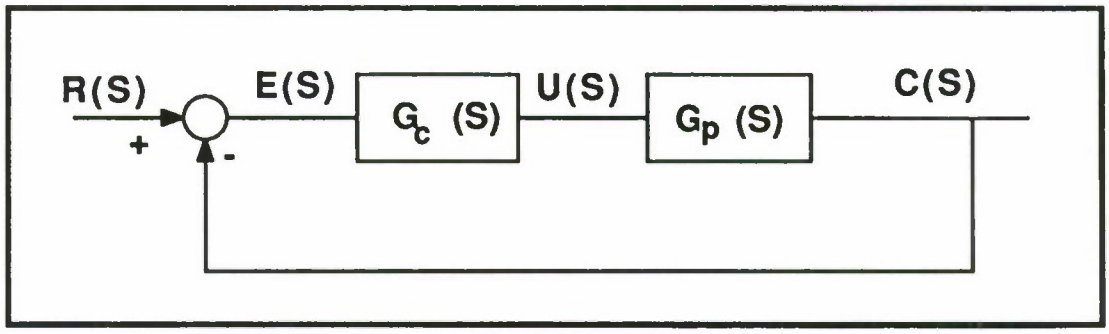

Figure 4.4: Block Diagram of System

where $G_c(S)$ is a cascade compensator and $G_p(S)$ is the plant function given as

$$G_p(S) = \frac{1.0}{S(1.0 + 0.1S)(1.0 + S)} \quad . \tag{4.5}$$

Assuming that the system's order was to be maintained and that no new roots were to be introduced, the standard forms of Table 4.2 gave the closed-loop transfer function as

$$\frac{C(S)}{R(S)} = \frac{\omega_0^3}{s^3 + 1.74\omega_0 S^2 + 2.15\omega_0^2 S + \omega_0^3} \quad . \tag{4.6}$$

Since

$$\frac{C(S)}{R(S)} = G_{cl}(S) = \frac{G_c(S)G_p(S)}{1 + G_c(S)G_p(S)} \quad , \tag{4.7}$$

then

$$G_c(S)G_p(S) = G_{eq}(S) = \frac{G_{cl}(S)}{1 - G_{cl}(S)} = \frac{\omega_0^3}{S(S^2 + 1.74\omega_0 S + 2.15\omega_0^2)} \quad . \tag{4.8}$$

Solving for $G_c(S)$,

$$G_c(S) = \frac{G_c(S)G_p(S)}{G_p(S)} = \frac{\omega_0^3(1.0 + 0.1S)(1.0 + S)}{S^2 + 1.74\omega_0 S + 2.15\omega_0^2} \quad . \tag{4.9}$$

If, based on the system's application, ω_0 was chosen to be 10.0 radians/second, then

$$G_c(S) = \frac{1000.0(1.0 + 0.1S)(1.0 + s)}{S^2 + 17.4S + 215.0} \quad . \tag{4.10}$$

Dividing the denominator polynomial by the numerator polynomial and factoring, the more easily realizable form of Equation 4.11 was obtained.

$$G_c(S) = \frac{100.0}{1 + \frac{6.4S+205.0}{S^2+11.0S+10.0}} = \frac{100.0}{1 + F_c(S)} \tag{4.11}$$

The block diagram of the cascade compensation is depicted in Figure 4.5.

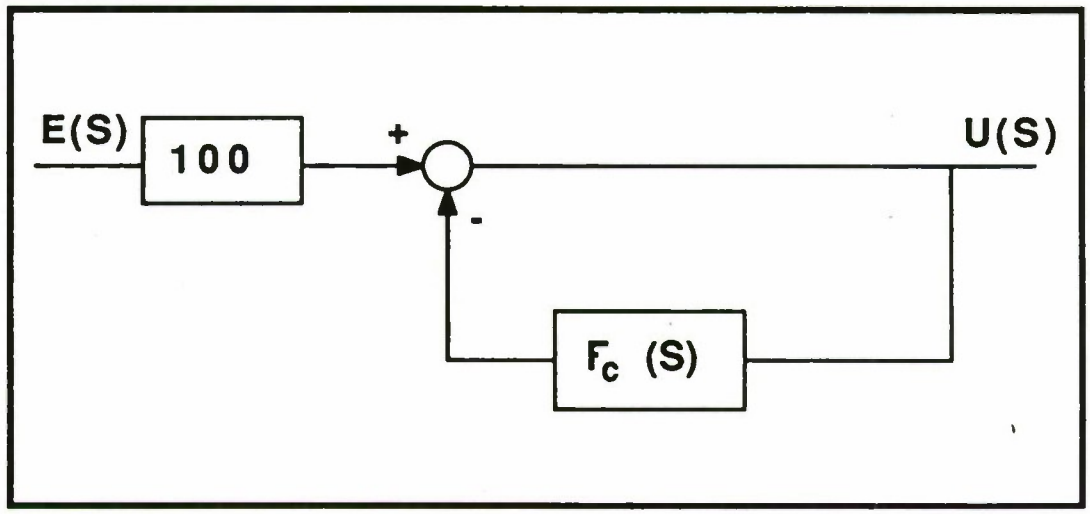

Figure 4.5: Block Diagram of Cascade Compensator

What remained was to realize the compensator in hardware. The quantity $F_c(S)$ was rewritten as

$$F_c(S) = \frac{20.5(1.0 + 0.03S)}{(1.0 + S)(1.0 + 0.1S)} \quad , \tag{4.12}$$

which was broken into

$$F_{c1}(S) = \frac{1}{1.0 + S} \tag{4.13}$$

and

$$F_{c2}(S) = \frac{20.5(1.0 + 0.03S)}{1.0 + 0.1S} \quad . \tag{4.14}$$

Equation 4.13 was realized using the network of Figure 4.6.

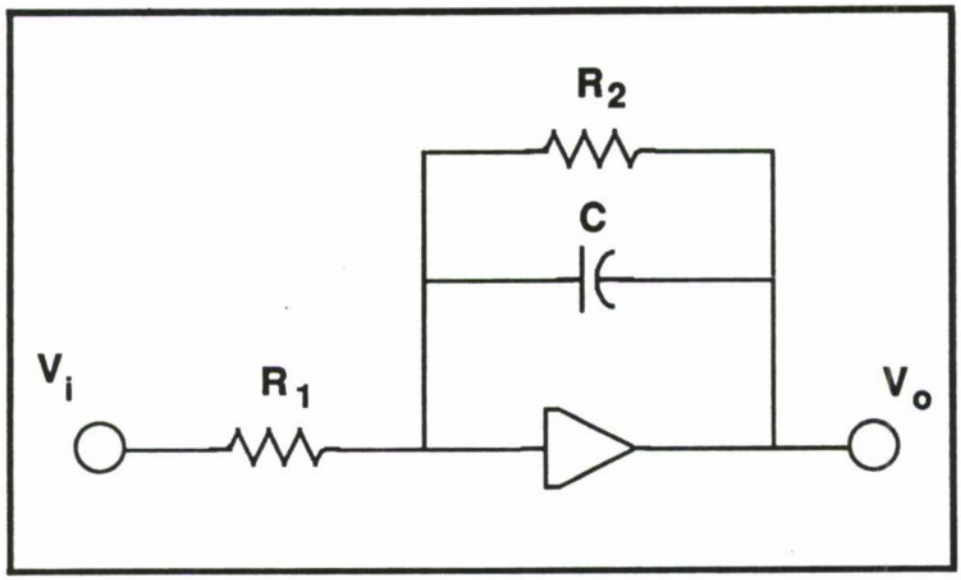

Figure 4.6: Network of $\frac{V_0}{V_i} = -\frac{R_2}{R_1(1+R_2CS)}$

Choosing values of $R_1 = R_2 = 1.0\ M\Omega$ and C = 1.0 μf provided Equation 4.13. To realize Equation 4.14, the network of Figure 4.7 was used.

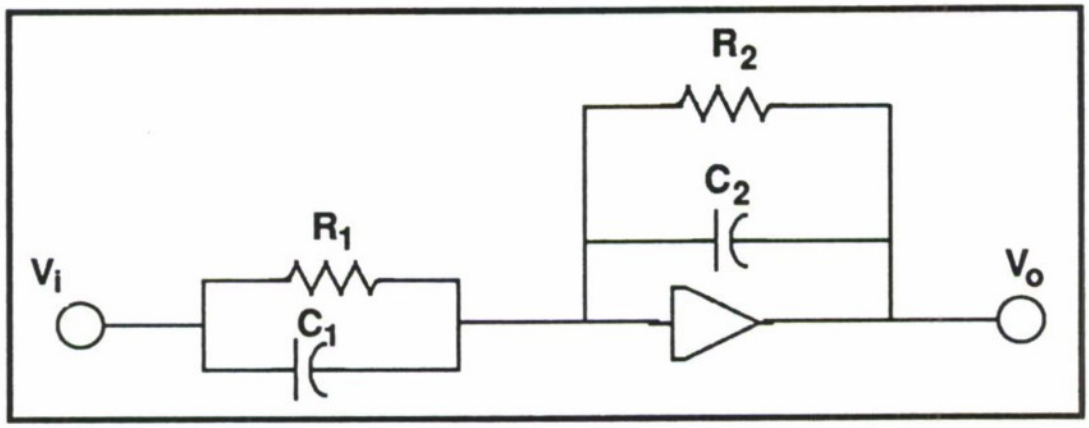

Figure 4.7: Network of $\frac{V_0}{V_i} = -\frac{R_2}{R_1}\frac{(1+R_1C_1S)}{(1+R_2C_2S)}$

Choosing $R_1 = 32.0\ K\Omega, R_2 = 1.0\ M\Omega, C_1 = 1.0\ \mu f, C_2 = 0.1\ \mu f$, and adding two potentiometers in order to provide the best possible fit, a possible compensation network was realized in Figure 4.8. [Ref. 6: pp. 86-149]

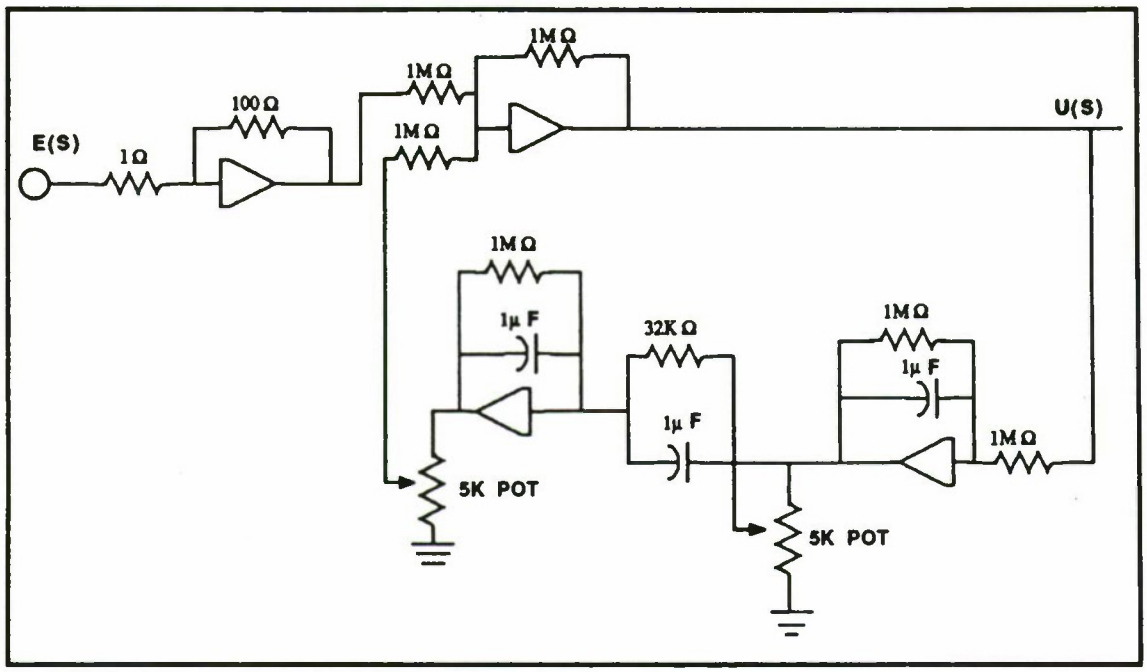

Figure 4.8: Possible Compensation Network

The key point here was not the hardware implementation of the compensator, but the fact that one could arrive at a design that would minimize the given cost index based solely on the use of the standard-form table.

The standard forms of Table 4.2 can most easily be applied with the use of full-state feedback. Consider the system of Figure 4.9.

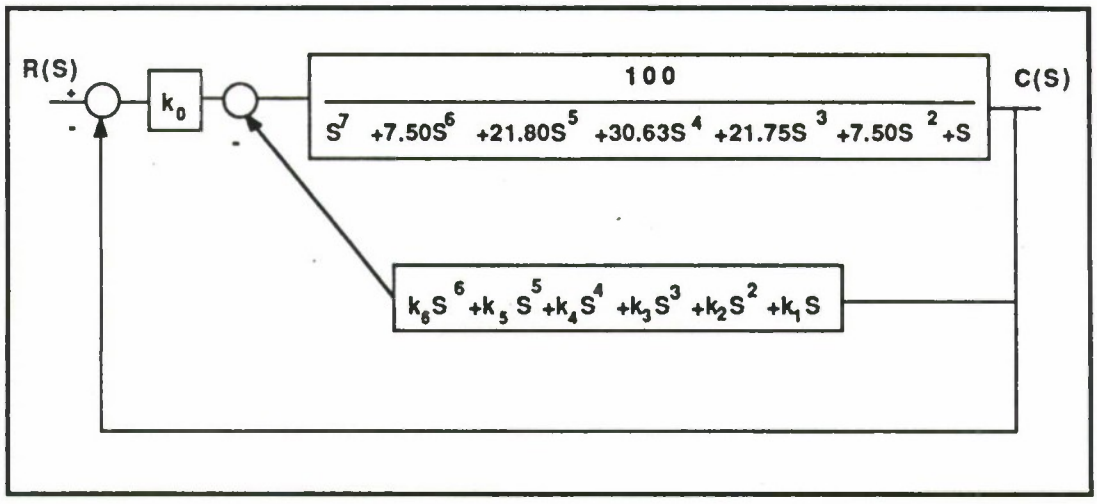

Figure 4.9: 7^{th}-Order System with Full State Feedback

After block diagram reduction, the system's transfer function was found to be

$$\frac{C(S)}{R(S)} = \frac{100.0k_0}{s^7 + (7.5 + 100k_6)S^6 + (21.8 + 100.0k_5)s^5 + (30.63 + 100.0k_4)S^4} \qquad (4.15)$$

$$\overline{+(21.75 + 100.0k_3)S^3 + (7.5 + 100.0k_2)S^2 + (1 + 100.0k_1)S + 100.0k_0} \; .$$

From Table 4.2, the standard form for a seventh-order system was

$$C.E. = S^7 + 1.59\omega_0 S^6 + 6.37\omega_0^2 S^5 + 7.57\omega_0^3 S^4 + 10.85\omega_0^4 S^3 + 7.82\omega_0^5 S^2 + 4.19\omega_0^6 S + \omega_0^7 \; . \qquad (4.16)$$

The bandwidth of the system was arbitrarily set at 5.0 radians/second. By equating coefficients of the system's characteristic equation to those of the standard form given in Equation 4.16, the optimal values were found to be $k_6 = 0.0045$, $k_5 = 1.37$, $k_4 = 7.16$, $k_3 = 67.60$, $k_2 = 244.30$, $k_1 = 654.68$ and $k_0 = 781.25$. Substituting these values into Equation 4.15, the transfer function became

$$\frac{C(S)}{R(S)} = \frac{78125.00}{S^7 + 7.95S^6 + 159.25S^5 + 946.25S^4 + 6781.25S^3 + 24437.5S^2 + 65468.75S + 78125.00} . \quad (4.17)$$

Using the standard forms developed by Graham and Lathrop, the optimal gains were $k_6 = 0.15$, $k_5 = 2.39$, $k_4 = 18.54$, $k_3 = 96.91$, $k_2 = 322.43$, $k_1 = 715.62$ and $k_0 = 781.25$. Substituting these values into Equation 4.15, the transfer function became

$$\frac{C(S)}{R(S)} = \frac{78125.00}{S^7 + 22.40S^6 + 260.50S^5 + 1885.00S^4 + 9712.50S^3 + 33250.00S^2 + 71562.50S + 78125.00} . \quad (4.18)$$

A comparison of the step responses of the two systems is presented in Figure 4.10. Clearly, the feedback gains derived from the standard forms of Table 4.2 provided a more optimal response than those derived from Graham and Lathrop's efforts. The revised system had a faster rise time, less over and undershoot, and a faster rate of decay.

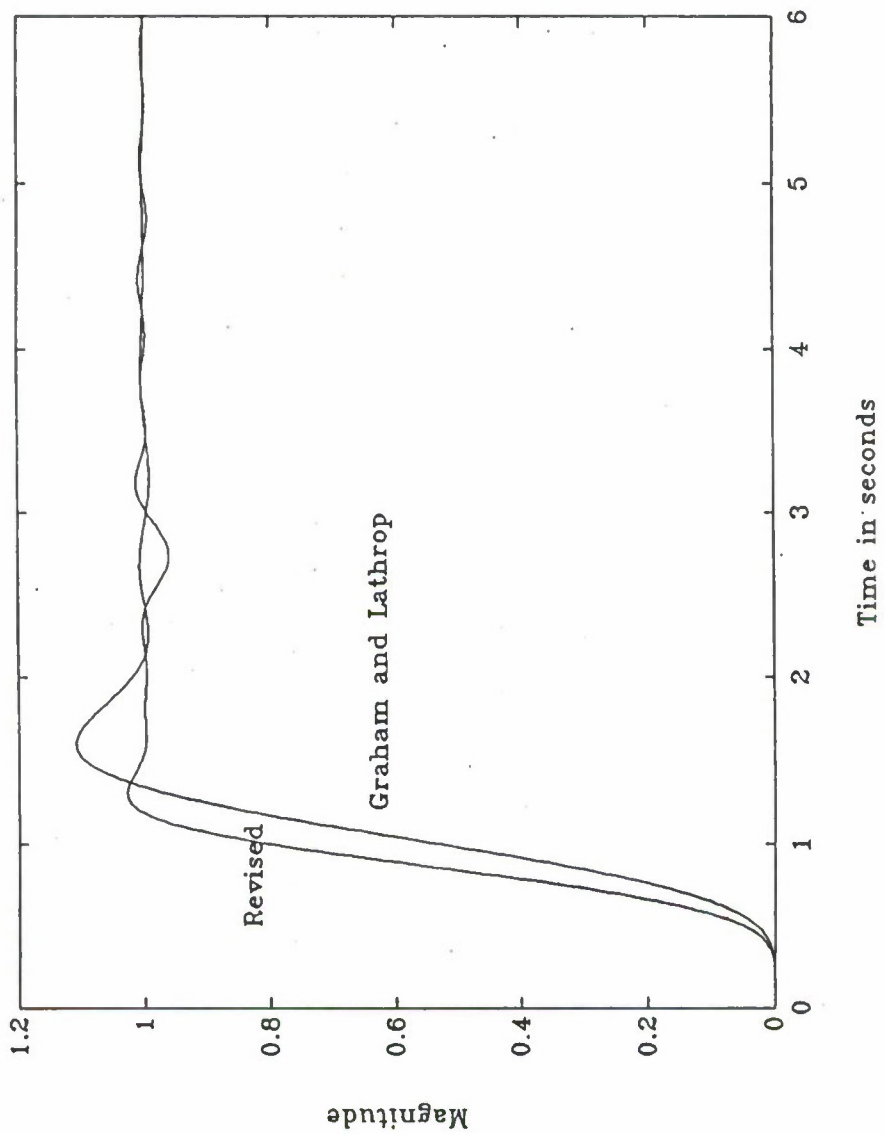

Figure 4.10: Comparison of Optimal Step Responses

V. THE EFFECT OF PENALIZING THE USE OF CONTROL

A. INTRODUCTION

The performance indices considered thus far assumed the availability of unlimited control input into the plant. Realistically, this is never the case and this limitation must be considered in any performance index utilized to optimize a system. Failure to do so often results in ridiculously high input values which cannot be attained by current technology; furthermore, the financial cost involved in the hardware implementation of the design must be considered. Higher control input necessitates correspondingly large, complex, and expensive system components. An economical system contains the lowest cost components possible to accomplish the task and utilizes these components to their full capacity. This philosophy indicates that the system is to be driven at its saturation limits to economically utilize its capabilities.

One of the most widely used linear-design techniques is the optimal linear quadratic regulator. A simplified version of this criterion is to find the control such that the performance index

$$J = \int_0^\infty \left[e^2(t) + qu^2(t)\right] dt \tag{5.1}$$

is minimized, where q is a weighting factor reflecting the relative importance or cost of control as compared to that of the system's total error. [Ref. 6:p. 340] The squaring of the terms reflect that it is the total error and control which are of importance, regardless of the relative direction of these values. This cost index has been well studied and analytical solutions formulated.

As discussed in Chapter I, the cost functional of the integral of time multiplied by the absolute value of error resulted in a system with a generally acceptable transient response. Based on this favorable response, the question arose as to what effect did the addition of a control cost to the index have on the system's transient response. It was the purpose of this section to answer this question. In particular, the investigation centered on the performance index of Equation 5.2,

$$J = \int_0^\infty \left[t\,|e(t)| + qu^2(t) \right] dt \tag{5.2}$$

where q was a relative weighting factor, $u(t)$ was the actual control input, t was time, and $e(t)$ was the error between the reference input and the actual system output. The nonlinear nature of Equation 5.2 eliminated an analytical solution; therefore, it was analyzed using simulation techniques.

B. LINEAR OPTIMIZATION

The cost index of Equation 5.2 was minimized for both a third- and fourth-order plant utilizing full-state feedback. The transfer function for the third-order plant was

$$G_p(S) = \frac{48.0}{S^3 + 3.0S^2 + 2.0S} \ , \tag{5.3}$$

and the transfer function for the fourth-order plant was

$$G_p(S) = \frac{10.0}{S^4 + 8.5S^3 + 16.0S^2 + 6.0S} \ . \tag{5.4}$$

A general block diagram of the system is presented in Figure 5.1.

In Chapter III, it was necessary to set the zero-derivative feedback gain to a fixed value in order for the cost index of time multiplied by the absolute value of the error to converge to some minimum value. With the addition of the $u^2(t)$ term in the cost index, this step was no longer necessary. This added constraint on

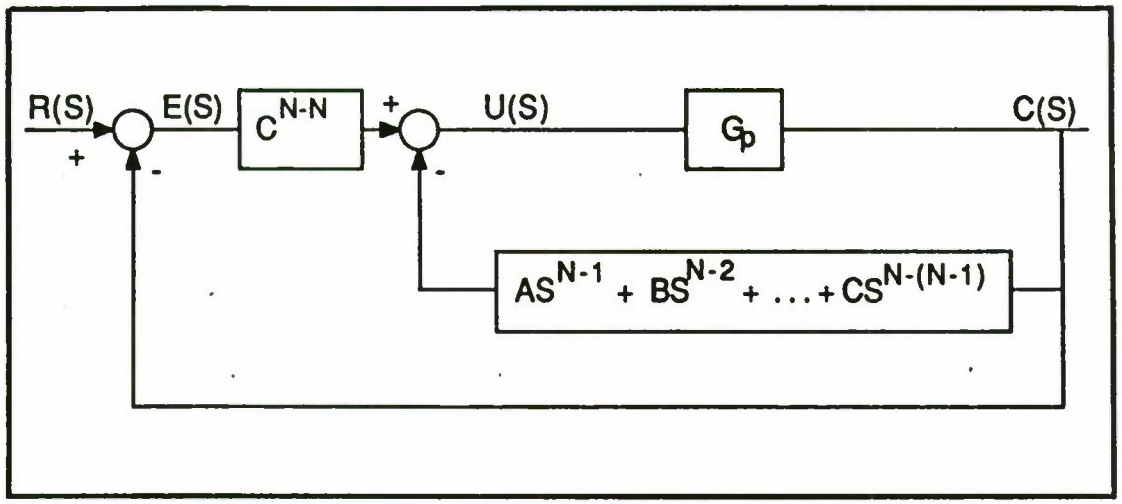

Figure 5.1: Block Diagram of System To Be Minimized Using $\int [t\,|e(t)| + qu^2(t)]\,dt$

the amount of control used did not allow the minimization routine to use unlimited control to speed-up the system. There was a minimum value of the cost index based on a compromise between the speed of the system and the amount of control used. This compromise was greatly affected by the value, chosen by the designer, of the weighting factor, q. Unfortunately, there was no magical value for q. It was, usually, arbitrarily chosen based on the components available in the system and the application for which the system was to be used.

Although it was not necessary to set the value of the zero-derivative feedback gain, the systems studied were minimized for both a fixed gain and a variable one. Zero-derivative feedback gains were, arbitrarily, chosen at 20.83 and 1000.00 for the third- and fourth-order systems, respectively. The results of the fixed gain cases are presented in Tables 5.1 and 5.2 for the third- and fourth-order systems. In both systems, trends were clearly evident. For the fixed gain, increases in the weighting of the control cost caused the optimal feedback gains to increase. This increase

in feedback gains caused the complex roots to retract to the real axis and all real roots to increase in absolute value. With all real roots, the system exhibited an exponential rise to steady state; however, it should be noted that relatively high values of q were used to force the roots to the real axis. In the case of the fourth-order system under study, a weighting factor of 100.0 was required. In most practical applications, this large of a weighting on control cost is not used by the designer. With the zero-derivative feedback gain variable, most of the reduction in the value of the performance index came from a reduction in the control cost. Since the control to the plant was the fixed value, k_0, multiplied by the plant gain and minus the derivative feedback, the feedback gains were increased to lower the plant input; consequently, the cost of control was reduced. As the value of the weighting index, q, was increased, the value of the cost functional increased. This indicated that the system was increasingly less capable of handling the compromise between the control cost and time multiplied by the absolute value of the error. Due to the fixed forward-path gain of the system and the squaring of the control cost, the system slowed rapidly for even small values of q. Figure 5.2 shows the third-order system's step responses for various values of q.

TABLE 5.1: Optimizing the Third-Order System, k_0 Fixed at 20.83

VALUE OF q	OPTIMAL PARAMETERS	VALUE OF COST INDEX	ROOT LOCATIONS
0.0	$k_0 = 20.83$ $k_1 = 4.48$ $k_2 = 0.31$	0.03	-7.34 -5.28 $\pm j$10.41
0.1	$k_0 = 20.83$ $k_1 = 10.90$ $k_2 = 2.55$	0.40	-121.13 -2.13 $\pm j$1.92
0.5	$k_0 = 20.83$ $k_1 = 15.31$ $k_2 = 4.92$	0.92	-236.06 -1.55 $\pm j$1.35
1.0	$k_0 = 20.83$ $k_1 = 18.78$ $k_2 = 7.48$	1.28	-359.54 -1.25 $\pm j$1.10
2.0	$k_0 = 20.83$ $k_1 = 22.94$ $k_2 = 11.97$	1.76	-575.65 -0.96 $\pm j$0.91
5.0	$k_0 = 20.83$ $k_1 = 33.48$ $k_2 = 25.60$	3.04	-1230.49 -0.65 $\pm j$0.62

TABLE 5.2: Optimizing the Fourth-Order System, k_0 Fixed at 1000.0

VALUE OF q	OPTIMAL PARAMETERS	MINIMIZATION PERIOD	ROOT LOCATIONS
0.0	k_0 = 1000.00 k_1 = 263.00 k_2 = 31.80 k_3 = 1.15	4.0	-4.01 $\pm j$12.97 -5.98 $\pm j$ 4.30
0.1	k_0 = 1000.00 k_1 = 948.00 k_2 = 376.00 k_3 = 50.00	5.0	-503.60 -4.03 -1.72 $\pm j$1.40
0.5	k_0 = 1000.00 k_1 = 1130.00 k_2 = 542.00 k_3 = 66.40	6.0	-665.35 -5.58 -1.29 $\pm j$1.02
1.0	k_0 = 1000.00 k_1 = 1220.00 k_2 = 628.00 k_3 = 75.10	6.0	-752.68 -6.03 -1.17 $\pm j$0.92
2.0	k_0 = 1000.00 k_1 = 1320.00 k_2 = 720.00 k_3 = 84.40	10.0	-845.16 -6.03 -1.07 $\pm j$0.84
5.0	k_0 = 1000.00 k_1 = 1450.00 k_2 = 845.00 k_3 = 97.30	15.0	-975.00 -6.70 -0.9995 $\pm j$0.733
10.0	k_0 = 1000.00 k_1 = 1550.00 k_2 = 929.00 k_3 = 106.00	15.0	-1063.90 -6.81 -0.97 $\pm j$0.66
100.0	k_0 = 1000.00 k_1 = 2110.00 k_2 = 1190.00 k_3 = 138.00	15.0	-1377.80 -6.41 -1.41 -0.81
1000.0	k_0 = 1000.00 k_1 = 2560.00 k_2 = 1370.00 k_3 = 161.00	15.0	-1613.40 -6.07 -1.92 -0.53
2000.0	k_0 = 1000.00 k_1 = 2610.00 k_2 = 1390.00 k_3 = 164.00	15.0	-1639.60 -6.03 -1.96 -0.52

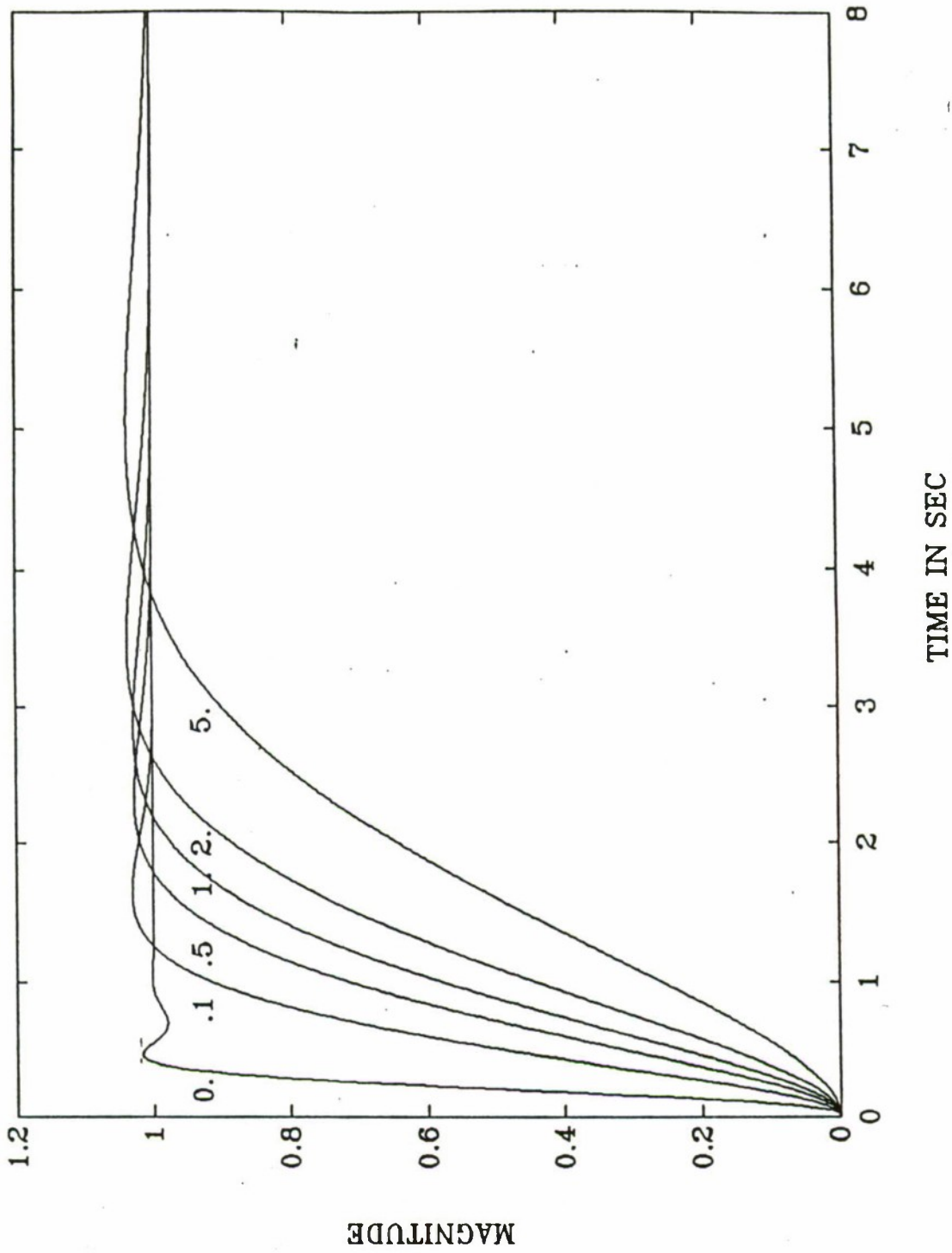

Figure 5.2: Step Responses for Various Values of q, Third-Order System

Tables 5.3 and 5.4 show the results of the third- and fourth-order, variable-gain systems. For weighting factors of less than or equal to 1.0, all of the feedback gains were reduced. This resulted in both the complex and real roots being reduced. For weighting factors in excess of 1.0, this trend ceased; moreover, the feedback gains optimized to more random patterns. A trend which did remain constant throughout the range of control weightings was the relative values of the feedback gains. In the fourth-order system of Table 5.4, the k_1 feedback gain remained the largest value, followed by the k_0, k_2, and k_3 feedback gains. Unlike the fixed gain systems, the complex roots of the variable-gain systems never returned to the real axis; however, the complex roots did progressively decrease in value. Since an increase in the control weighting translated to less power being supplied to the plant, the result was a slower response. To accomplish this reduction in speed, the dominant roots became smaller in value. Since the natural frequency was measured as the radial distance from the origin of the s-plane to the complex roots, this reduction in the absolute value of the dominant roots implied a reduction in the bandwidth of the system. In an attempt to find a definitive root pattern to which the roots converged, control weightings up to and including 10,000.00 were used. No progressive patterns were found. As with the fixed-gain systems, increasing values of q caused increasing values of the performance index.

TABLE 5.3: Optimizing the Third-Order System with k_0 Variable

VALUE OF q	OPTIMAL PARAMETERS	VALUE OF COST INDEX	OPTIMAL ROOTS	SYSTEM BANDWIDTH**
0.0	(Will not converge)			
0.1	$k_0 = 3.310$ $k_1 = 1.380$ $k_2 = 0.180$	0.178 F.T. = 4.0*	-3.62 $\pm j$4.83 -4.37	5.42
0.5	$k_0 = 1.420$ $k_1 = 0.753$ $k_2 = 0.114$	0.284 F.T. = 4.0*	-2.63 $\pm j$3.78 -3.22	4.09
1.0	$k_0 = 1.052$ $k_1 = 0.612$ $k_2 = 0.099$	0.349 F.T. = 4.0*	-2.41 $\pm j$3.37 -2.94	3.69
2.0	$k_0 = 0.754$ $k_1 = 0.480$ $k_2 = 0.081$	0.430 F.T. = 4.0*	-2.14 $\pm j$3.06 -2.60	3.30
5.0	$k_0 = 0.502$ $k_1 = 0.356$ $k_2 = 0.062$	0.569 F.T. = 4.0*	-1.86 $\pm j$2.68 -2.27	2.88
10.0	$k_0 = 0.356$ $k_1 = 0.274$ $k_2 = 0.048$	0.773 F.T. = 4.0*	-1.66 $\pm j$2.39 -2.01	2.59
100.0	$k_0 = 0.121$ $k_1 = 0.112$ $k_2 = 0.015$	1.610 F.T.=4.0*	-1.16 $\pm j$1.66 -1.41	1.79
1000.0	$k_0 = 0.034$ $k_1 = 0.023$ $k_2 = -0.016$	3.70 F.T.=10.0*	-0.70 $\pm j$1.21 -0.84	1.77
2000.0	$k_0 = 0.025$ $k_1 = 0.012$ $k_2 = -0.017$	4.98 F.T.=10.0*	-0.68 $\pm j$1.00 -0.84	1.06
5000.0	$k_0 = 0.020$ $k_1 = 0.005$ $k_2 = -0.006$	7.50 F.T.=20.0*	-0.48 $\pm j$0.55 -1.74	0.99
10000.0	$k_0 = 0.009$ $k_1 = 0.002$ $k_2 = -0.025$	10.10 F.T.=30.0*	-0.77 $\pm j$1.04 -0.27	0.76

* Finishing Time (F.T.) or integration time over which the system was minimized; units=seconds.

**The system bandwidth was approximated by the $\sqrt[r]{\omega_o}$. The value of ω_o was defined as shown in the standard forms of Table 2.2.

TABLE 5.4: Optimizing the Fourth-Order System with k_0 Variable

VALUE OF q	OPTIMAL PARAMETERS	VALUE OF COST INDEX F.T.=10.0 SEC*	OPTIMAL ROOTS	SYSTEM BANDWIDTH
0.0	(Will not converge)			
0.1	$k_0 = 5.366$ $k_1 = 6.591$ $k_2 = 2.382$ $k_3 = 0.361$	1.586	-8.23 -1.48 -1.19 $\pm j1.73$	2.71
0.5	$k_0 = 2.482$ $k_1 = 3.551$ $k_2 = 1.293$ $k_3 = 0.226$	2.594	-10.27 -1.14 -0.93 $\pm j1.31$	2.34
1.0	$k_0 = 1.705$ $k_1 = 2.593$ $k_2 = 0.852$ $k_3 = 0.145$	3.242	-6.47 -1.09 -0.91 $\pm j1.19$	1.99
5.0	$k_0 = 1.201$ $k_1 = 2.345$ $k_2 = 1.292$ $k_3 = 0.627$	5.724	-14.83 -1.27 -0.59 $\pm j0.63$	1.93
10.0	$k_0 = 1.075$ $k_1 = 2.368$ $k_2 = 1.677$ $k_3 = 1.044$	7.545	-17.13 -0.68 -0.57 $\pm j0.78$	1.81
100.0	$k_0 = 0.279$ $k_1 = 0.560$ $k_2 = 0.456$ $k_3 = 0.666$	20.190	-13.72 -0.63 -0.40 $\pm j0.40$	1.29
1000.0	$k_0 = 0.149$ $k_1 = 0.424$ $k_2 = 1.212$ $k_3 = 1.074$	68.45 F.T.=20 sec*	-17.68 -1.12 -0.23 $\pm j0.16$	1.10

* Finishing Time (F.T.) or integration time over which the system was minimized.

Two problems inherent to the cost index were found while investigating the variable-gain systems. These problems were due to the mathematical formulation of the index. Although the index considered the duration of the total error and the amount of control used, it did not equally weight these conflicting values. The duration and amount of error was found by multiplying time by the absolute value of the error; on the other hand, the control cost was found by squaring the control input. The difference between the squared value and the multiplied value required that a long minimization period be used during the system's optimization. If this procedure was not followed, an optimal solution could not be assured. This problem is best shown by an example. Consider the fourth-order plant of Equation 5.4. Prior to optimization, the random feedback gains were $k_0 = 1000.0$, $k_1 = 263.0$, $k_2 = 31.8$, and $k_3 = 1.15$. With these gains, the response of Figure 5.3 was obtained. This system had a settling time of approximately two seconds. The system was then optimized using the performance index of Equation 5.2. Using a control weighting factor of 5.0 and minimization periods of 2.0, 4.0, 6.0, and 10.0 seconds, the optimal step responses of Figure 5.4 were obtained. As can be seen from the figure, different optimal responses were obtained for each minimization period. As the minimization or integration period was increased, the step response became more optimal. This dependence was also seen in the optimal feedback gains. The optimal feedback gains and the values of the cost functional for a 10.0 second simulation are shown in Table 5.5. As the minimization period was increased, the value of the cost index was decreased; furthermore, the feedback gains moved closer to their optimal values. The problem was magnified as the value of the control weighting was increased. Progressively longer minimization periods were required to ensure a truly optimal solution. The explanation of this phenomenon was straightforward. For short time periods and larger control weightings, the minimization routine realized the most

cost savings by cutting the mathematically favored control cost. This artificial optimal solution could only be corrected by increasing the integration period over which the problem was solved. For a given control weighting, there was no exact way of predicting the required minimization period needed to optimize the system. The only solution was to steadily increase the solution time until no further reductions in cost were realized. For the systems under study, large multiples of the original system's settling time were used.

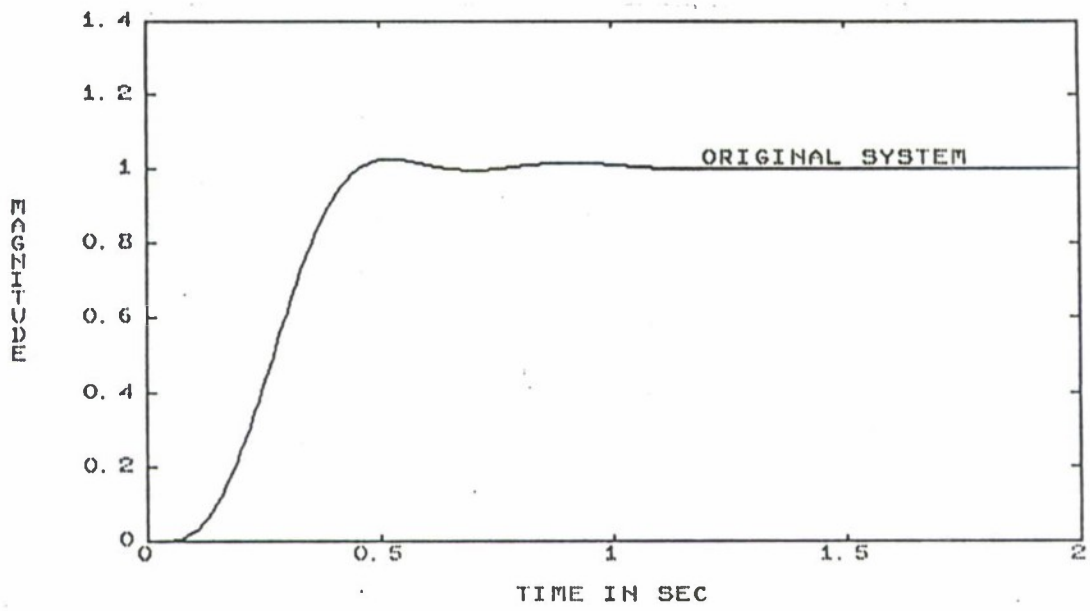

Figure 5.3: Step Response of System Before Minimization

TABLE 5.5: Optimal Feedback Gains Corresponding to Figure 5.3

MINIMIZATION PERIOD (SEC)	OPTIMAL FEEDBACK GAINS	VALUE OF COST INDEX AFTER 10.0 SEC. SIMULATION
2.0	$k_0 = 0.14$ $k_1 = 5.87$ $k_2 = 1.14$ $k_3 = 0.88$	43.60
4.0	$k_0 = 1.04$ $k_1 = 1.31$ $k_2 = 1.53$ $k_3 = 0.64$	10.19
6.0	$k_0 = 1.05$ $k_1 = 2.03$ $k_2 = 0.83$ $k_3 = 0.71$	6.08
10.0	$k_0 = 1.20$ $k_1 = 2.35$ $k_2 = 1.29$ $k_3 = 0.63$	5.72

The second problem encountered in the optimization was with the contour of the performance-index surface. As the control weighting was increased, the cost surface became flatter. The flatness of the surface made it difficult to find the absolute or global minimum. For a q value of 5.0, Table 5.4 reflects optimal feedback gains of $k_0 = 1.39$, $k_1 = 2.81$, $k_2 = 1.76$, and $k_3 = 0.88$. The associated value of the cost index was 5.73. For the same system and control weighting, feedback gains of $k_0 = 0.67$, $k_1 = 0.83$, $k_2 = 0.60$, and $k_3 = 0.67$ resulted in a cost of 5.82. The two sets of optimal feedback gains were relatively far apart, but gave nearly the same value for the cost index. This indicated a nearly flat cost surface. As the value of the control weighting was increased, the cost surface became even flatter.

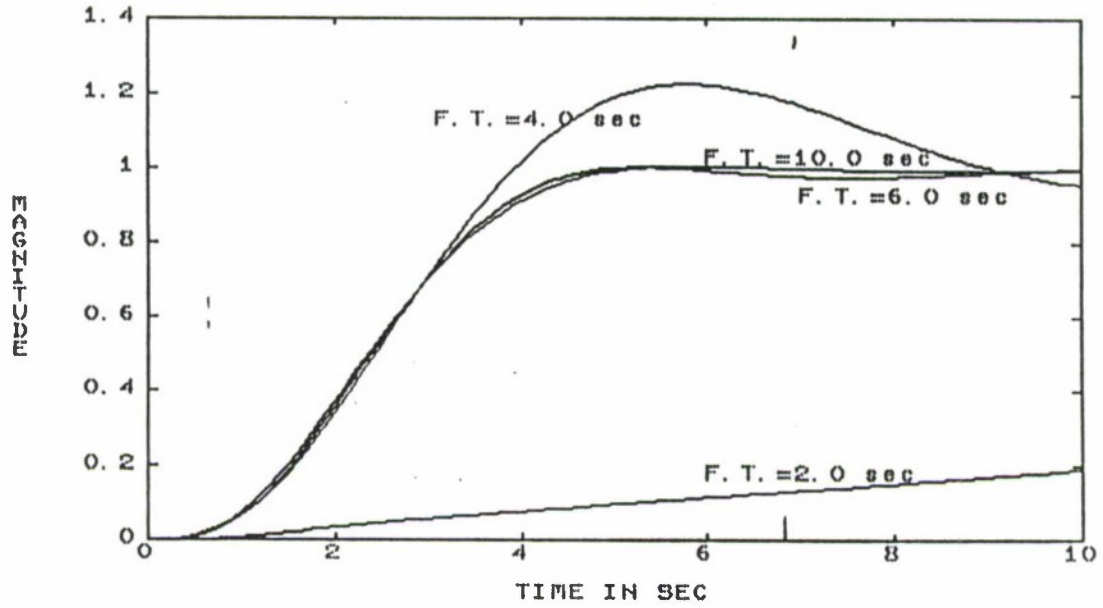

Figure 5.4: Optimal Step Responses Using Various Minimization Periods (F.T. = Finishing Time of Minimization)

The above problems translated to the fact that the index of Equation 5.2 could not be easily and reliably used for control weightings above 1.0.

C. NONLINEAR PERFORMANCE OF THE LINEAR OPTIMIZATION

For a linear control system, the characteristic response to a step input remains the same regardless of the magnitude of the step. The number of overshoots and undershoots, as well as the settling time, remains constant. These characteristics can only be changed by redesigning the system. For a system with signal limitations, the time required to carry out a step command increases with the size of the step. No prediction can be made as to the characteristic nature of the transient response. If the objective is to simply reduce the response time to its minimum value, the ideal operating procedure is to use a saturated drive at all times. The

concept is that maximum forward drive is applied at $t = 0$ and is reversed at a proper instant $t = t_{REVERSE}$, so that deceleration under maximum reverse drive reduces the velocity to zero at precisely the commanded value of the output. [Ref. 8:p. 433] This emphasis on total response time neglects the amount of total error in the response and places a hard limit on the amount of control input allowed; conversely, the cost functional of Equation 5.2 penalizes the amount of system error and effectively places an adjustable soft limit on the amount of control used. In the absence of any saturating elements, the amount of control used is only limited by the usage penalty imposed by Equation 5.2. The optimal control value determined by minimizing Equation 5.2 may or may not saturate any nonlinear element which is later introduced to the system. The question then arises as to what effect the introduction of a saturating element has on the optimal transient response of the linear system. To answer this question, the fourth-order plant of Equation 5.4 was employed with the feedback compensation scheme presented in Figure 5.1. The system was then optimized using the cost index of Equation 5.2. The control weighting, q, was set at 0.1, and a step input of 1.0 was used in the optimization. The optimal step response is presented in Figure 5.5. A saturating element was then introduced into the system as shown in Figure 5.6. Using the linear optimal solution, the nonlinear system was simulated for a 10.0 second period using various saturation limits. The results of these simulations are presented in Table 5.6. For saturation limits of ± 5.0 and above, no limiting effects were noted. The response time remained at approximately 3.5 seconds. As the saturation limits were lowered, the duration of the limiting increased. This increased limiting caused a corresponding increase in both the response time and the value of the cost index. It was noted that decreasing the saturation limits had the same effect as increasing the step size. The method of

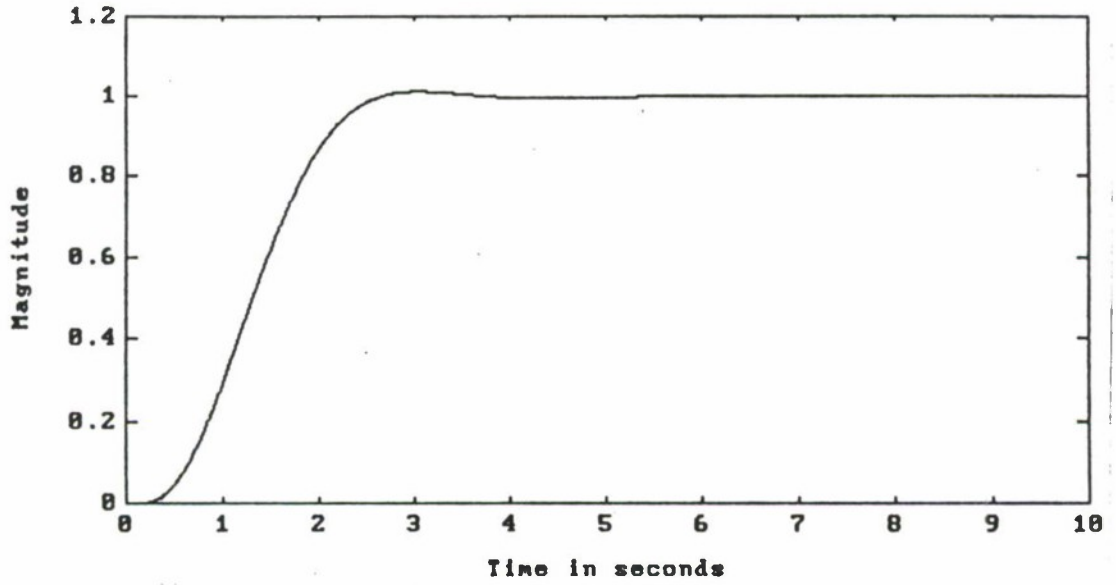

Figure 5.5: Step Response of Optimal Linear System

decreasing the saturation limits was chosen so as to allow the use of a common scale in the comparison of the performance criteria.

A graphical portrayal of selected trials from Table 5.6 are presented in Figures 5.7 and 5.8. Figure 5.7 shows the value of control used as a function of time for saturation limits of ± 5.0, $\pm$ 1.0, and $\pm$ 0.5. At a saturation limit of $\pm$ 5.0, no limiting occurred. When the saturation limits were lowered to ± 1.0 and ± 0.5, the system was constrained by the upper limit for progressively longer periods. The lower limits were never reached. Figure 5.8 shows the corresponding step responses of the systems portrayed in Figure 5.7. As the saturation limits were increased, the system became slower; however, the general form of the transient response was relatively unchanged. Although the percent overshoot was slightly reduced, the only significant adjustment was a slower rise time.

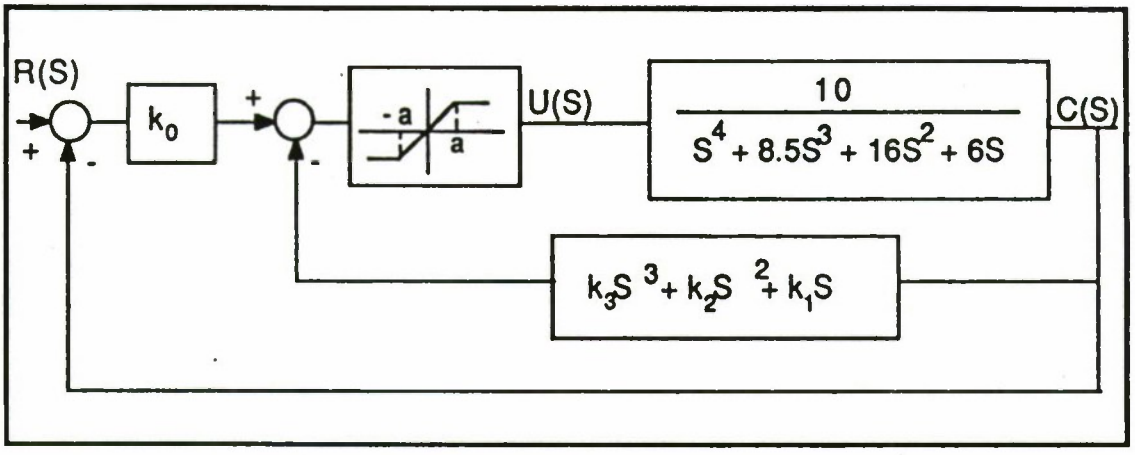

Figure 5.6: Block Diagram of Nonlinear System

TABLE 5.6: Linear System Optimization Employed with Nonlinear System; Step Size = 1.0, $q = 0.1$, Varying Saturation Limits

SATURATION LIMITS	VALUE OF $\int [t\,\|E\| + qU^2]\,dt$	DURATION OF SATURATION (SEC)	SETTLING TIME (SEC)
± 5.0	1.586	0.00	3.5
± 4.0	1.575	0.20	3.5
± 3.0	1.572	0.35	3.5
± 2.0	1.634	0.50	3.8
± 1.0	2.074	1.25	4.2
± 0.5	3.240	2.20	5.2

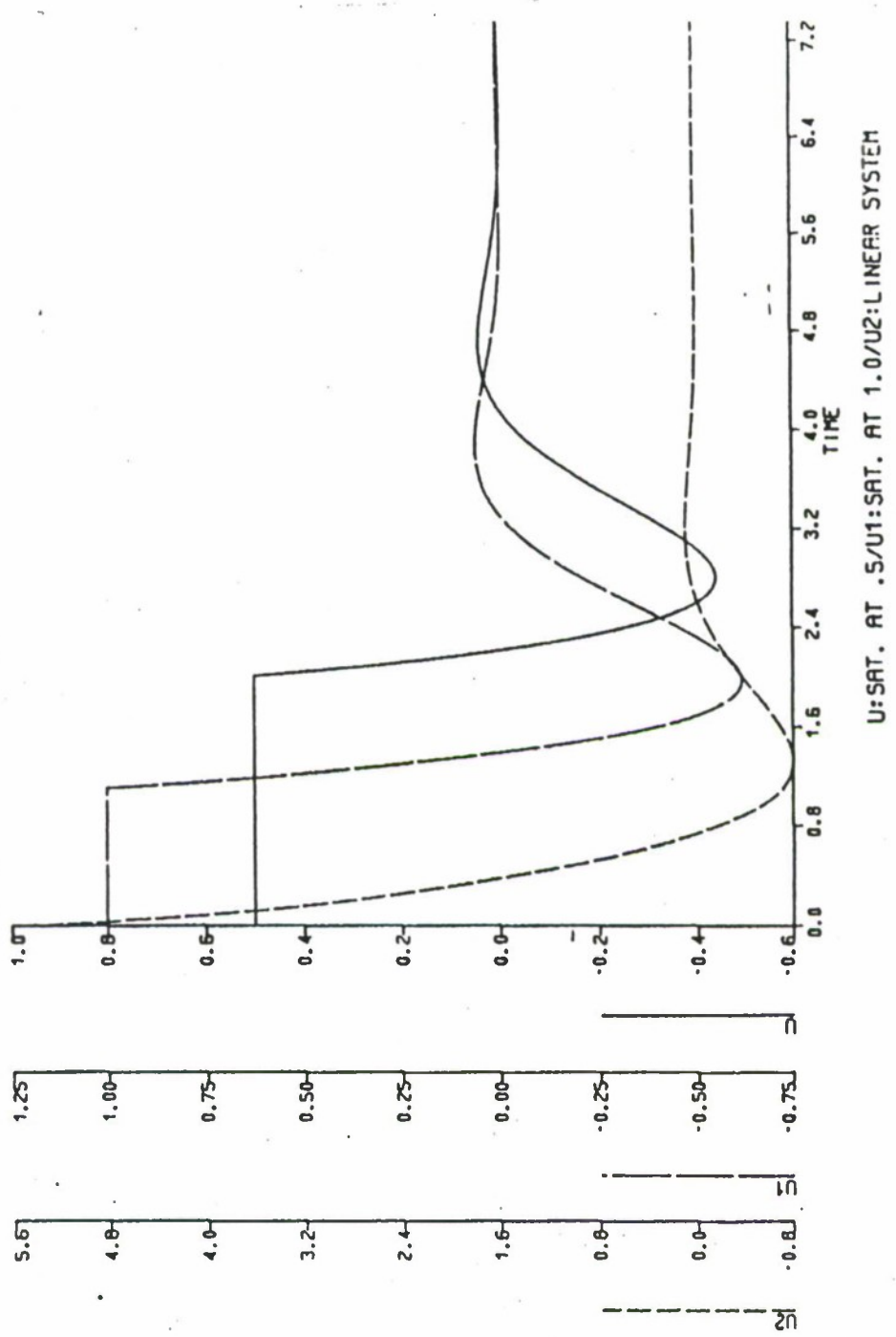

Figure 5.7: Control Input Response Curve for Saturation Limits of ± 5.0, ± 1.0, and ± 0.5. Saturation of ± 5.0 is Effectively a Linear System

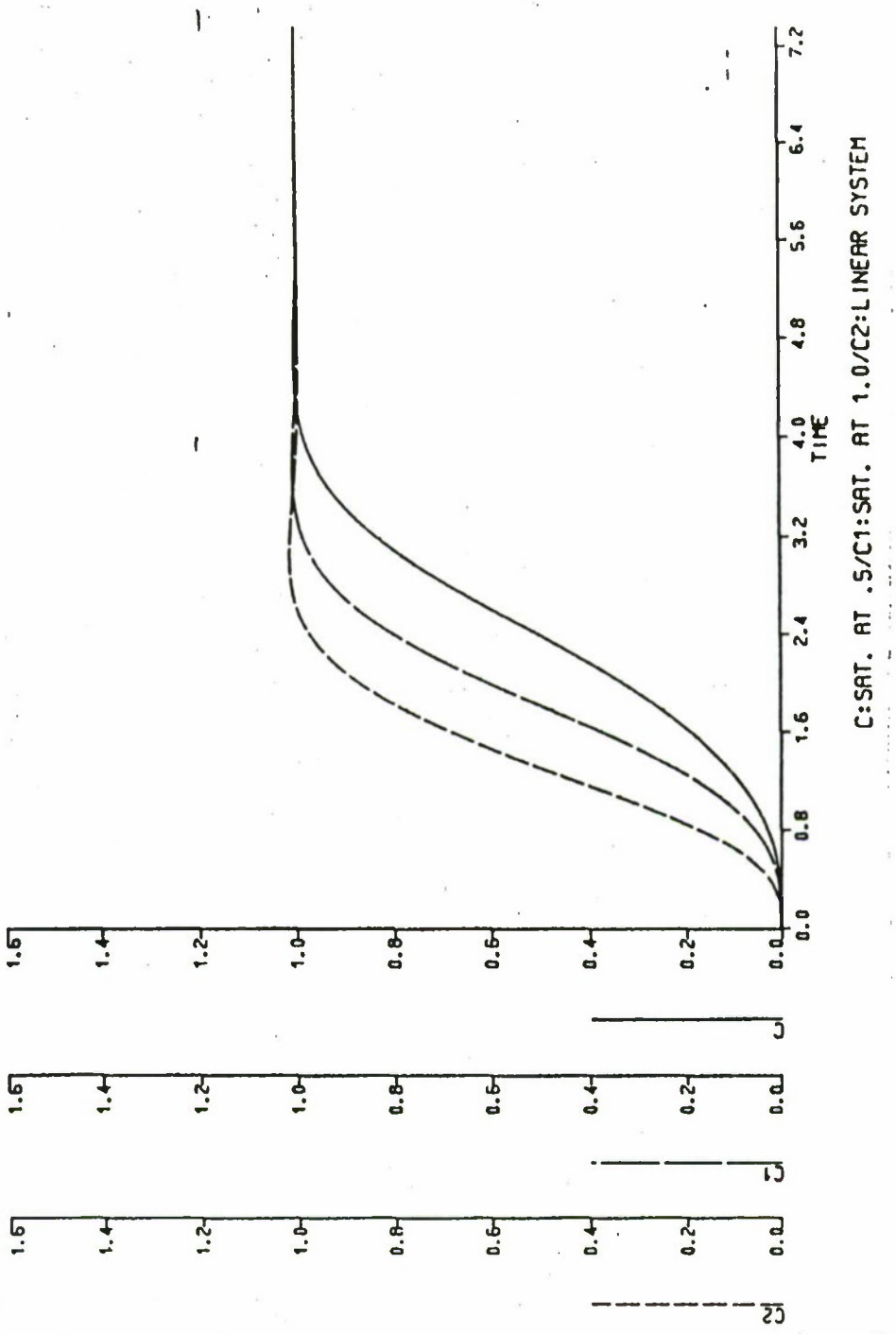

Figure 5.8: Step Responses of Systems Depicted in Figure 5.7

As previously mentioned, decreasing the saturation limits had the same effect as increasing the step input to the system; however, decreasing the limits was the most expedient way to heavily saturate the system. In order to provide this extreme saturation, saturation limits were set at ±5.0 and step inputs from 1.0 to 100.0 were used. Table 5.7 shows the results of the simulations. The general trends remained the same as those obtained by varying the saturation limits. As the step input was increased, the value of the cost index and the duration of the saturation and settling time were increased. The linear system was optimized to a specific control input

TABLE 5.7: Linear System Optimization Employed with Nonlinear System; $q = 0.1$, Saturation Limit = 5.0, Varying Step Size Input

SIZE OF STEP INPUT	VALUE OF $\int [t \lvert E \rvert + qu^2(t)]\, dt$	DURATION OF SATURATION (SEC)	SETTLING TIME (SEC)
1.0	1.586	0.00	3.5
1.5	2.675	0.20	5.0
2.0	3.784	0.40	5.2
5.0	13.362	1.20	5.8
10.0	38.490	2.00	6.2
50.0	847.460	8.81	11.8
100.0	4342.500	14.82	16.5

based on a control cost of 0.1 multiplied by the square of the control input. The optimal feedback gains reflected the best compromise between this value and the

value of time multiplied by the absolute value of the error. When the limiter was added to the system, the amount of control used was reduced during the period of saturation. The compromise was no longer valid. As the step input was increased, the system remained in saturation for longer periods of time. Longer saturation periods resulted in larger deviations from the compromise and, correspondingly, higher values for the cost index. During these saturation periods, the system was operating in an open loop mode, at full capacity, trying to correct the system error.

The control and output responses are depicted for selected step inputs in Figures 5.9 and 5.10, respectively. The general shape of the transient response remained unchanged, while the rise time became slower with increasing step size. It was of interest to note that even in the heavily saturated case of a step input equal to 100.0, the transient response maintained its characteristic one-overshoot, no-undershoot response.

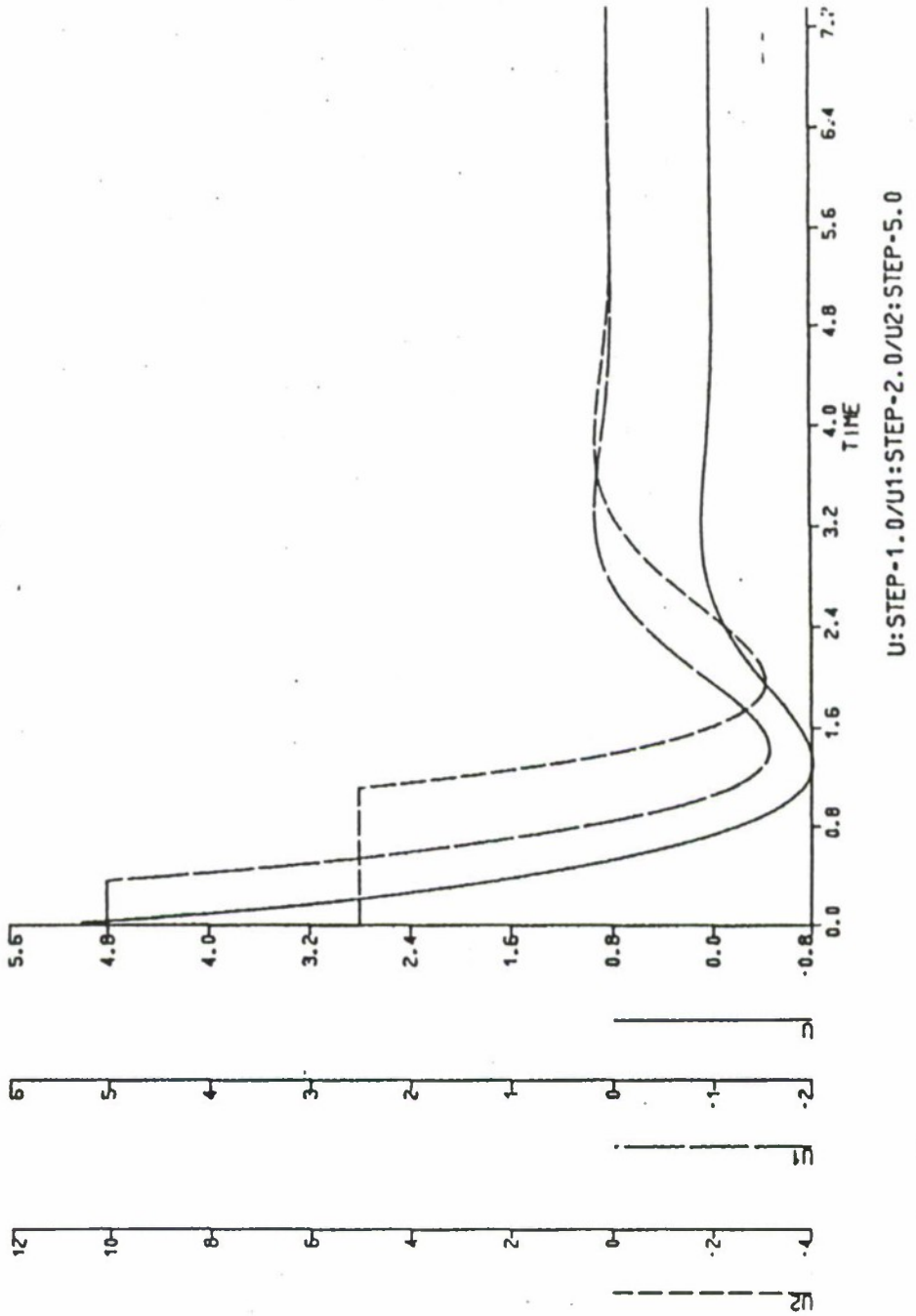

Figure 5.9: Control Input Response for Step Inputs of 5.0, 2.0, and 1.0

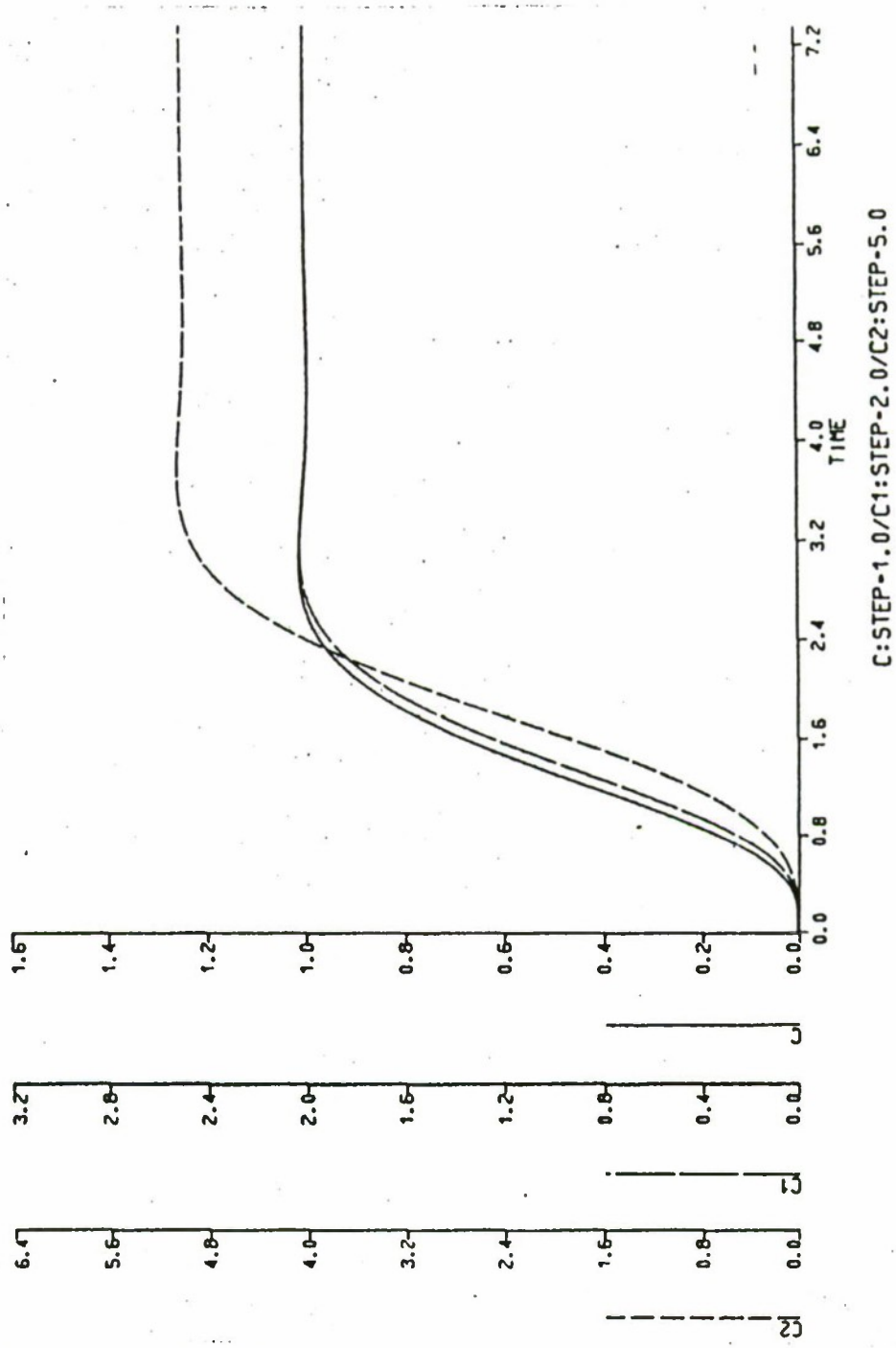

Figure 5.10: Step Responses for Step Inputs of 5.0, 2.0, and 1.0

D. COMPARISON OF COST INDEXES

In his work with the linear quadratic regulator of Equation 5.1, Sheldon S. L. Chang [Ref. 9] suggested that a linear system which had been optimized using this cost index was superior to one which had not. Chang asserted that when a saturating element was placed in the circuit, the system which was optimized using the cost function of the linear quadratic regulator showed a far superior transient response over a system which was not optimized using this cost index. The theory behind his allegation centered around the presence of the control cost within the performance index. He implied that the presence of this control cost reduced the magnitude of the control signal; consequently, the amount of saturation experienced by the system was reduced. Because of the reduced saturation, he forecast a much better transient response in terms of overshoot, undershoot, and settling time. [Ref. 9:pp. 11-30]

From Chang's work, a logical extension of theory was that the cost function of Equation 5.2 would exhibit the same traits as that of the linear quadratic regulator. Specifically, a linear system which was optimized using Equation 5.2 would perform better in the presence of a limiter than a system which was designed with no constraint on the amount of control used. The purpose of this section was to investigate this conjecture.

Using a control weighting of 0.1 in Table 5.4, it was found that the minimization of the cost index of Equation 5.2 resulted in optimal feedback gains of $k_0 = 5.37$, $k_1 = 6.59$, $k_2 = 2.38$, and $k_3 = 0.36$. Following the same procedure as was outlined in Chapter III, the fourth-order system was optimized using the integral of time multiplied by the absolute value of error. With the zero-derivative feedback gain set at 5.37, the optimal feedback gains were determined to be $k_1 = 4.90$, $k_2 = 0.97$, and $k_3 = -0.244$. This exercise provided two systems of the same bandwidth;

however, each system was designed by minimizing a different cost index. The performance index of the first system included a control cost with a weighting of $q = 0.1$, while the performance index of the second system provided no limit on the use of control input. Both optimizations were then simulated in the nonlinear system of Figure 5.6. The saturation limits of the limiter were varied and the value of the cost index of Equation 5.2 evaluated. The results of these simulations are presented in Table 5.8. System 1 refers to the minimization of the integral of time multiplied by the absolute value of the error, and system 2 refers to the minimization of Equation 5.2 with $q = 0.1$. Since system 2 was optimized with a constraint on the amount of control used, lower absolute saturation limits were needed before any limiting effects were seen. In this case, limiting effects were noted at the limits of ± 3.00. System 1 reached saturation with limits of $\pm$ 6.00. From the saturation limits of $\pm$ 6.00 to $\pm$ 1.00, the value of the cost index for system 1 exceeded the value of system 2. At the limit $\pm$ 1.00, the value of the cost indexes for the two systems became equal. System 1 had a saturation period of 2.6 seconds, which was more than double that of system 2. This did not imply that the control input of the two systems were equal; however, it did imply that the value obtained by adding the total system error to the control input was equal for the two systems. For absolute limiting values of less than $\pm$ 1.0, the value of the cost index for system 1, again, exceeded the value of system 2.

In Figures 5.11 and 5.12 are presented the control input and the step responses for the two systems at saturation limits of ± 5.0 and ± 1.0. Figure 5.11 shows that at a saturation limit of ± 5.0, system 1 was in saturation and system 2 was not. At the saturation limit of ± 1.0, system 2 was saturated by the upper limit while system 1 was saturated by both the upper and lower limit. Figure 5.12 shows the corresponding step responses for these systems. Even in the presence of heavy

TABLE 5.8: Simulation Results for Systems Optimized Using Different Cost Indices. System 1: Optimized Using $\int [t\,|e(t)|]\,dt$, System 2: Optimized Using $\int [t\,|e(t)| + 0.1u^2(t)]\,dt$, Step Input = 1.0, Simulation Period = 8.0 seconds.

SATURATION LIMITS	SATURATION PERIOD (SEC)		VALUE OF $\int [t\,\|e(t)\| + 0.1u^2(t)]\,dt$	
	SYSTEM 1	SYSTEM 2	SYSTEM 1	SYSTEM 2
± 6.00	0.2	0.0	2.38	1.59
± 5.00	0.4	0.0	2.21	1.59
± 3.00	0.7	0.3	1.79	1.57
± 1.00	2.6	1.2	2.07	2.07
± 0.50	3.9	1.8	3.43	3.24
± 0.25	5.8	4.6	6.35	5.93

saturation, system 1 remained faster; however, it experienced more overshoot of the steady-state position. In terms of which system responded best in the presence of a limiter, system 2 had a very slight advantage. When the limit was moved from no saturation at limits of ±5.0 to heavy saturation at limits of ±1.0, the transient response of system 2 maintained its basic shape. The major change was a slower rise time accompanied by a slightly lower percent overshoot. System 1 also decreased its rise time, but increased its percent overshoot as well. System 1 maintained its faster response to the first steady-state crossing throughout the range of limiting values. The question of which was the better response remained a question of the use for which the system was to be used; however, the results did not indicate a large advantage for including a control cost in the performance index. When placed in heavy saturation, neither system exhibited any type of rapid deterioration of the

response. Inclusion of the control cost in the performance index of the linear system did provide a slightly more favorable and predictable response when subjected to a limiter; specifically, the response stayed, essentially, the same with a predictable decrease in rise time.

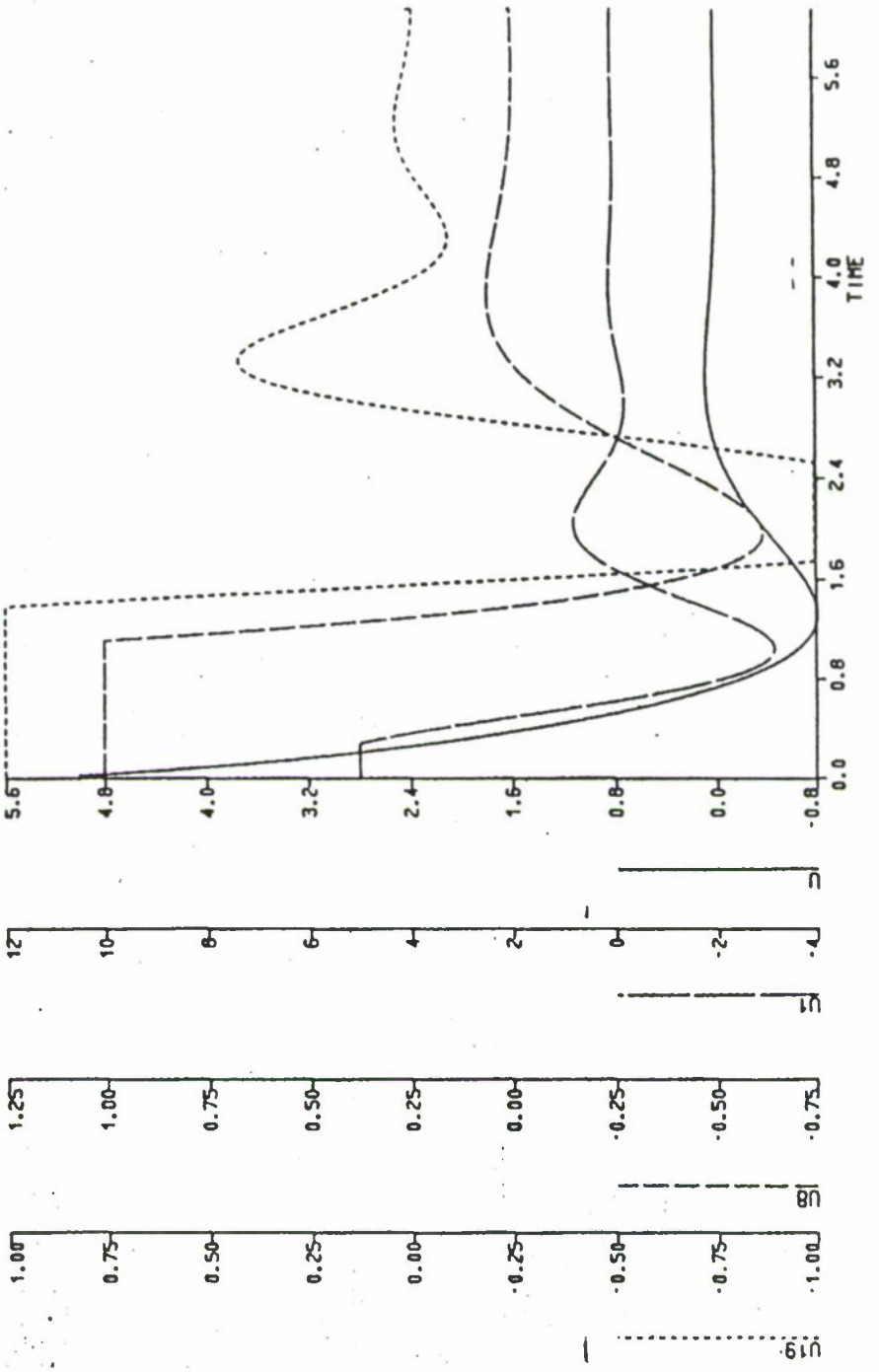

Figure 5.11: Control Input Response
U: System 2 with Limiter at ±5.0
U1: System 1 with Limiter at ±5.0
U8: System 2 with Limiter at ±1.0
U19: System 1 with Limiter at ±1.0

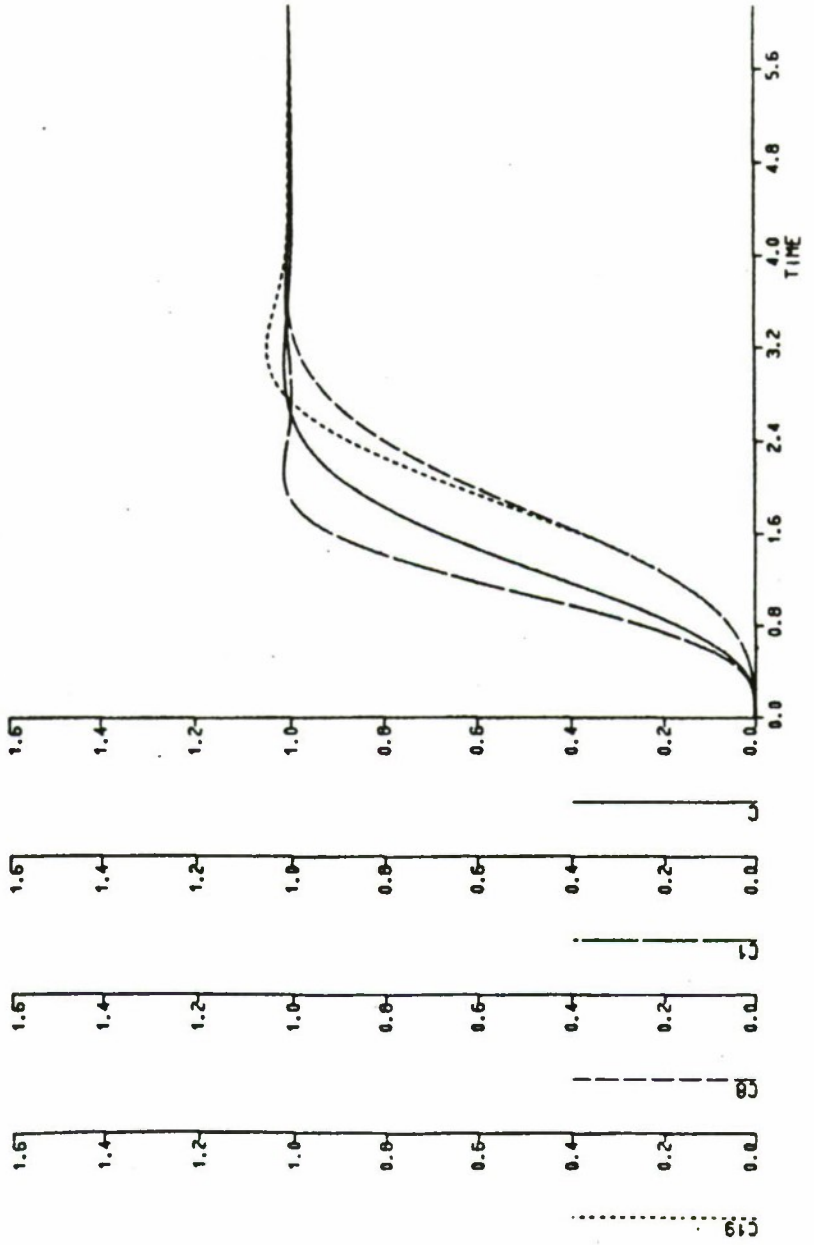

Figure 5.12: Step Response
C: System 2 with Limiter at ±5.0
C1: System 1 with Limiter at ±5.0
C8: System 2 with Limiter at ±1.0
C19: System 1 with Limiter at ±1.0

E. THE LINEAR QUADRATIC REGULATOR

Based on the results of the previous section, it was of interest to further investigate Chang's work with the linear quadratic regulator. Chang based his conclusions on the results of a single example. It was the purpose of this section to repeat this example to determine if the results could be duplicated. Chang's design process was not questioned, only the performance of and the conclusions drawn from the final design.

A hydraulic system for position control was designed with the specifications of 15.0 percent overshoot or less, and a response time of approximately 0.01 seconds. The transfer function of the hydraulic valve and servomotor system is given in Equation 5.5,

$$G_p(S) = \frac{K}{S\left[1.0 + 0.4\left(\frac{S}{\omega}\right) + \left(\frac{S}{\omega}\right)^2\right]} \tag{5.5}$$

where K=200.0 radians/second and ω = 157.0 radians/second. Chang proposed two cascade compensation schemes. The first of these was designed by conventional root-locus techniques with no regard to the amount of control input used. The second design was based on a root-square-locus plot which attempted to minimize the amount of control used in accordance with the linear quadratic regulator. Equal weighting was given to the total system error and the amount of control used. The transfer functions of the conventional and root-square-locus compensation are presented in Equations 5.6 and 5.7, respectively.

$$G_{c1}(S) = \frac{1.04\left[1.0 + 0.4\left(\frac{S}{\omega}\right) + \left(\frac{S}{\omega}\right)^2\right]}{\left[1.0 + 0.615\left(\frac{S}{\omega}\right)\right]\left[1.0 + 0.069\left(\frac{S}{\omega}\right)\right]} \tag{5.6}$$

$$G_{c2}(S) = \frac{0.859\left[1.0 + 0.4\left(\frac{S}{\omega}\right) + \left(\frac{S}{\omega}\right)^2\right]}{1.0 + 0.453\left(\frac{S}{\omega}\right) + 0.110\left(\frac{S}{\omega}\right)^2} \tag{5.7}$$

The system utilizing the compensation of Equation 5.7 was called the optimum system, and the system employing the compensation scheme of Equation 5.6 was called the conventional system. Note that both compensation schemes employed the compensator zeros to cancel the plant's poles, and replaced these poles with the poles of the compensator. [Ref. 10:pp. 81-87] To determine the performance of these systems in the presence of a limiter, the compensation schemes were simulated in the system of Figure 5.13 with step inputs of 1.0. Setting saturation limits of ± 10.0, the responses of Figures 5.14 and 5.15 were obtained. Figure 5.14 gives the responses of signals $X(S)$ and $U(S)$, and shows that neither system was in saturation. The corresponding output responses are shown in Figure 5.15. Both systems were operating in the linear region and had nearly identical step responses.

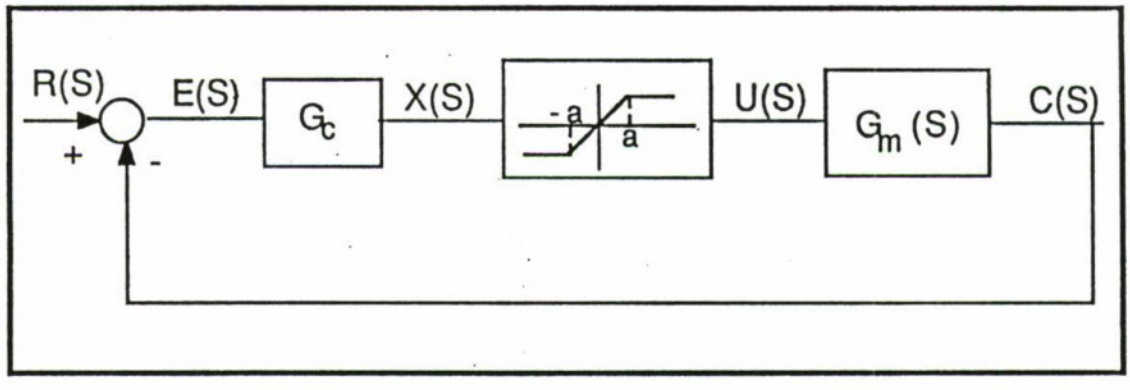

Figure 5.13: Block Diagram of Nonlinear System Used in Chang's Example

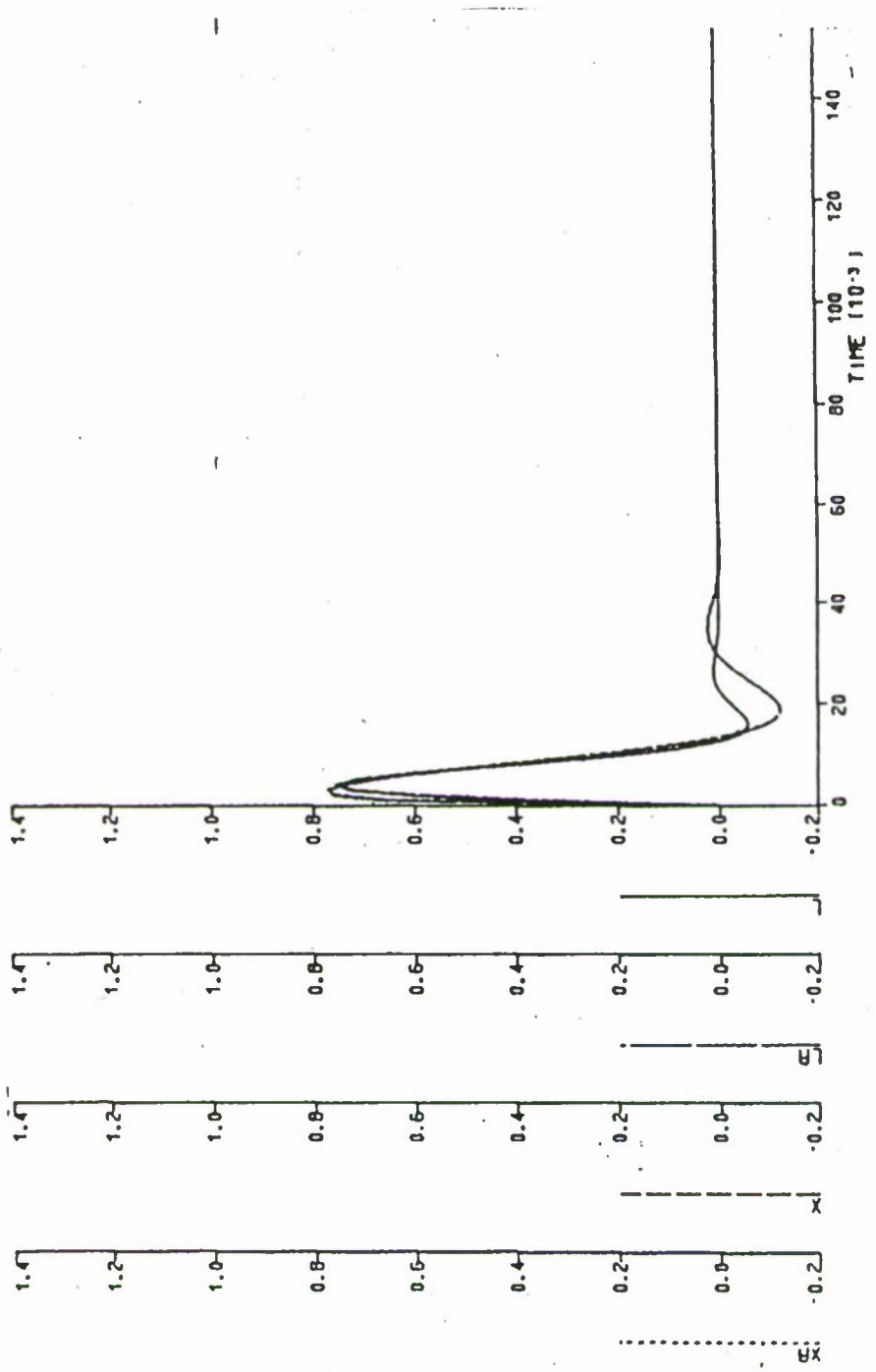

Figure 5.14: Signals $X(S)$ and $U(S)$ Corresponding to Figure 5.13, Limits = ±10.0.
L: Optimal $U(S)$ Signal
LA: Conventional $U(S)$ Signal
X: Optimal $X(S)$ Signal
XA: Conventional $X(S)$ Signal

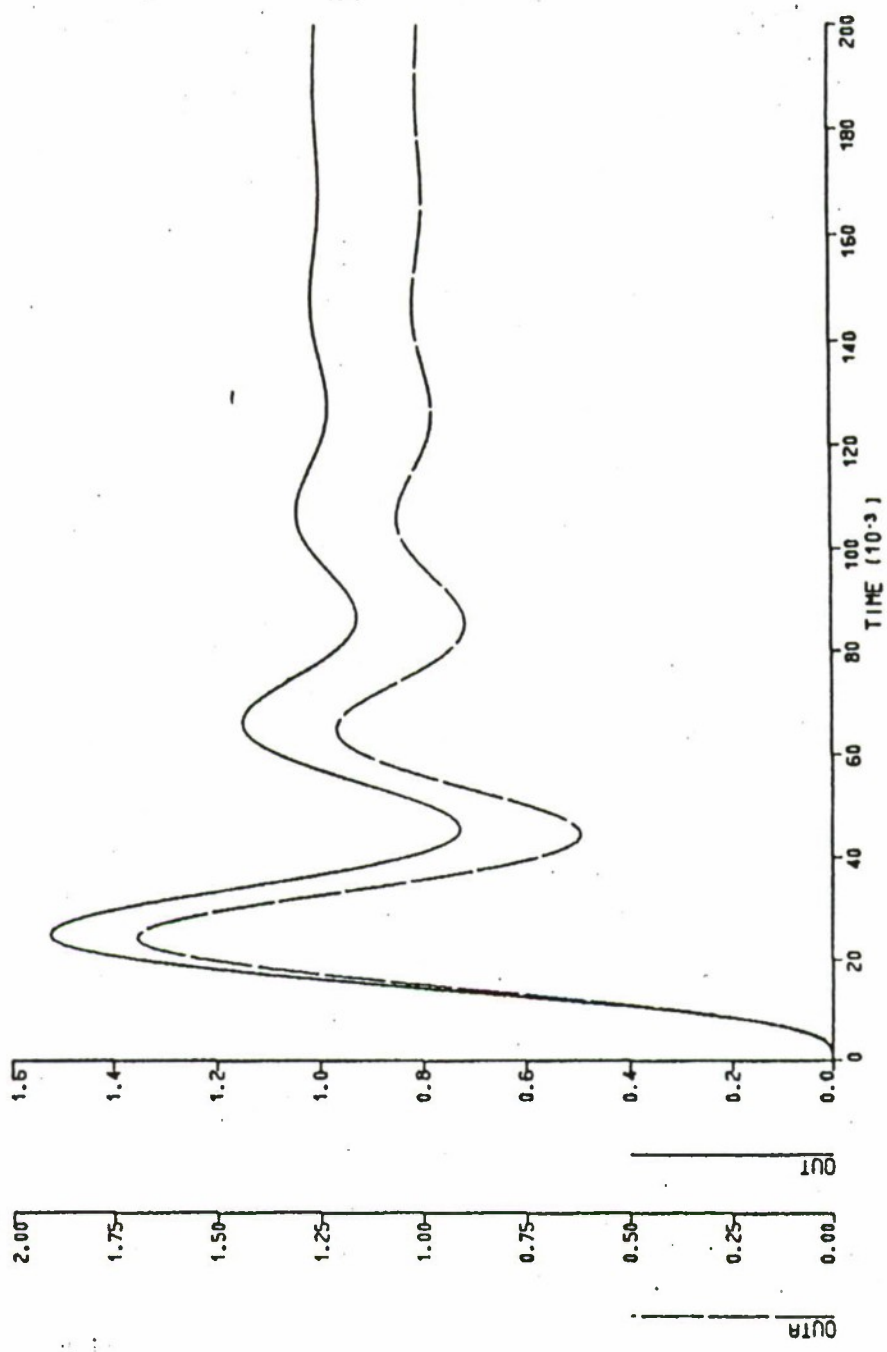

Figure 5.15: Step Responses of Optimal and Conventional Systems, Limits = 10.0
OUT: Output of Optimal System
OUTA: Output of Conventional System

Noting that the input to the limiter reached a maximum of approximately 0.75 for both systems, the saturation point was successively moved to lower saturation values to find the point of greatest divergence between the two step responses. Saturation limits of ± 0.4 were found to provide the largest variance between the optimal and conventional systems. The graphical results of this simulation is provided in Figures 5.16 and 5.17. Figure 5.16 shows that the conventional system remained in saturation slightly longer than the optimal system, resulting in the differing step responses of Figure 5.17. Although the conventional system had larger overshoots and undershoots than the optimal system, these oscillations quickly damped-out to a settling time of 0.15 seconds for both systems. The rapid deterioration of the conventional system, alluded to by Chang, was never obtained.

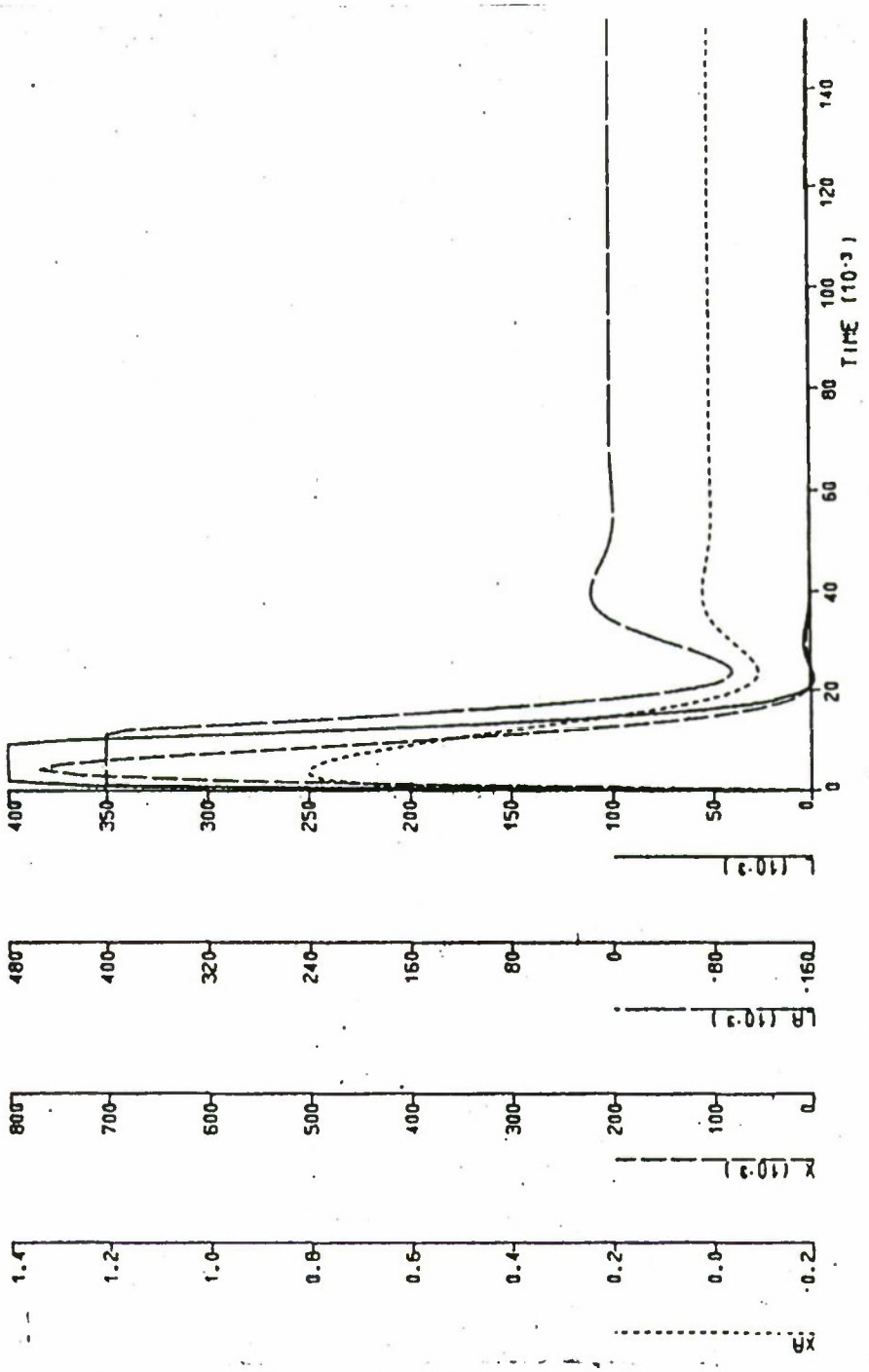

Figure 5.16: Signals $X(S)$ and $U(S)$ Corresponding to Figure 5.13, Limits = 0.4
L: Optimal $U(S)$ Signal
LA: Conventional $U(S)$ Signal
X: Optimal $X(S)$ Signal
XA: Conventional $X(S)$ Signal

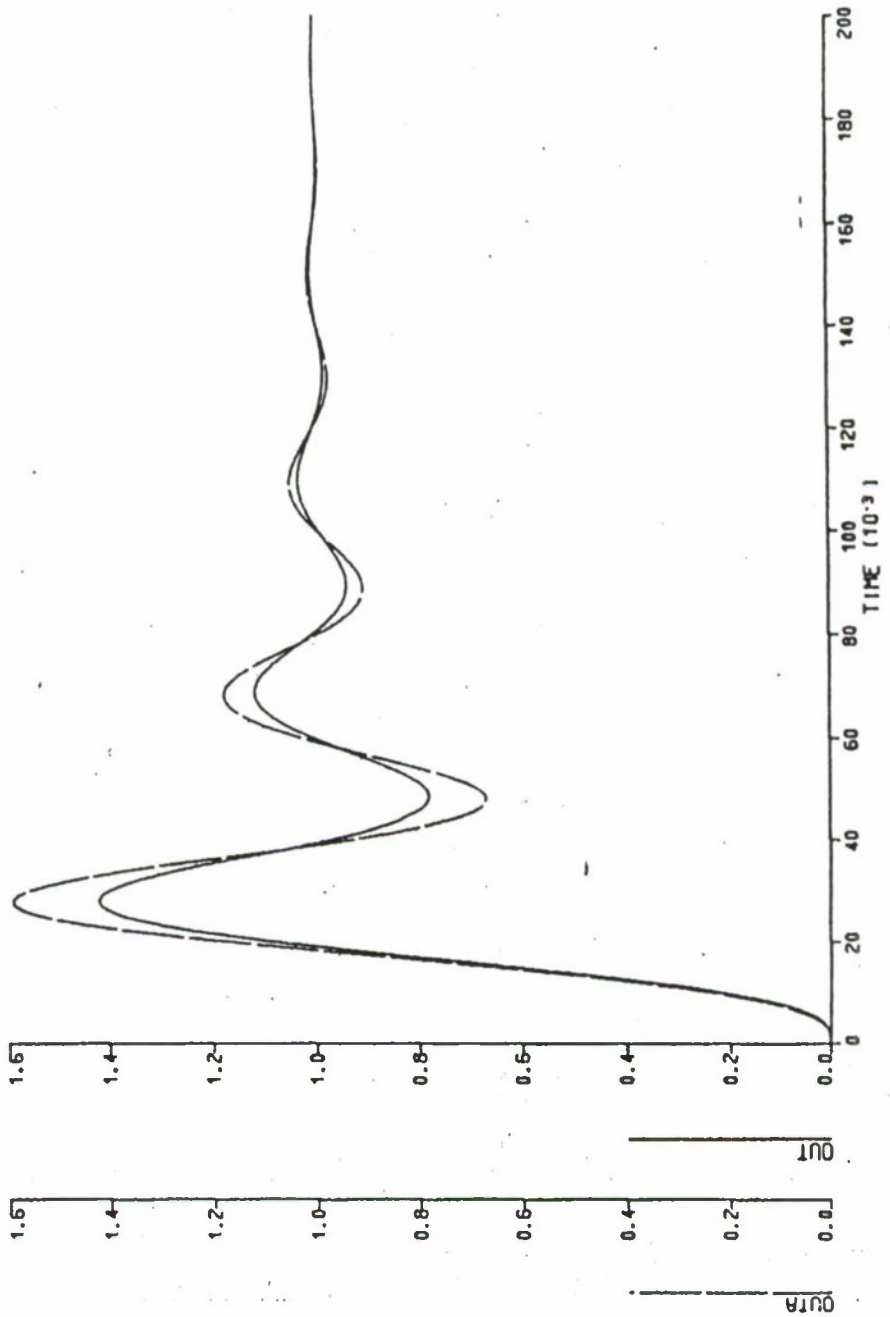

Figure 5.17: Step Responses of Optimal and Conventional Systems, Limits = ±0.4
OUT: Output of Optimal System
OUTA: Output of Conventional System

Chang argued that since the conventional system's input to the limiter was larger than that of the optimal system, the conventional system would saturate more heavily and result in a much poorer response. In light of the results of this investigation, as well as those of the previous section, it could only be concluded that the presence of a control cost in the performance index did little to enhance the performance of a nonlinear system.

F. LINEAR PERFORMANCE OF A NONLINEAR OPTIMIZATION

Thus far, the study dealt with the effects of inserting a saturating nonlinearity into an optimal linear system. It was the purpose of this section to optimize the nonlinear system and evaluate its performance after the nonlinearity had been removed.

To investigate this possibility, the nonlinear system of Figure 5.6 was optimized using the cost index of Equation 5.2. Various values of the control weighting were used. It is important to note that before optimizing the nonlinear system, it was necessary to ensure that the saturation limits were small enough to allow operation in the nonlinear region. If the limits were too large, the optimization would have been, in essence, a linear optimization. For the system of Figure 5.6, saturation limits of ± 3.0 and ± 1.0 were used. The results of the nonlinear optimization are presented in Table 5.9. If Table 5.9 is compared to the linear optimization of Table 5.4, the effect of the nonlinearity can be seen. At saturation limits of ± 3.0, the nonlinear system was in saturation for only a short time with the remainder of the transient period operating in the linear region; consequently, there was little difference between the nonlinear optimal parameters and the linear optimal parameters. At the saturation limits of ± 1.0, the nonlinear system remained saturated for approximately one-half

of the transient period; consequently, substantially different optimal feedback gains were obtained.

Removing the nonlinearity from the system of Figure 5.6 and employing the nonlinear optimal gains of Table 5.9, the step responses of Figure 5.18 were obtained. They represent nonlinear optimal parameters employed in a linear system. As the value of the control weighting was increased, the optimal parameters resulted in slower system responses. The reason for this trend could be seen by examining the nonlinear optimization process. During optimization, the system operated in either the saturated or linear region. When the system was in saturation, the amount of control was set by the limiter. When the system was operating in the linear region, the amount of control was determined by the value of the control weighting. As the control weighting was increased, the amount of control used during the linear operation decreased; consequently, less control input resulted in slower systems.

TABLE 5.9: Optimizing the Nonlinear System Using $\int [t\,|e(t)| + qu^2(t)]\,dt$, Step Input = 1.0, Integration Time = 10.0 sec.

VALUE OF LIMITS	VALUE OF OF q	VALUE OF COST INDEX	OPTIMAL FEEDBACK GAINS
±3.0	0.1	1.582	$k_0 = 5.417$ $k_1 = 6.585$ $k_2 = 2.343$ $k_3 = 0.319$
±3.0	0.5	2.596	$k_0 = 2.485$ $k_1 = 3.611$ $k_2 = 1.322$ $k_3 = 0.255$
±3.0	1.0	3.320	$k_0 = 2.476$ $k_1 = 4.069$ $k_2 = 1.965$ $k_3 = 0.595$
±3.0	5.0	5.979	$k_0 = 2.111$ $k_1 = 4.681$ $k_2 = 3.661$ $k_3 = 1.994$
±3.0	10.0	7.641	$k_0 = 1.431$ $k_1 = 3.391$ $k_2 = 2.831$ $k_3 = 1.781$
±3.0	100.0	20.246	$k_0 = 0.382$ $k_1 = 0.988$ $k_2 = 1.205$ $k_3 = 1.203$
±1.0	0.1	1.968	$k_0 = 7.356$ $k_1 = 7.320$ $k_2 = 1.918$ $k_3 = -0.029$
±1.0	0.5	2.655	$k_0 = 4.687$ $k_1 = 6.044$ $k_2 = 2.324$ $k_3 = 0.343$
±1.0	1.0	3.278	$k_0 = 4.521$ $k_1 = 4.521$ $k_2 = 2.608$ $k_3 = 0.389$
±1.0	5.0	5.813	$k_0 = 3.477$ $k_1 = 7.642$ $k_2 = 6.146$ $k_3 = 2.864$
±1.0	10.0	7.545	$k_0 = 1.100$ $k_1 = 2.412$ $k_2 = 1.694$ $k_3 = 0.992$
±1.0	100.0	21.792	$k_0 = 0.732$ $k_1 = 2.314$ $k_2 = 5.686$ $k_3 = 1.013$

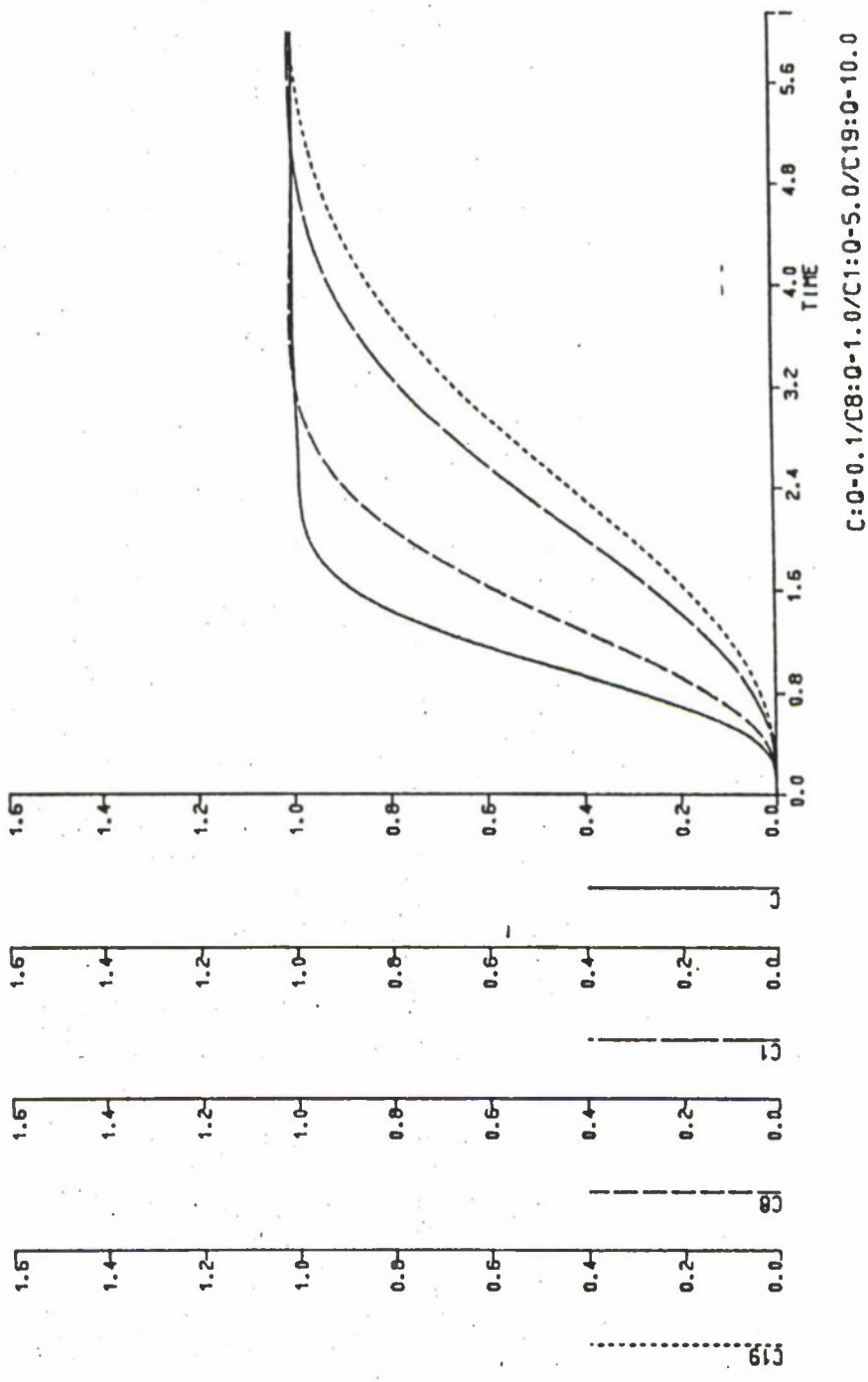

Figure 5.18: Step Responses of Nonlinear Optimal Gains (Limits = ±1.0) When Employed in a Linear System

G. COMPARISON OF NONLINEAR AND LINEAR OPTIMAL SYSTEMS

In order to better determine the differing effects between the optimization of a linear system and a nonlinear system, a battery of simulations was conducted using the feedback gains presented in Tables 5.4 and 5.9. The values of Table 5.4 reflect the results of the fourth-order linear optimization, and Table 5.9 reflects the results of the fourth-order nonlinear optimization. For each control weighting, the optimal linear and nonlinear gains were simulated in both a nonlinear and linear system. The results of the nonlinear system simulations are presented in Figures 5.19 through 5.24. Referring to Figures 5.19 and 5.20, which reflect a control weighting of 0.1, the nonlinear optimization remained in saturation much longer than that of the linear optimization. The heavy saturation of the nonlinear optimization resulted in a faster and less costly step response. The nonlinear gains had a performance index value of 1.968, while the linear gains resulted in a value of 2.073. The nonlinear gains utilized the system to its full capacity for nearly the entire transient period.

As the control weighting was increased to higher values, the superiority of the nonlinear gains decreased. For a control weighting of 1.0, the value of the performance indices were nearly equal for the two systems. The nonlinear gains resulted in a cost of 3.278, and the linear gains gave a cost of 3.261. As shown in Figure 5.21, both systems saturated only at the upper limit with the nonlinear system remaining in saturation for a longer period of time. As shown in Figure 5.22, the nonlinear gains resulted in a faster rise time for the step response.

The difference between the nonlinear and linear responses continued to decrease as the control weighting was increased to 5.0. Figures 5.23 and 5.24 show that neither system remained in saturation for long periods of time, and the step responses were nearly identical.

The above results reinforce the knowledge that the most efficient system is one that utilizes its components to their full capacity. If the control weighting is small enough to allow the system to saturate, a more optimal system is attained through the optimization of the nonlinear system. In the system under study, control weightings of below 1.0 were required. In other performance indices, such as the linear quadratic regulator, the range of control weightings which cause saturation will expand. This means that nonlinear optimization remains superior for higher values of the control weighting. As the control weightings are increased to values which do not allow long saturation periods, linear and nonlinear optimal gains perform equally as well.

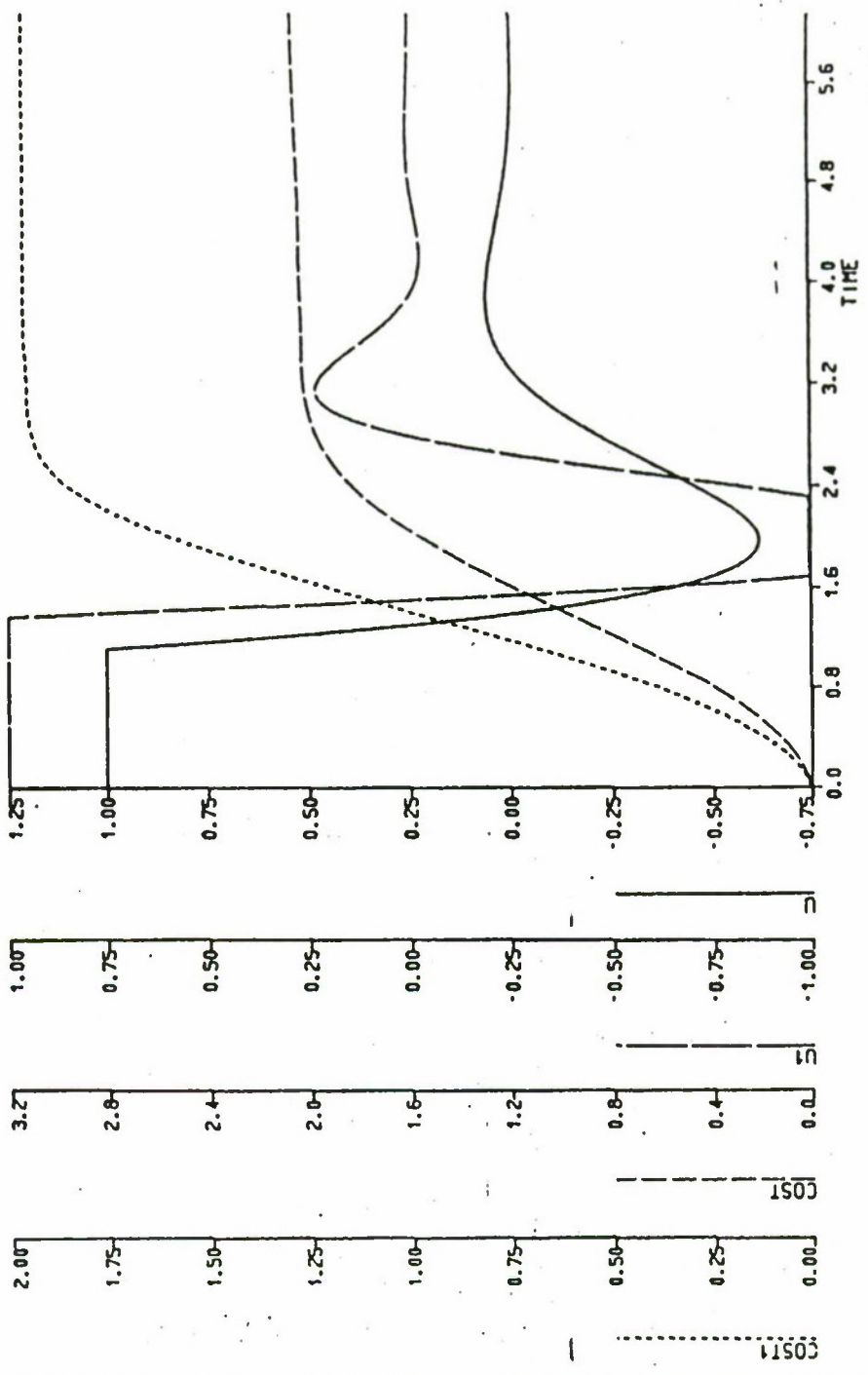

Figure 5.19: Linear Versus Nonlinear Optimal Gains in a Nonlinear System, q=0.1
U: Control Signal for Linear Gains
$U1$: Control Signal for Nonlinear Gains
COST: Value of Cost Index for Linear Gains
COST1: Value of Cost Index for Nonlinear Gains

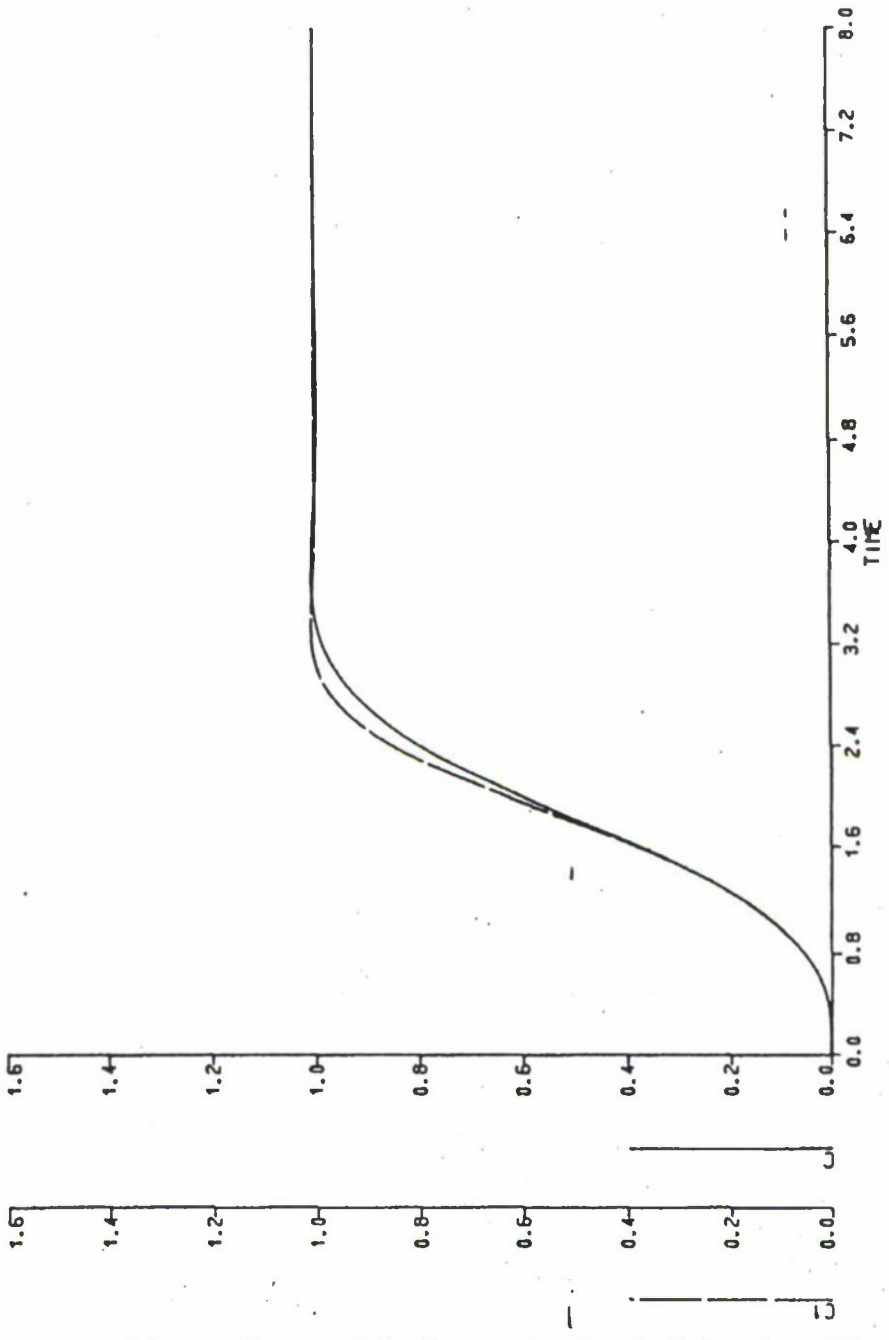

Figure 5.20: Linear Versus Nonlinear Optimal Gains in a Nonlinear System, q=0.1
C: Control Signal for Linear Gains
$C1$: Control Signal for Nonlinear Gains

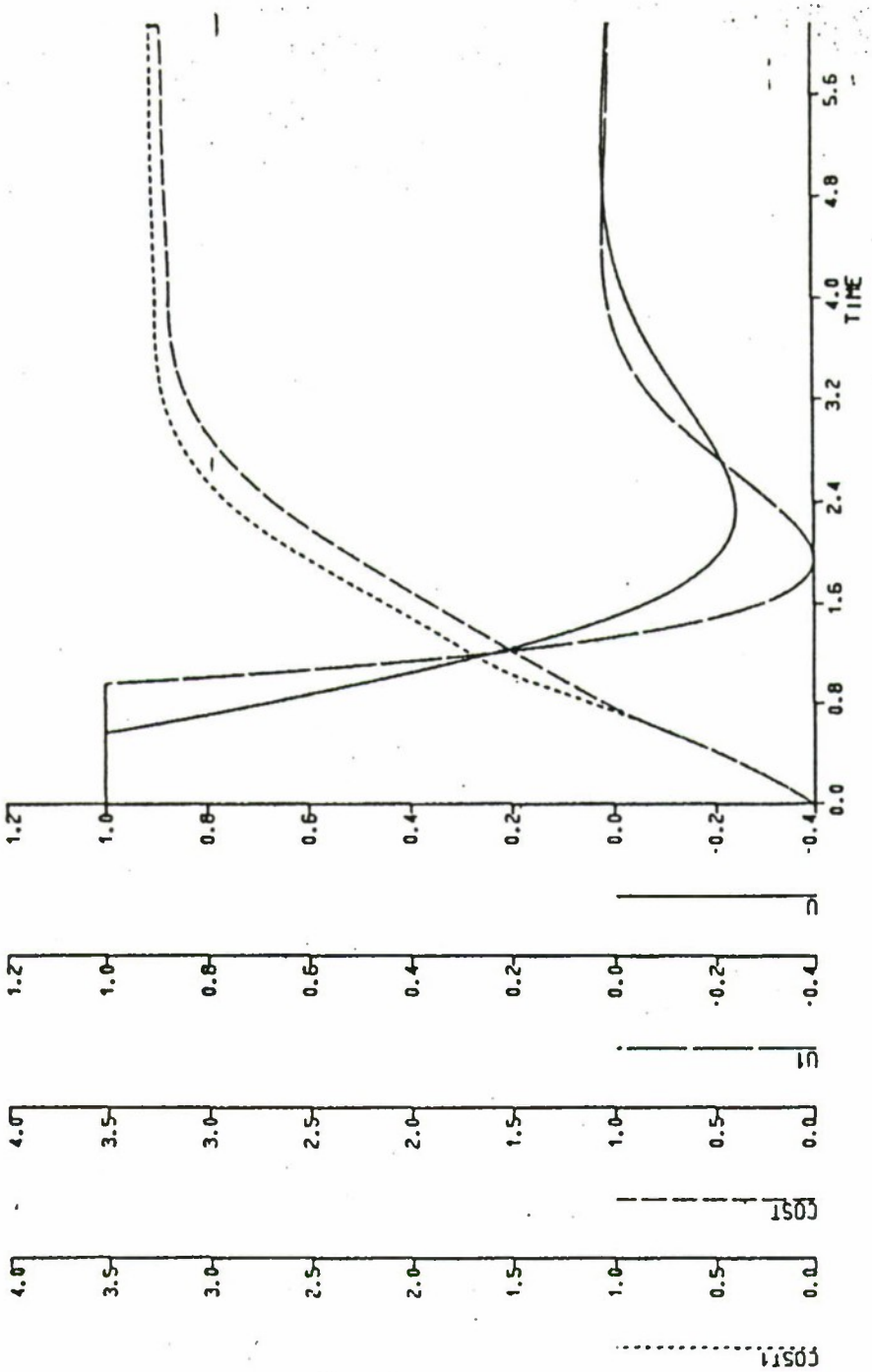

Figure 5.21: Linear Versus Nonlinear Optimal Gains in a Nonlinear System, q=1.0
U: Control Signal for Linear Gains
$U1$: Control Signal for Nonlinear Gains
COST: Value of Cost Index for Linear Gains
COST1: Value of Cost Index for Nonlinear Gains

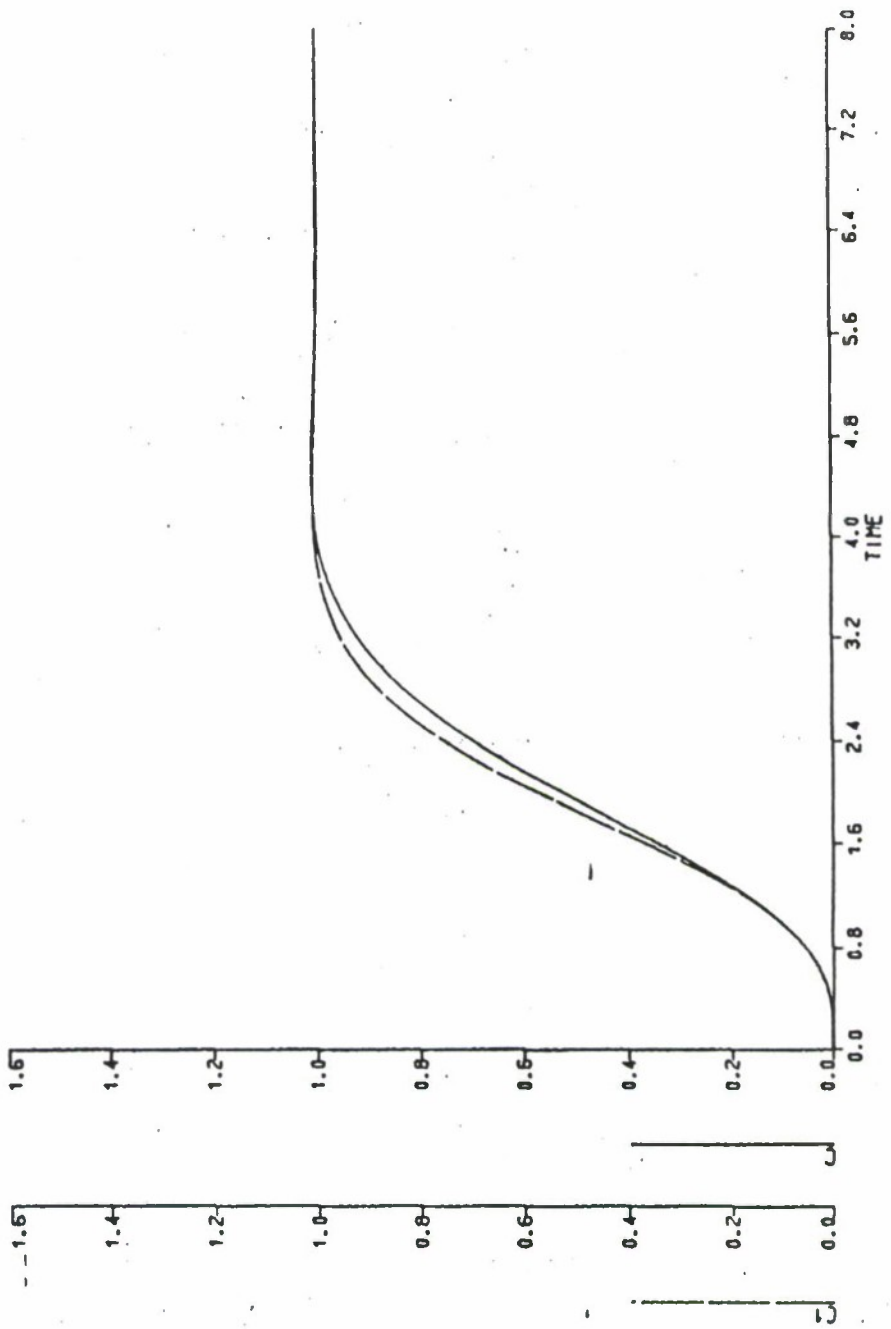

Figure 5.22: Linear Versus Nonlinear Optimal Gains in a Nonlinear System, q=1.0
C: Control Signal for Linear Gains
$C1$: Control Signal for Nonlinear Gains

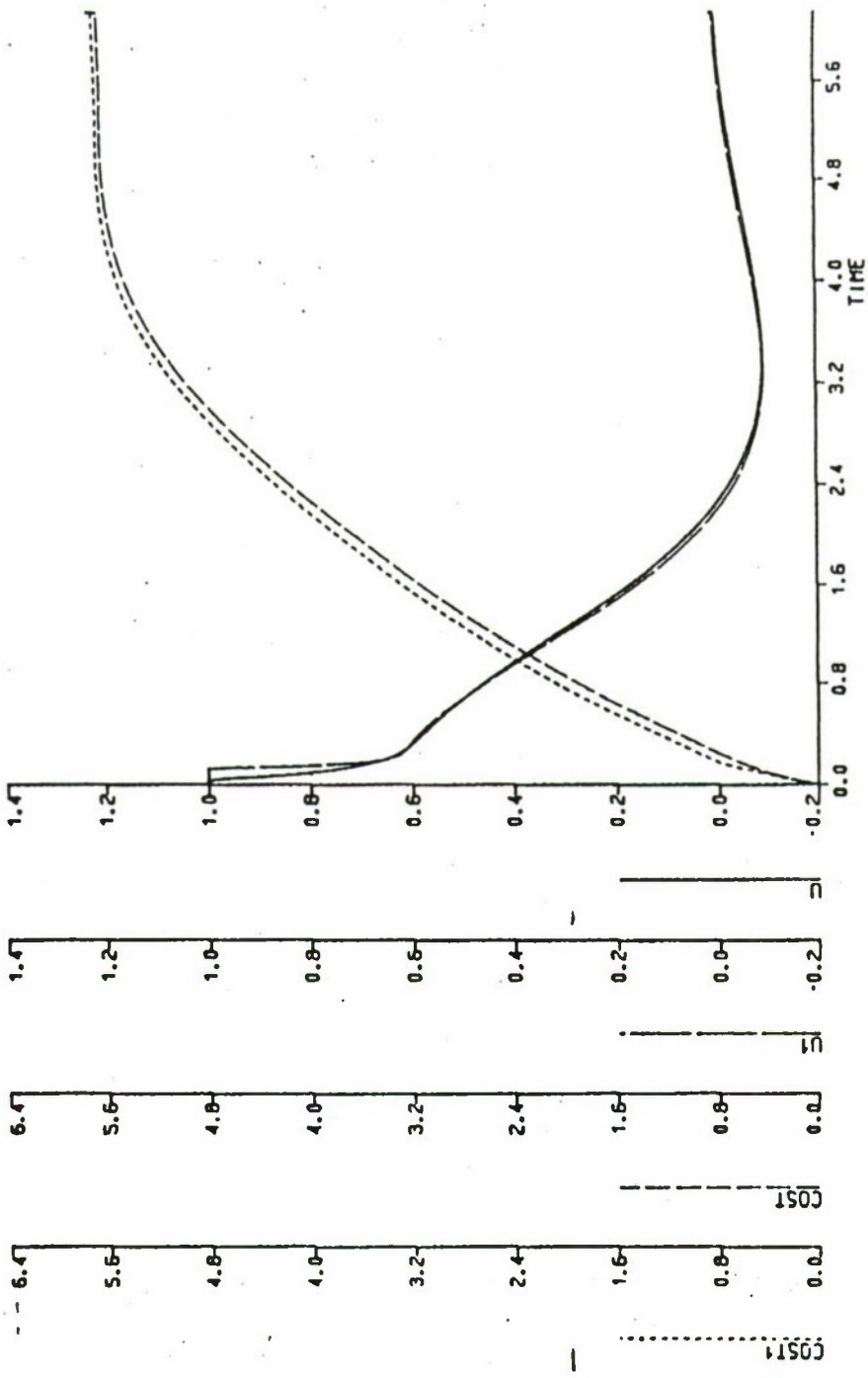

Figure 5.23: Linear Versus Nonlinear Optimal Gains in a Nonlinear System, q=5.0
U: Control Signal for Linear Gains
$U1$: Control Signal for Nonlinear Gains
COST: Value of Cost Index for Linear Gains
COST1: Value of Cost Index for Nonlinear Gains

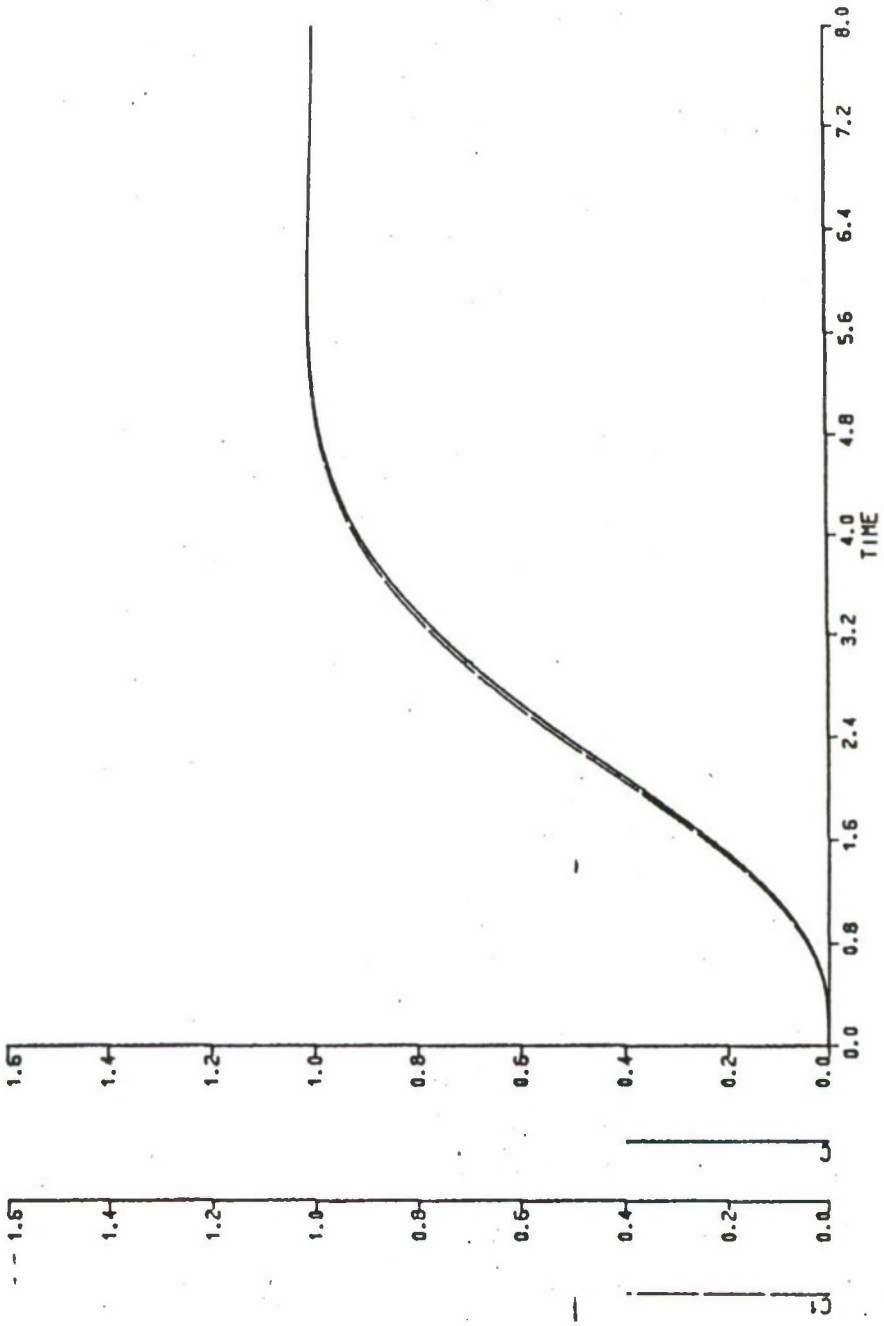

Figure 5.24: Linear Versus Nonlinear Optimal Gains in a Nonlinear System, q=5.0
C: Control Signal for Linear Gains
$C1$: Control Signal for Nonlinear Gains

Following the above studies, the linear and nonlinear optimal gains were simulated in a linear system. The graphical results of these simulations are presented in Figures 5.25 through 5.27. For all values of the control weighting, the nonlinear gains resulted in a faster response and a higher value of the performance index.

For a cost weighting of 0.1, the graphs of Figures 5.25 and 5.26 show that the control signal of the nonlinear system had more overshoot and undershoot than that of the linear system. During the optimization of the nonlinear system, the minimization of the cost function attempted to keep the system in constant saturation. The value of the cost index was reduced by operating the system near saturation. The value of time multiplied by the absolute value of the error was reduced by increasing the rise time and decreasing the overshoot. In the linear optimization, the optimal cost reduction was attained by reducing the control signal. The smaller control signal resulted in a slower rise time and more overshoot. The minimization of the cost index was a trade-off between the amount of control and the integral of time multiplied by the absolute value of error. In the nonlinear optimization, the greatest reduction in the index came from a reduction of time multiplied by the absolute value of error. In the linear system optimization, the greatest reduction came from a reduction of the control signal. When the results of both systems were placed in a linear system, the optimal nonlinear gains resulted in a faster system with less overshoot. The nonlinear gains were not optimal for the linear system and resulted in a higher value of the cost index. The value of the cost index for the linear system was 1.58, while that of the nonlinear system was 2.25.

As the value of the control weighting was increased to 5.0, the nonlinear and linear gains gave an almost identical response. This control weighting precluded the nonlinear optimization from operating in constant saturation and bounded it to the

linear region for the majority of the transient period. As shown in Figures 5.27 and 5.28, the characteristics of the two systems became nearly identical.

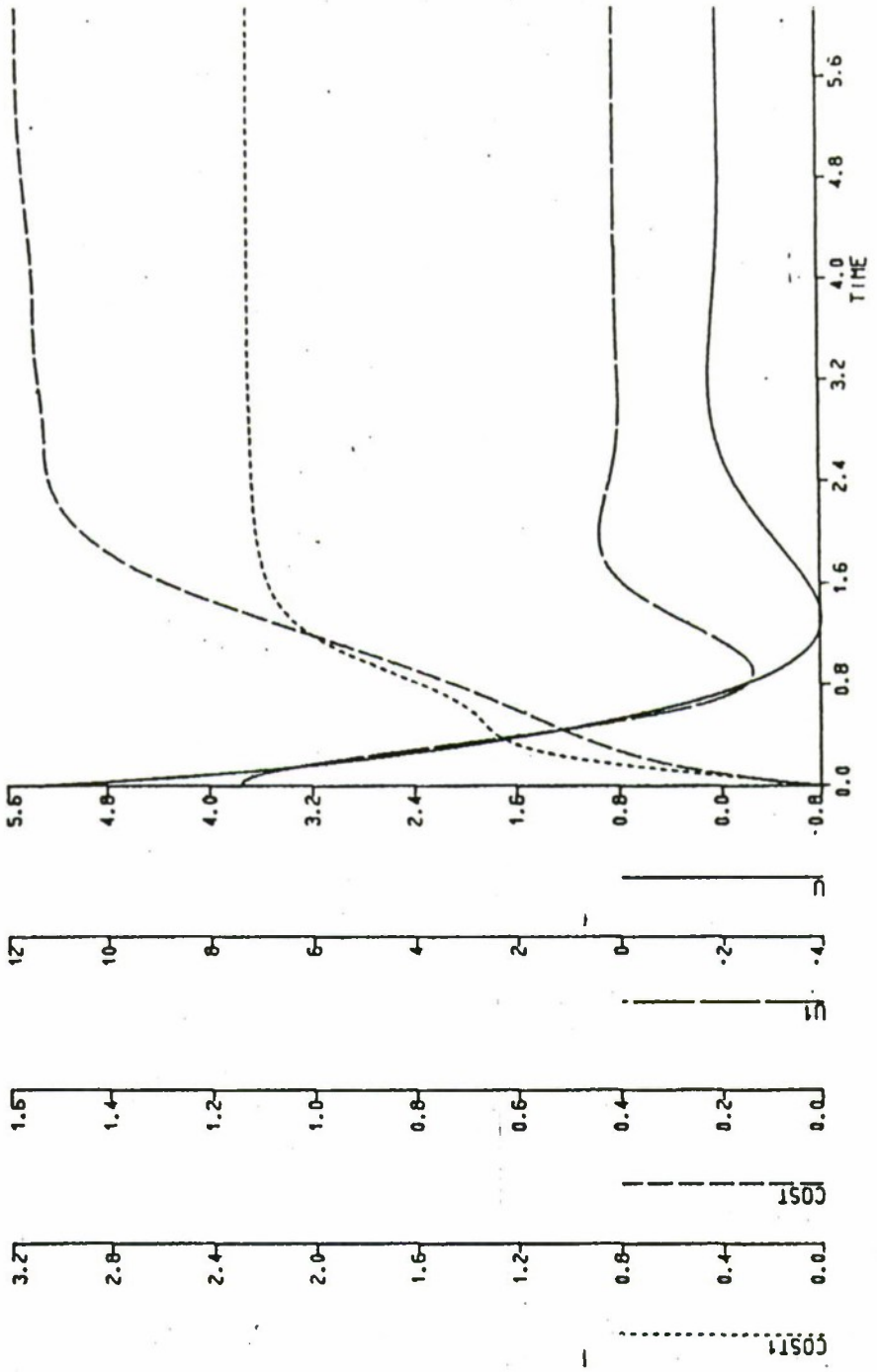

Figure 5.25: Linear Versus Nonlinear Optimal Gains in a Linear System, q=0.1
U: Control Signal for Linear Gains
$U1$: Control Signal for Nonlinear Gains
COST: Value of Cost Index for Linear Gains
COST1: Value of Cost Index for Nonlinear Gains

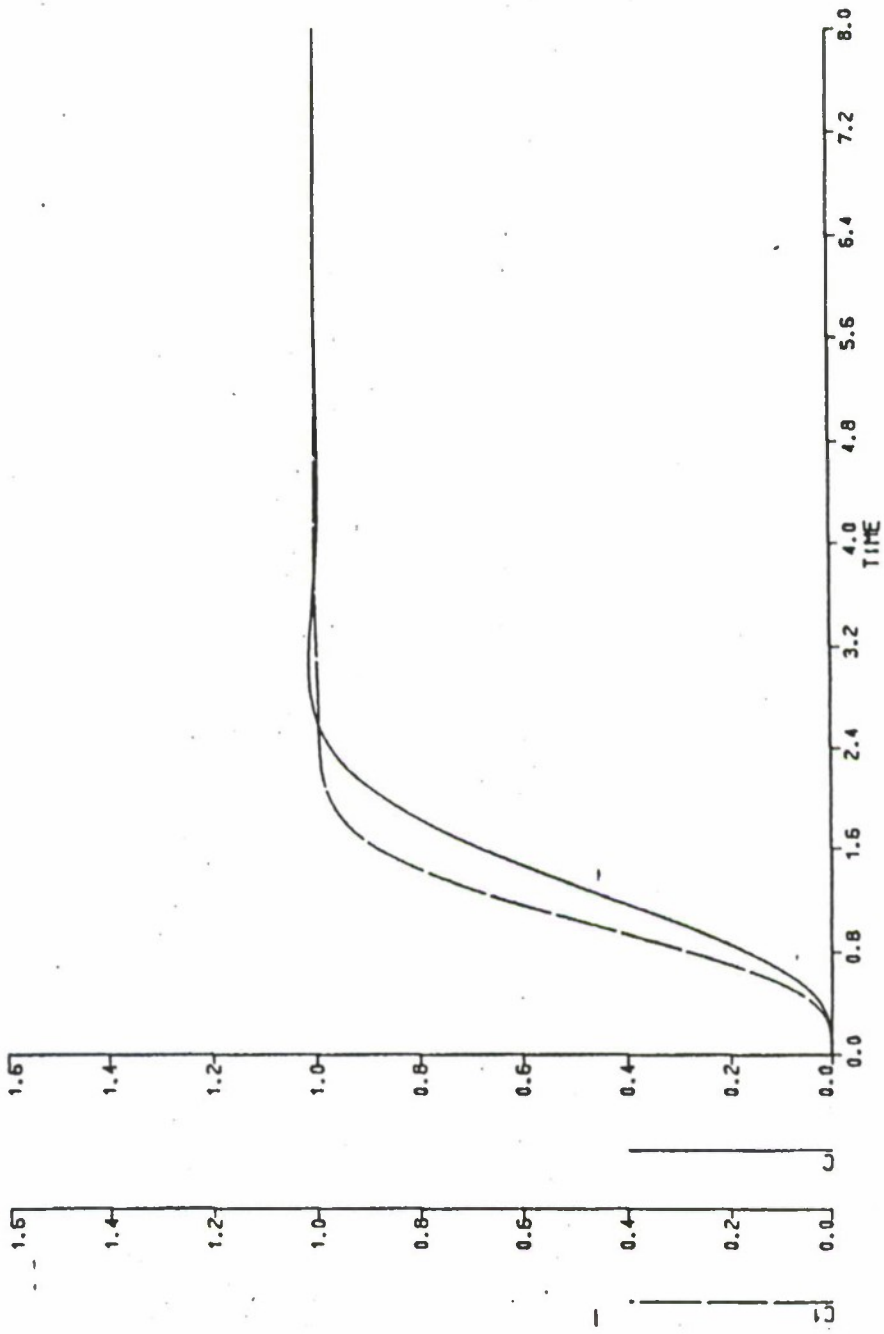

Figure 5.26: Linear Versus Nonlinear Optimal Gains in a Linear System, q=0.1
C: Control Signal for Linear Gains
$C1$: Control Signal for Nonlinear Gains

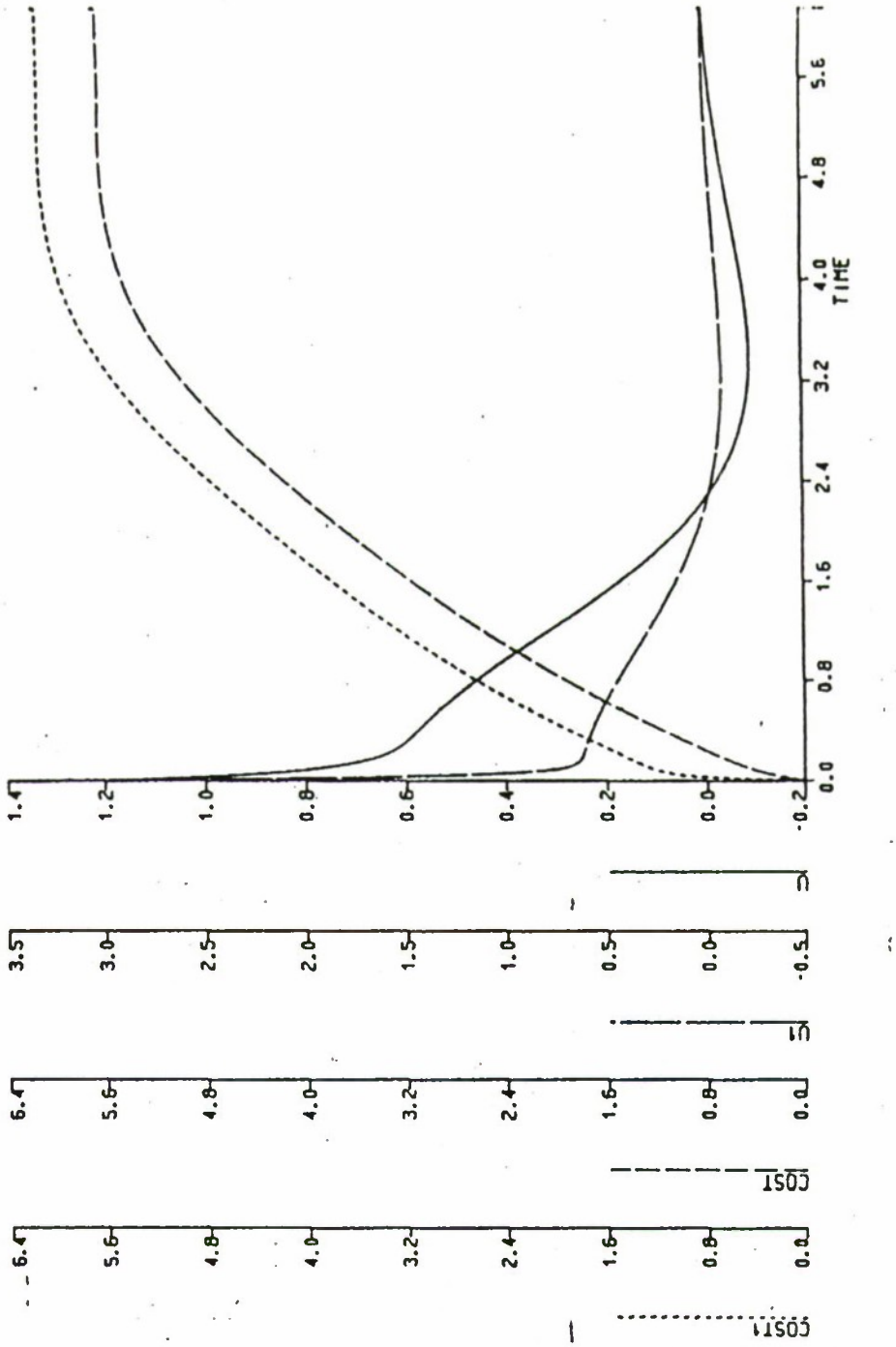

Figure 5.27: Linear Versus Nonlinear Optimal Gains in a Linear System, q=5.0
U: Control Signal for Linear Gains
$U1$: Control Signal for Nonlinear Gains
COST: Value of Cost Index for Linear Gains
COST1: Value of Cost Index for Nonlinear Gains

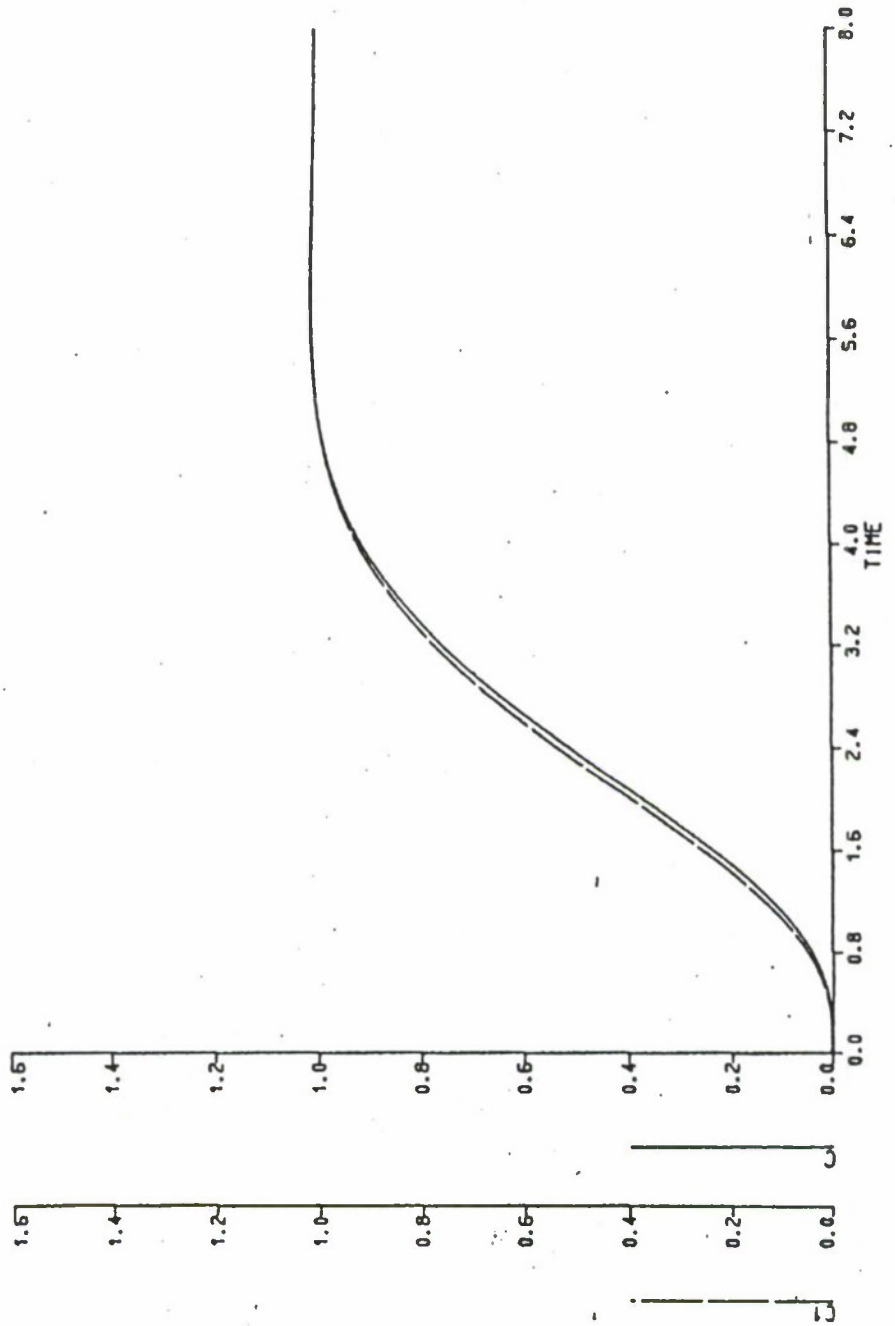

Figure 5.28: Linear Versus Nonlinear Optimal Gains in a Linear System, q=5.0
C: Control Signal for Linear Gains
$C1$: Control Signal for Nonlinear Gains

VI. SUMMARY AND CONCLUSIONS

This study dealt solely with all-pole plants with one pole located at the origin. This implied zero steady-state error. All optimizations were conducted using full-state-feedback compensation in the minor loop. Based on the preliminary work done by Graham and Lathrop, the integral of time multiplied by the absolute value of error was accepted as the best performance criterion due to its reliability, ease of application and selectivity; however, it was emphasized that this criterion represented a compromise between the conflicting characteristics of the percent overshoot of the steady-state position and the time required to reach the first zero-error signal. The cost function was unrealistic in its assumption of the availability of infinite control signal. To correct this inadequacy, an alternative performance index was introduced which penalized the use of control. It was found that the cost function was a mathematical tool used to artificially define an optimal system. Its use may or may not have resulted in a system which met the specifications needed in the design. It was concluded that it may be possible for an experienced designer to apply the appropriate weightings within the index to reflect his needs, but no precise relationships between specifications and weightings were established.

In the utilization of the integral of time multiplied by the absolute value of the error, it was concluded that systems utilizing full-state-feedback compensation could not be optimized. The zero-order derivative feedback acted as a variable gain for the system, resulting in unrealistic bandwidths. The system attempted to duplicate an ideal step function. Fixing the zero-order derivative to a constant value fixed the bandwidth of the system and allowed the performance index to reach a true minimum. It was concluded that there was only one optimal solution for a

given N^{th}-order system; therefore, there was only one optimal root pattern. Since the use of full-state feedback allowed the placement of the roots at any location, the roots remained at their optimal positions regardless of the parameters of the plant. Any change in the plant's parameters was offset by a corresponding increase or decrease in the feedback gains, returning the roots to their optimal locations. In the presence of a saturating element at the plant input, the system's damping was reduced; however, the general characteristics of the linear system were maintained. The system maintained its characteristic one-overshoot, one-undershoot response. When the system was optimized in the presence of the nonlinearity, a more optimal response was obtained. The presence of the saturating element limited the speed of the system and resulted in a reduction of the performance index based, mainly, on eliminating the error; whereas, the linear optimization realized most of its reduction by increasing the speed of the system. When the saturating element was moved to the system input, opposite effects were found. Employing the linear optimal gains, this configuration provided more damping. When optimized with the nonlinearity at the new location, the damping was reduced and the response became more oscillatory. It was concluded that the two different positions of the nonlinearity provided a direct contrast in terms of its effect on the response of the system. These results held true for any-order, all-pole system utilizing full-state-feedback compensation. Given a saturation nonlinearity at either the system or plant input, it was postulated that a designer could use these general trends to intelligently determine the compensation.

The standard forms derived by Graham and Lathrop were studied to determine their validity. It was concluded that although their results were impressive, Graham and Lathrop failed to find the absolute or global minimum. New standard forms were derived which showed a definitive and progressive root pattern. The superiority and

usefulness of these standard forms were shown through the use of examples which utilized active networks in their compensation schemes.

A control cost was added to the criterion in the form of the squared value of the input control signal. A weighting factor was included which reflected the relative importance of the control signal. Optimizations were conducted for third and fourth-order systems utilizing fixed and variable-forward-gain scenarios. In the fixed gain cases, it was concluded that increases in the weighting of the control cost caused optimal gains to increase and the complex roots to retract to the real axis. Due to the mathematical structure of the index, the system was highly sensitive to the value of the control weighting. In the variable-gain cases, the complex roots optimized to more random patterns. Increases in the control weighting translated to less power being supplied to the plant and a slower system with smaller bandwidths. No definitive root pattern was established. Two problems were uncovered which made the minimization of the index difficult. The flatness of the cost-index contour and a high dependence on the integration period negated any assurance of finding the absolute or global minimum.

Using the linear optimal gains, a saturating nonlinearity was inserted into the system. Simulations were conducted using various step and limit sizes. It was found that the presence of the limiter destroyed the compromise between speed and error that had been established in the optimization of the linear system. As the step sizes were increased so as to cause saturation, the system responded with an increase in both the response time and the value of the cost index. It was concluded that the general form of the transient response remained unchanged, i.e., there was no rapid deterioration of the response.

A comparison of the two cost indices was conducted in terms of their performance in the presence of a saturating nonlinearity. Specifically, the theory that a

linear system which was optimized with a performance index that included a cost constraint performed better in the presence of saturation was investigated. It was found that although the inclusion of a control cost resulted in a small reduction of overshoot, there was no overriding advantages for using one index over the other. Based on this result, Sheldon S. L. Chang's work with the linear quadratic regulator was investigated. Chang's results supporting the superiority of the regulator were not duplicated. The conclusion was that the addition of a control cost to the performance index did little to enhance nonlinear performance.

In order to thoroughly investigate the cost functions under study, the effects of a nonlinear optimization when employed in a linear system were investigated. It was found that as the value of the control weighting was increased, the response of the linear system became slower. The explanation of this trend was found by examining the nonlinear optimization process. During the saturation periods, the amount of control was set by the limiter. During linear operation, the amount of control was determined by the value of the control weighting. As the control weighting was increased, the amount of control used during the linear operation decreased; consequently, less control input resulted in a slower system response.

APPENDIX A
Computer Code for the Optimization of the Fourth-Order System using the ITAE Criterion

```
*    EXAMPLE OF A TYPICAL MINIMIZATION ROUTINE FOR
*    THE INTEGRAL OF TIME MULTIPLIED BY THE ABSOLUTE
*    VALUE OF THE ERROR PLUS A WEIGHTING FACTOR
*    MULTIPLIED BY THE SQUARE OF THE CONTROL INPUT
*************************************************************
*    NUMEROUS SUCH PROGRAMS WERE USED IN THE COURSE OF
*    THE STUDY
*************************************************************
*    INITIALIZE ARGUMENTS TO BE USED IN MINIMIZATION SUBROUTINE
D       COMMON/HANDJ/FLAG,ERRFN,K00,K11,K22,K33
*************************************************************
TITLE    OPTIMIZATION OF FOURTH ORDER NONLINEAR SYSTEM
*************************************************************
*       ESTABLISH CONSTANTS TO BE USED IN THE PROGRAM
CONST    Q=100.,A=1.0,IC=0.0
*************************************************************
*       ASSIGN INITIAL VALUES TO THE PARAMETERS
*       TO BE OPTIMIZED
PARAM    K0=5.41,K1=6.58,K2=2.34,K3=.319
*************************************************************
*       INITIALIZE THE PARAMETERS
INITIAL
        IF (FLAG.LT.0.)    K11=K1
        IF (FLAG.LT.0.)    K22=K2
        IF (FLAG.LT.0.)    K33=K3
        IF (FLAG.LT.0.)    K00=K0
*************************************************************
*       INPUT A STEP FUNCTION
DYNAMIC
        R=A*STEP(0.0)
*************************************************************
*      SIMULATE THE SYSTEM
DERIVATIVE
*-----------------COMPENSATED SYSTEM-------------------------
        E=R-C
        EPG=K00*E
        Z=EPG-F
        U=LIMIT(-1.0,1.0,1.0*Z)
        B=REALPL(IC,.50,U*5.0)
        CDOT3=B-H
        CDOT2=INTGRL(IC,CDOT3)
        CDOT=INTGRL(IC,CDOT2)
        C=INTGRL(IC,CDOT)
        H=6.5*CDOT2+3.0*CDOT
        F=K11*CDOT+K22*CDOT2+K33*CDOT3
*************************************************************
*       CALCULATE THE PERFORMANCE INDEX
NOSORT
        IF(E.LT.0.0) THEN
        EA=-E
        ELSE
        EA=E
        ENDIF
```

```
SORT
        EAT=EA*TIME
        USQD=U*U
        PCOST=Q*USQD+EAT
        COST=INTGRL(IC,PCOST)
*************************************************************
*       DEFINE THE CRITERIA TO BE USED IN THE MINIMIZATION
*       ROUTINE
TERMINAL
      ERREN = COST
*************************************************************
*       DEFINE THE INTEGRATION METHOD TO BE USED
METHOD   RK5
*************************************************************
*       DEFINE THE PERIOD OF INTEGRATION
CONTROL  FINTIM=10.0
*************************************************************
* END OF MAIN PROGRAM
END

STOP
*************************************************************
*       MINIMIZATION SUBROUTINE
FORTRAN
        IMPLICIT REAL*8 (A-H,O-Z)
*************************************************************
*       SET UP THE WORKING ARRAYS
        DIMENSION X(4),STEP(4),Q(4),QQ(4),W(4)
*************************************************************
*       ESTABLISH THE INITIAL STEP SIZES TO BE USED IN THE SEARCH
        STEP(1)=1.
        STEP(2)=1.0
        STEP(3)=1.0
        STEP(4)=.10
*************************************************************
*       DEFINE THE NUMBER OF PARAMETERS
        N=4
*************************************************************
*       DEFINE THE NUMBER OF FUNCTION CALLS TO BE PERFORMED
        ITMAX = 2000.0
*************************************************************
*       DEFINE THE ERROR IN THE CRITERION FUNCTION TO BE REACHED
*       BEFORE THE PROGRAM TERMINATES
        CETOL = 1.0D-6
*************************************************************
*       SET THE STEPSIZE REDUCTION FACTORS TO BE USED IN THE SEARCH
        ALPHA = 2.0D0
        BETA = 0.5D0
*************************************************************
*       ADMINISTRATIVE DATA TO TELL THE PROGRAM THAT THIS IS A
*       MINIMIZATION ROUTINE
        IPRINT = 0
        MINMAX = -1
*************************************************************
*       CALL THE MINIMIZATION SUBROUTINE
        CALL HOOKE(X,STEP,N,ITMAX,CETOL,ALPHA,BETA,
     *             CE,Q,QQ,W,IPRINT,MINMAX)
        STOP
        END
```

APPENDIX B

Computer Code for the Optimization of the Fourth-Order System Using the Cost Function of $\int_0^\infty [t\,|e(t)| + qu(t)^2]\,dt$

```
*    EXAMPLE OF A TYPICAL MINIMIZATION ROUTINE
*    FOR THE INTEGRAL OF TIME MULTIPLIED BY THE
*    ABSOLUTE VALUE OF THE ERROR
*************************************************
*    NUMEROUS SUCH PROGRAMS WERE USED IN THE
*    COURSE OF THE STUDY
*************************************************
*    INITIALIZE ARGUMENTS TO BE USED IN MINIMIZATION SUBROUTINE
D       COMMON/HANDJ/FLAG,ERRFN,K11,K22,K33
*************************************************
TITLE    OPTIMIZATION OF FOURTH ORDER LINEAR SYSTEM
*************************************************
*     ESTABLISH CONSTANTS TO BE USED IN THE PROGRAM
CONST    A=1.0,IC=0.0,K0=5.366
*************************************************
*     ASSIGN INITIAL VALUES TO THE PARAMETERS
*     TO BE OPTIMIZED
PARAM    K1=6.5910,K2=2.3820,K3=.361
*************************************************
*     INITIALIZE THE PARAMETERS
INITIAL
        IF (FLAG.LT.0.)    K11=K1
        IF (FLAG.LT.0.)    K22=K2
        IF (FLAG.LT.0.)    K33=K3
*************************************************
*     INPUT A STEP FUNCTION
DYNAMIC
        R=A*STEP(0.0)
*************************************************
*     SIMULATE THE SYSTEM
DERIVATIVE
*-------------------COMPENSATED SYSTEM-------------------------
        E=R-C
        EPG=K0*E
        U=EPG-F
        B=REALPL(IC,.50,U*5.0)
        CDOT3=B-H
        CDOT2=INTGRL(IC,CDOT3)
        CDOT=INTGRL(IC,CDOT2)
        C=INTGRL(IC,CDOT)
        H=6.5*CDOT2+3.0*CDOT
        F=K11*CDOT+K22*CDOT2+K33*CDOT3
*************************************************
*     CALCULATE THE PERFORMANCE INDEX
NOSORT
        IF(E.LT.0.0) THEN
        EA=-E
        ELSE
        EA=E
        ENDIF
SORT
        EAT=EA*TIME
        COST=INTGRL(IC,EAT)
```

```
**********************************************
*     DEFINE THE CRITERIA TO BE USED IN THE MINIMIZATION
*     ROUTINE
TERMINAL
       ERRFN = COST
**********************************************
*     DEFINE THE INTEGRATION METHOD TO BE USED
METHOD    RK5
**********************************************
*     DEFINE THE PERIOD OF INTEGRATION
CONTROL   FINTIM=10.0
**********************************************
*     END OF MAIN PROGRAM
END
STOP
**********************************************
*     MINIMIZATION ROUTINE
FORTRAN
        IMPLICIT REAL*8 (A-H,O-Z)
**********************************************
*     SET-UP THE WORKING ARRAYS
        DIMENSION X(3),STEP(3),Q(3),QQ(3),W(3)
**********************************************
*     ESTABLISH THE INITIAL STEP SIZES TO BE USED IN THE SEARCH
        STEP(1)=.1
        STEP(2)=.10
        STEP(3)=.01
**********************************************
*     DEFINE THE NUMBER OF PARAMETERS
        N=3
**********************************************
*     DEFINE THE NUMBER OF FUNCTION CALLS TO BE PERFORMED
        ITMAX = 600.0
**********************************************
*     DEFINE THE ERROR IN THE CRITERION FUNCTION TO BE REACHED
*     BEFORE  THE PROGRAN TERMINATES
        CFTOL = 1.0D-3
**********************************************
*     SET THE STEPSIZE REDUCTION FACTORS TO BE USED IN THE
*     SEARCH
        ALPHA = 2.0D0
        BETA = 0.5D0
**********************************************
*     ADMINISTRATIVE DATA TO TELL THE PROGRAM THAT THIS IS A
*     MINIMIZATION ROUTINE
        IPRINT = 0
        MINMAX = -1
**********************************************
*     CALL THE MINIMIZATION SUBROUTINE
        CALL HOOKE(X,STEP,N,ITMAX,CFTOL,ALPHA,BETA,
     *             CF,Q,QQ,W,IPRINT,MINMAX)
        STOP
        END
```

LIST OF REFERENCES

1. Graham, D. and Lathrop, R., "The Synthesis of Optimum Transient Response: Criteria and Standard Forms", *AIEE Applications and Industry*, No. 9, pp. 273-288, 1953.

2. Graham, D. and Lathrop, R., "The Transient Performance of Servomechanisms with Derivative and Integral Control", *AIEE Applications and Industry*, No. 11, pp. 10-17, 1954.

3. International Business Machines, *Dynamic Simulation Language/VS: Language Reference Manual*, IBM Corporation.

4. D'Azzo, J. J. and Houpis, C. H., Feedback Control System Analysis and Synthesis, McGraw-Hill Book Co., 1966.

5. Butterworth, S., "On the Theory of Filter Amplifiers", *Wireless Engineering*, No. 7, pp. 536-541, 1930.

6. Sedra, Adel S. and Smith, Kenneth C., *Microelectronic Circuits*, Holt, Rhinehart and Winston Publishing Co., 1987.

7. Frankline, G. F., Powell, J. D. and Emami-Naeini, A., *Feedback Control of Dynamic Systems*, Addison-Wesley Publishing Co., 1986.

8. Thaler, George J., *Automatic Control Systems*, West Publishing Co., 1989.

9. Chang, Sheldon S. L., *Control Systems Engineering*, McGraw-Hill Book Co., 1961.

10. Chang, Sheldon S. L., *Root Square Locus Plot - A Geometrical Method for Synthesis of Optimum Servo Systems*, IRE Convention Record, 1958.

INITIAL DISTRIBUTION LIST

		No. of Copies
1.	Defense Technical Information Center Cameron Station Alexandria, Virginia 22304-6145	2
2.	Library, Code 0142 Naval Postgraduate School Monterey, California 93943-5002	2
3.	Chairman, Code 62 Department of Electrical and Computer Engineering Naval Postgraduate School Monterey, California 93943-5000	1
4.	Professor George J. Thaler, Code 62Tr Department of Electrical and Computer Engineering Naval Postgraduate School Monterey, California 93943-5000	1
5.	Professor Harold A. Titus, Code 62Ts Department of Electrical and Computer Engineering Naval Postgraduate School Monterey, California 93943-5000	1
6.	Commander Missile and Space Intelligence Center Redstone Arsenal, Alabama 35898-5500	1
7.	Darrell R. Davis Route 2, Box 306 Wheelersburg, Ohio 45694	2